



SILVER NANOPARTICLES IN GLASS IONOMER CEMENTS: SYNTHESIS,  
CHARACTERIZATION AND VALIDATION OF THE ANTIBACTERIAL ACTIVITY

Lílian Fernanda Santos Paiva

Tese de Doutorado apresentada ao Programa de Pós-graduação em Engenharia Metalúrgica e de Materiais, COPPE, da Universidade Federal do Rio de Janeiro, como parte dos requisitos necessários à obtenção do título de Doutor em Engenharia Metalúrgica e de Materiais.

Orientador(es): Rossana Mara da Silva Moreira  
Thiré  
Karine Anselme

Rio de Janeiro  
Março de 2015

SILVER NANOPARTICLES IN GLASS IONOMER CEMENTS: SYNTHESIS,  
CHARACTERIZATION AND VALIDATION OF THE ANTIBACTERIAL ACTIVITY

Lílian Fernanda Santos Paiva

TESE SUBMETIDA AO CORPO DOCENTE DO INSTITUTO ALBERTO LUIZ  
COIMBRA DE PÓS-GRADUAÇÃO E PESQUISA DE ENGENHARIA (COPPE) DA  
UNIVERSIDADE FEDERAL DO RIO DE JANEIRO COMO PARTE DOS  
REQUISITOS NECESSÁRIOS PARA A OBTENÇÃO DO GRAU DE DOUTOR EM  
ENGENHARIA DE MATERIAIS.

Examinada por:

---

Prof. Rossana Mara da Silva Moreira Thiré, D.Sc.

---

Dr. Karine Anselme, Ph.D.

---

Dr. Lydie Ploux, Ph.D.

---

Prof. Luiz Carlos Pereira, D.Sc.

---

Prof. Raphael Hirata Junior, D.Sc.

---

Prof. Angela Maria Moraes, D.Sc.

RIO DE JANEIRO, RJ - BRASIL

MARÇO DE 2015

Paiva, Lílian Fernanda Santos

Silver nanoparticles in glass ionomer cements: synthesis, characterization and validation of the antibacterial activity / Lílian Fernanda Santos Paiva. – Rio de Janeiro: UFRJ/COPPE, 2015.

X, 162 p.: il.; 29,7 cm.

Orientadores: Rossana Mara da Silva Moreira Thiré  
Karine Anselme

Tese (doutorado) – UFRJ/ COPPE/ Programa de Engenharia Metalúrgica e de Materiais, 2015.

Referências Bibliográficas: p. 127-146.

1. Cimentos ionômeros de vidro. 2. Nanopartículas de prata. 3. Biofilmes. I. Thiré, Rossana Mara da Silva Moreira *et al.* II. Universidade Federal do Rio de Janeiro, COPPE, Programa de Engenharia Metalúrgica e de Materiais. III. Título.

Resumo da Tese apresentada à COPPE/UFRJ como parte dos requisitos necessários para a obtenção do grau de Doutor em Ciências (D.Sc.)

## NANOPARTÍCULAS DE PRATA EM CIMENTOS IONÔMERO DE VIDRO: SÍNTESE, CARACTERIZAÇÃO E VALIDAÇÃO DA ATIVIDADE ANTIBACTERIANA

Lílian Fernanda Santos Paiva

Março/2015

Orientadores: Rossana Mara da Silva Moreira Thiré  
Karine Anselme

Programa: Engenharia Metalúrgica e de Materiais

O objetivo deste estudo foi atribuir propriedades antibacterianas para a superfície de um cimento de ionômero de vidro (CIV) experimental, inerente à presença de nanopartículas de prata (AgNP). As nanopartículas mantiveram-se como uma solução coloidal estável, com tamanhos médios variando de 7 a 10 nm, ao longo de um período de monitoramento maior que 180 dias. Foi realizada a caracterização dos CIV com quantidades crescentes de sal de prata (Without Ag, Low Ag, Medium Ag e High Ag). A síntese de AgNP na matriz polimérica do CIV mostrou não prejudicar a sua resistência à compressão, ou o seu tempo de cura. Em High Ag, a maior concentração de prata aumentou a resistência à compressão dos cimentos, devido à ancoragem de cadeias de polímero. Todos os grupos contendo prata induziram zonas de inibição do crescimento bacteriano estatisticamente significativas sobre placas de agar. Medium Ag mostrou possuir a concentração de sal de prata em que a adesão bacteriana e os parâmetros de formação de biofilme (biomassa, espessura média, distância de difusão e superfície/bio-volume) foram significativamente afetados em relação ao controle, causando a formação de grandes agregados ou biofilmes em forma de teia. Além disso, Medium Ag manteve as viabilidades bacterianas e de células de fibroblastos gengivais inalteradas.

Abstract of the Thesis presented to COPPE/UFRJ as a partial fulfillment of the requirements for the degree of Doctor of Science (D.Sc.)

SILVER NANOPARTICLES IN GLASS IONOMER CEMENTS: SYNTHESIS,  
CHARACTERIZATION AND VALIDATION OF THE ANTIBACTERIAL ACTIVITY

Lílian Fernanda Santos Paiva

March/2015

Advisors: Rossana Mara da Silva Moreira Thiré

Karine Anselme

Department: Metallurgical and Material Engineering

The aim of this study was to attribute antibacterial properties to the surface of an experimental glass ionomer cement (GIC), inherent to the presence of silver nanoparticles (AgNP). The nanoparticles remained as a stable colloidal solution, with average sizes ranging from 7 to 10 nm, over monitoring period of more than 180 days. Characterization of the GIC with increasing amount of silver salt (Without Ag, Low Ag, Medium Ag and High Ag) was pursued in order to verify any significant changes on their properties. Synthesizing AgNP into the polymer matrix of GIC showed not to affect their final compression strength or net setting time. In High Ag, the concentration of silver in the matrix increased compressive strength of the cements, due to the anchoring of polymer chains. All groups containing Ag induced statistically significant bacterial growth inhibition zones on agar plates. Medium Ag showed to have the concentration of silver salt in which bacterial adhesion and biofilm formation parameters (biomass, mean thickness, diffusion distance and surface to bio-volume) were significantly affected compared to control, causing formation of large aggregates or web-like biofilms, and in which bacterial and fibroblast cell viabilities remained unaltered.

Résumé de la Thèse présenté à COPPE/UFRJ comme un accomplissement partiel des exigences pour le diplôme de Docteur en Sciences (D.Sc.)

NANOPARTICULES D'ARGENT DANS DES CIMENTS VERRES IONOMÈRES:  
SYNTHÈSE, CARACTÉRISATION ET VALIDATION DE LEUR ACTIVITÉ  
ANTIBACTÉRIENNE

Lílian Fernanda Santos Paiva

Mars/2015

Encadrants: Rossana Mara da Silva Moreira Thiré

Karine Anselme

Département: Génie Métallurgique et des Matériaux

Le but de cette étude était d'attribuer à la surface d'un ciment verre ionomère (CVI) expérimental des propriétés anti-bactériennes, grâce aux propriétés des nanoparticules d'argent (AgNP). Les nanoparticules sont restées sous forme d'une solution colloïdale stable sur une période de suivi de 180 jours, avec tailles moyennes allant de 7 à 10 nm. La caractérisation des ciments verre ionomères chargés en nanoparticules d'argent (AgNP-CVI) avec une quantité croissante de sel d'argent (Without Ag, Low Ag, Medium Ag et High Ag) a été approfondie afin de vérifier d'éventuelles modifications importantes de leurs propriétés. Synthétiser AgNP dans la matrice polymérique du CVI a montré de ne pas nuire à leur résistance à la compression (CS) et leur réaction de prise. À High Ag, la concentration d'argent dans la matrice a augmenté la CS des ciments, du fait de l'ancrage des chaînes de polymères. Tous les groupes contenant de l'Ag induisent des zones d'inhibition de croissance de *E. coli* (SCC1) sur les plaques de gélose significatives statistiquement. Medium Ag a montré avoir la concentration de sel d'argent pour laquelle l'adhésion bactérienne et la formation de paramètres du biofilm (biomasse, épaisseur moyenne, la distance de diffusion et de surface sur bio-volume) ont été affectés de façon significative par rapport au contrôle, causant la formation de grands agrégats ou de biofilms en toiles d'araignée, alors que les viabilités cellulaires restent inchangées.

## ACKNOWLEDGEMENTS

I would like to express my special appreciation and thanks to my advisors Professor Dr. Rossana THIRE and Dr. Karine ANSELME. Thank you for encouraging my research and for allowing me to grow as a research scientist. Your advice on both research as well as on my career have been priceless. I would also like to thank Professor Dr. Gloria SOARES, you have been a tremendous mentor for me.

I would like to thank my co-advisor Dr. Lydie PLOUX, without her supervision and constant help this thesis would not have been possible. I would also like to express the deepest appreciation to Professor Dr. Robert HILL, who kindly received me in his laboratory, and have shown the attitude and the substance of a genius, whose passion for “dental materials” had lasting effect.

A special thanks to Professor Dr. Luis Pereira da COSTA, who helped me to develop the main idea of this project, and continually conveyed a spirit of adventure in regard to research and scholarship, as well as an excitement in regard to teaching.

In addition, I want to thank to Dr. Lavinia BALAN, Professor Dr. Lucianne Copple MAIA and Dr. Tatiana Kelly FIDALGO for technical support and specially the valuable collaboration in this work.

I would also like to thank for serving as my jury members, Professor Dr. Angela Maria MORAES, Professor Dr. Raphael HIRATA JUNIOR and Professor Dr. Luiz Carlos PEREIRA. I also want to thank you for letting my defense be an enjoyable moment, and for your brilliant comments and suggestions, thanks to you.

I thank valuable help of Dr. Carlos Wanderlei from EMBRAPA and Epaminondas for providing ICP analyses, and also Dr. Andre ROSSI from CBPF for TEM analyses to my thesis.

I also thank CAPES and CNPq for their financial support granted through doctoral fellowship.

I would especially like to thank technicians and colleagues of the Metallurgical and Materials Department (PEMM) and of the *Institut de Science des Matériaux de Mulhouse* (IS2M). Ana Paula, Márcia, Laércio, Carla, Aline, Marcus, Francisco, Bruno, Paulo, Fábio, Renata, Marta, Rafael, Marianna, Bruna, Paulo Henrique, Carol, Camila, Raquel, Taíla, Emilia, Nelly, Helena, Laura, Jules, William, Tatiana, Loïc, Eric, Patrick, Samar, Laurent, Gautier, Sylvie, all of you have been there to support me when I recruited your help, and also for turning work in a more pleasant place.

A special thanks to my family. Words cannot express how grateful I am to my mother, and father for all of the sacrifices that you've made on my behalf. Your prayer for me was what sustained me thus far.

I would also like to thank all of my friends who supported me in writing, and incited me to strive towards my goal. I would like to express special appreciation to those who were always my support in the moments when there was no one to answer my queries.

## SUMMARY

|   |    |
|---|----|
| I. INTRODUCTION   | 1  |
| II. LITERATURE REVIEW                                       | 4  |
| 2.1. GLASS IONOMER CEMENT (GIC)                             | 4  |
| 2.1.1. Development of GIC                                   | 4  |
| 2.1.2. Structure of GIC                                     | 7  |
| 2.1.3. The setting reaction for convencional GIC            | 9  |
| 2.1.4. Classification and clinical application of GIC       | 14 |
| 2.2. RESTORATIVE DENTISTRY                                  | 16 |
| 2.2.1. Dental caries  | 16 |
| 2.2.2. Minimal Intervention Dentistry (MID)                 | 19 |
| 2.2.3. Biofilms, the environment and interfaces             | 23 |
| 2.2.4. Oral biofilms and ecological succession              | 25 |
| 2.2.5. Development of antibacterial dental materials        | 28 |
| 2.2.6. Antibacterial activity of silver (Ag)                | 35 |
| 2.3. SILVER NANOPARTICLES (AgNP)                            | 39 |
| 2.3.1. Optical properties of AgNP                           | 39 |
| 2.3.2. Synthesis of AgNP                                    | 43 |
| III. OBJECTIVES   | 55 |
| 3.1. GENERAL  | 55 |
| 3.2. SPECIFIC OBJETIVES                                     | 55 |
| IV. MATERIALS AND METHODS                                   | 56 |
| 4.1. GLASS IONOMER CEMENT COMPOSITION                       | 56 |
| 4.2. SYNTHESIS OF SILVER NANOPARTICLES                      | 57 |
| 4.3. PREPARATION OF THE IONOMER GLASS                       | 58 |
| 4.4. PREPARATION OF THE CEMENTS                             | 59 |
| 4.5. CHARACTERIZATION OF THE GIC                            | 60 |
| 4.5.1. Net Setting Time                                     | 60 |
| 4.5.2. Compressive Strength (CS)                            | 60 |
| 4.5.3. Analysis of the Silver Content                       | 62 |
| 4.5.4. Surface Chemical Composition                         | 63 |
| 4.6. <i>IN VITRO</i> CYTOTOXICITY TEST (INDIRECT MTT ASSAY) | 64 |

|   |     |
|---|-----|
| 4.7. AGAR PLATE DIFFUSION TEST ( <i>E. coli</i> )       | 65  |
| 4.8. SPECIFIC ANTIBACTERIAL ASSAYS ( <i>S. mutans</i> ) | 66  |
| 4.8.1. Bacterial adhesion and biofilm development       | 66  |
| 4.8.2. MTT metabolic activity of <i>S. mutans</i>       | 69  |
| 4.9. STATISTICAL ANALYSES                               | 69  |
| V. RESULTS AND DISCUSSION                               | 70  |
| 5.1. SYNTHESIS OF AgNP                                  | 70  |
| 5.1.1. Synthesis by direct electron transfer method     | 75  |
| 5.2. THE IONOMER GLASS                                  | 86  |
| 5.3. CHARACTERIZATION OF THE GIC                        | 87  |
| 5.4. IN VITRO CYTOTOXICITY (INDIRECT MTT ASSAY)         | 97  |
| 5.5. AGAR PLATE DIFFUSION TEST                          | 99  |
| 5.6. SPECIFIC ANTIBACTERIAL ASSAYS                      | 102 |
| VI. FINAL CONSIDERATIONS                                | 120 |
| VII. CONCLUSION   | 124 |
| VIII. PROPOSAL OF FUTURE STUDIES                        | 126 |
| VIII. REFERENCES  | 127 |
| ANEXX (Cotutelle UFRJ-UHA)                              | 147 |

# I. Introduction

---

Dental caries is still a serious oral health problem in most economically developed countries, affecting some of school children and the majority of adults [1]. The pathology and medical complications are very frequent, despite the marked improvement in recent decades in all industrialized countries. It is also the most prevalent oral disease in many countries in Asia and Latin-America, but seems to be less common and less severe in most African countries [1].

The preferred treatment of caries with cavitation in dentin is removal of demineralized and contaminated tooth tissue through cavity preparation, followed by restoration of lost tissues with dental materials, such as metal alloys, composite resins, glass ionomer and ceramics.

Glass-ionomer cements (GIC), a particular category of bioactive dental materials, were first introduced by Wilson and Kent [2]. They were invented because of the need of replacement material to mercury-based amalgams in dentistry. These glass polyalkenoate cements formed from ion leachable fluoro-alumino-silicate glasses and poly(acrylic acid) solution are still one of the most promising bioactive dental materials, although they have been successfully applied in dentistry for more than 30 years. An acid-base reaction occurs forming a composite gel phase (carboxylate salts) encrusted with not reacted glass particles.

GIC are often used in clinical practice due to their singular characteristics. The importance of these cements is attributed to their role in the clinical management of caries, in Minimal Intervention Dentistry (MID), and Caries Management by Risk Assessment (CAMBRA). Their anticariogenic properties such as fluoride release, the ion exchange between GIC and tooth at the internal interface, the direct adhesion to tooth structure and base metals, minimized microleakage at the tooth–enamel interface, linear thermal expansion coefficient similar to dentin and low cytotoxicity are unique properties that enable specific application of such cements. Disadvantages such as early water sensitivity, low compressive strength and reduced wear resistance have limited the use of conventional GIC in some clinical applications, which demand long term restorations. Despite these issues, GIC has a specific field of application in Pediatric Dentistry, in which dental caries presents high morbidity. Considering the reduced chair timing and other treatment difficulties inherent to children’s behavior, GIC is indicated because of simplicity of the technique and preventive effects observed only in this class of materials. Thus, differently from dental composite resins used for definitive restoration of dental caries, it remains as the chosen material suitable for short- to medium-term restorations for many dental practice situations.

The use of fluoride in preventing caries is already established in Dentistry, however currently it has emerged the need to expand the arsenal of preventive products through effective antibacterial therapies, causing prevention to become less dependent on fluoride products [3]. In this context, silver nanoparticles (AgNP) have been shown to be great allies if retained on materials as they may change their surface charge, hydrophobicity, and other physicochemical characteristics of great importance to the accession process and maturation of bacterial biofilm causing caries [4]. Moreover, immobilization of AgNP in

polymer matrix seems advantageous for reducing toxicity of the nanoparticles, since it should prevent mammalian cells to their direct uptake, which would function as a reservoir of silver ions [5].

Recently, resin-based nanocomposites filled with AgNP start to be widely investigated as antibacterial materials for dental applications. Those materials are applied to permanent restorations, which require high color stability and durable mechanical properties. However, resin-based materials are not as bioactive as water-based GIC due to the flux of unbound water through the material. Bioactivity of water-based materials is a major requirement for combating active caries, and also the main reason for the applicability of GIC in modern cariology approaches, such as MID. The originality of this work consists of synthesizing AgNP in the water-based GIC formulation attributing antibacterial properties to this material by the release of silver ions. Such activity allied to the known release of fluoride might also imply cariostatic function to GIC, thus contributing to enhance their performance in fight against caries.

Prompted by the motivation of attributing antibacterial properties to the surfaces of GIC, we hypothesized whether the presence of AgNP would alter properties of the conventional GIC. The aim of this study was to synthesize and characterize novel silver nanoparticles poly(acrylic acid) (AgNP-PAA) via photoreduction technique, and evaluate *in vitro* properties of the formed GIC, validating antibacterial properties by analyses of bacterial adhesion and biofilm formation on the surfaces of the cements.

## II. Literature Review

---

### 2.1. GLASS IONOMER CEMENTS (GIC)

#### *2.1.1. Development of GIC*

Dental silicates used to be the principal material for anterior teeth restorations, and represented, along with metal alloys, the two types of most used dental materials. In the early 1960s, due to their poor clinical performance, the Department of Scientific and Industrial Research set up the Committee for Research into Dental Materials and Equipment to coordinate research and development in United Kingdom universities and Government research establishments in order to improve properties of silicate cements [6]. Wilson's collaboration with Kent and Lewis resulted on finding that aluminium and calcium phosphates constitute part of the Silicate cement matrix, and such discovery conducted them to assume that replacement of phosphoric acid with polymeric chelating agents might improve the cement. Finally in 1965, after numerous trials with a number of acids, Wilson mixed dental silicate glass with 25% poly (acrylic acid) and found an hydrolytically stable cement after 24 hours, however with little or no working time. This study showed that improvement of dental silicate cement, even if possible, was going to be a long-term undertaking [6].

After a decade of intensive research, the Laboratory of the Government Chemist (LGC, UK) achieved the composition of ion-leachable aluminosilicate glasses and an

aqueous solution of poly (acrylic acids) that was the first commercially usable cement termed ASPA - Alumino Silicate Poly (acrylic acid) or glass ionomer cement (GIC) [2, 7]. However the first glass ionomer ASPA I (De Trey Division, Dentsply International) set gingerly, was susceptible to moisture while setting and had a very low translucency. The reason was high fluoride content and crystallization of the glass, resulting in poor aesthetics and limited use in practice [8]. Then, improving the handling properties of the cements became the new challenge.

Five years later, a significant discovery made by Wilson and Crisp showed that tartaric acid (TA) acts as an accelerator, aiding in the extraction of ions from the aluminosilicate glass and facilitates their binding to the polyanion chains. TA chelates metal ions and thus delays the cross-linking of polyacid chains, and possibly forms a cross-linking unit, where a pair of metal ions are bridged by the ligand. This would significantly increase postgelation hardening and extend working time. This formulation known as ASPA II, constituted the first practical glass ionomer cement, which contained TA, in addition to glass powder and poly (acrylic acid) [9]. However, ASPA II solution of poly (acrylic acid) tended to form a gel over time. To overcome this problem, Wilson and Crisp added methyl alcohol to poly (acrylic acid) solutions to inhibit the ordering of structures in solution, which was termed ASPA III [10]. The same authors developed a copolymer of acrylic and itaconic acid, which was less liable to form intermolecular hydrogen bonds and gel. This cement, designated ASPA IV, formed the basis of modern commercial glass ionomer cement [10].

Further studies led to understand that an excess of tartaric acid above the optimum (5 to 10 % wt.) retards setting and weakens the cement, presumably because the

concentration of metal-TA chelate units is too great [11]. Polyalkenoic acid and tartaric acid may also be vacuum dried and incorporated into the glass powder, to overcome cytotoxicity owing to polymerization process of the polymers and to improve homogeneity in powder to liquid mixing. The powder is then mixed with water or dilute tartaric acid solution to the cement [8].

In 1980, Sced and Wilson found that the addition of metal powder or metal fibres can improve strength of GIC, but the resistance to abrasion was reduced [12]. The abrasion resistance and strength were improved by sintering the metal (silver particles) and glass powders together, and they called CERMETS [13]. Other modification to the cements includes incorporation of crystallites of corundum, rutile and tielite in order to improve the strength. However, in water-setting systems, cement strength was shown to be critically dependent on the glass-polyacid ratio [14].

In 1986, Antonucci have developed resin-modified glass ionomers to overcome moisture sensitivity and the lack of command set of the cements. The addition of a small quantity of resin such as hydroxyethyl methacrylate (HEMA) or Bis-GMA to the liquid produced advantageous physical properties. The photopolymerizable resin added to the polyacid liquid component hardens the material substantially when a visible light beam is applied. Once the resin component has been cured, the glass ionomer hardening reaction continues, protected from moisture and overdrying by the hard resin framework [15]. Since then, the term conventional GIC refers to those materials not containing resin in their components.

### 2.1.2. Structure of GIC

Conventional glass ionomer cements are formed by a finely divided fluoro-alumino-silicate glass powder reacted with aqueous solutions of poly (acrylic acid) and other poly (alkenil acids) [2]. The basic component of GIC is calcium or strontium based alumino-silicate glasses with high fluoride content [7, 16]. Glasses for this application are usually called an ionomer glass and generally contain 20–36wt.% SiO<sub>2</sub>, 15–40% Al<sub>2</sub>O<sub>3</sub>, 0–35% CaO, 0–10% AlPO<sub>4</sub>, 0–40% CaF<sub>2</sub>, 0–5% Na<sub>3</sub>AlF<sub>6</sub> and 0–6% AlF<sub>3</sub> [17].

The formulation of the original glass are listed below in increasing order of complexity [18]:

- 1- SiO<sub>2</sub>-Al<sub>2</sub>O<sub>3</sub>-CaF<sub>2</sub>;
- 2- SiO<sub>2</sub>-Al<sub>2</sub>O<sub>3</sub>-CaF<sub>2</sub>-Al<sub>3</sub>PO<sub>4</sub> ;
- 3- SiO<sub>2</sub>-Al<sub>2</sub>O<sub>3</sub>-CaF<sub>2</sub>-Al<sub>3</sub>PO<sub>4</sub>-Na<sub>3</sub>AlF<sub>6</sub>.

Currently four main types of ionomer glasses have been used for cement forming:

1. Alumino-silicate glasses, which have been mainly studied by Wilson and co-workers in the early 1970's and are based on the systems SiO<sub>2</sub>- Al<sub>2</sub>O<sub>3</sub>-CaO or SiO<sub>2</sub>-Al<sub>2</sub>O<sub>3</sub>-CaF<sub>2</sub>;

2. Alumino-borate glasses based mainly on the system Al<sub>2</sub>O<sub>3</sub>- B<sub>2</sub>O<sub>3</sub>- ZnO - ZnF<sub>2</sub>;

3. Zinc-silicate glasses based on the systems CaO-ZnO-SiO<sub>2</sub> or Al<sub>2</sub>O<sub>3</sub>-ZnO-SiO<sub>2</sub> and

4. Alumino-phospho-silicate glasses based on the system SiO<sub>2</sub>-Al<sub>2</sub>O<sub>3</sub>-P<sub>2</sub>O<sub>5</sub>-CaO-CaF<sub>2</sub>

[19].

The glasses can be prepared by mixing the appropriate oxides and melting of ingredients in the temperature range of 1100 °C to 1590 °C, depending on the composition. Then the melt is shock-cooled either onto a metal plate and then into water or directly into water. Many other components such as sodium, potassium, aluminium, barium and silver are incorporated to provide specific properties [13]. The glass is then ground further by dry milling in a ball mill or a gyro mill to a particle size less than 45 µm for a filling grade cement or less than 15 µm for a fine grained luting cement [20].

When glass ionomer cement was first developed, the liquid component was aqueous poly (acrylic acid) that turned into a gel on storage [20]. For this reason, itaconic acid and maleic acid copolymers were added to prevent gelation. Tartaric acid is also added to extend the working time and promotes a snap set [21].

A dry form of poly (acrylic acid) has been introduced to increase the molecular weight, without making the liquid very viscous. Tartaric acid can also be incorporated in the powder. Therefore the liquid can be simple distilled water or an aqueous solution of tartaric acid [22].

The fully set cement is a composite of residual glass particles embedded in a siliceous hydrogel all bonded in a metal-polyacrylate matrix [23].

Nicholson [15] have categorized the modifications in the glass ionomers into:

- (i) the use of alternative polymers, such as acrylic/maleic acid, as the polyacid component, enabling stability of the solution over time;

- (ii) the use of dried polymer powders blended with the glass, and activated by the addition of water, in order to enhance reactivity of the glass particles during agglutination of the cement;
- (iii) the development of cermet-containing cements, in which the filler consists of a CERMET (i.e. a ceramic—metal hybrid, in this case being calcium fluoro-alumino-silicate glass fused to silver) rather than a pure glass. These materials are used in situations where radiopacity is required, and for core build-up under crowns.
- (iv) metal-reinforced cements, where a metal, such as silver—tin alloy or stainless steel, is added to an otherwise conventional glass-ionomer in an attempt to reinforce the set cement;
- (v) resin-modified cements, in which the conventional acid—base components are complemented with monomers and initiators capable of undergoing photochemical polymerization.

### *2.1.3. The setting reaction for conventional GIC*

The setting reaction is an acid base reaction in which the ion leachable glass acts as a base and the acid being poly(acrylic acid) or one of its copolymers [24]. This reaction results in the release of metal cations,  $\text{Al}^{3+}$ ,  $\text{Ca}^{2+}$  etc. by surface dissolution of the glass particles, which ultimately crosslink the polyacid network, to form a rigid polysalt matrix. It has also been suggested that fluorine complexes such as  $\text{AlF}^{2+}$  is released from the glass [25].

Glass ionomer cements undergo three distinct and overlapping setting reactions. The three phases in the setting reaction of glass-ionomer cement [26] are:

- Phase 1: The decomposition or dissolution of the glass powder
- Phase 2: Gelation-precipitation phase
- Phase 3: Maturation phase

The first phase is the decomposition of the glass powder, when hydrated protons (hydrogen ions), which are formed from the ionization of the poly(acrylic acid) in the water, attack the surface of the glass particles (Figure 2.1A). This process results in the releasing of calcium, aluminium, and fluoride ions and forming a silica-based hydrogel around the involved glass particles. The pH rises as the poly(acrylic acid) is converted into polyacrylates [24]. This is illustrated in Figure 2.1B.

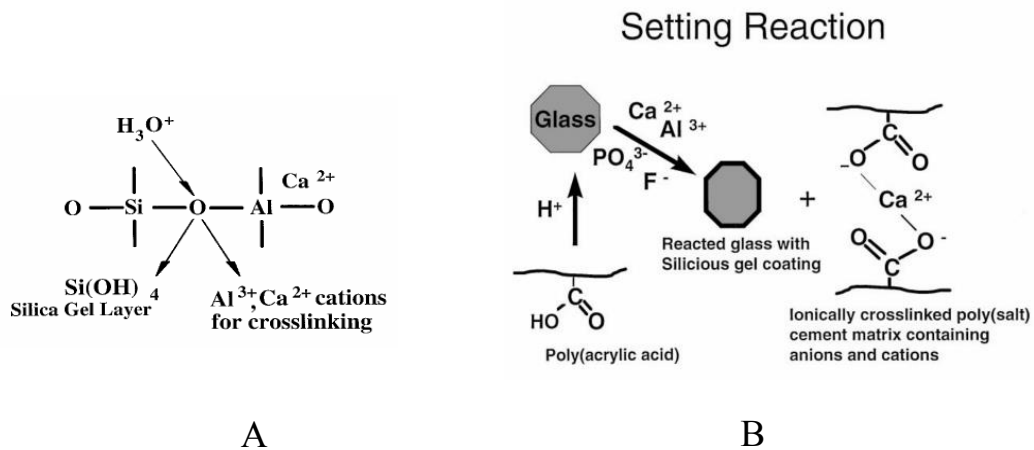


**Figure 2.1** Schematic illustration of A: acid degradation of an aluminosilicate network and B: setting reaction in a glass ionomer cement [27].

During gelation, the second phase of the reaction, the  $\text{Al}^{3+}$  and  $\text{Ca}^{2+}$  ions migrate from the silica hydrogel into the matrix phase. As the pH increases, polysalts (specifically as polycarboxylates) precipitate and ionically crosslink the polyanion chains, causing the cement to harden. The cement has relatively poor physical properties at first when calcium polycarboxylates form over 5 minutes, while the stronger and more stable aluminium polycarboxylates form over 24 hour [23, 28].

The maturation phase is the last stage of the glass-ionomer cement's setting reaction. The cement is very sensitive to moisture contamination in the first 24 hours [23]. The ability of the cement to dehydrate or uptake water decreases as it matures, becoming increasingly rigid as it ages. This is a unique characteristic of these cements among all other dental cements. The strength of glass-ionomer cements are directly related to the bound (non-evaporated) water/evaporated water ratio, or the degree of hydration. This ratio decreases with time; the amount of unbound or loose water becomes less and less in comparison to bound water [15].

The details of the setting chemistry of glass-ionomers was first studied by Crisp *et al.* [28] with infrared spectroscopy. Interpretation of spectra show that in the early stages of the reaction the calcium salt alone is formed, resulting on gelation and the initial set; the aluminum salt formed later is responsible for the final hardening. The difference in the rates of salt formation is attributed to the low mobility of the aluminum ion consequent on its hydration, the morphology of cations in the glass surface, and the stringent steric requirements of crosslinking by  $\text{Al}^{3+}$  ions. In the fully hardened cement a siliceous hydrogel is formed together with both polyacrylate salts of calcium and aluminum. However, a minor proportion of  $-\text{COOH}$  remains unconverted to  $-\text{COO}^-$  groups possibly because they

are inaccessible for steric reasons, and also because when the polyacrylate chain is largely ionized, the remaining hydrogen becomes very firmly bound by electrostatic forces. In effect they have little acidic function and are replaced by cations with difficulty [28].

The addition of tartaric acid (TA) to the GIC was also investigated by FTIR spectroscopy and has confirmed previous results that (+)-tartaric acid reacts more readily with glass than does poly(acrylic acid), thereby delaying the setting of the cement (prolonged working time). Subsequently, (+)-TA rapidly yields calcium tartrate, disponibilizing ions for reaction with the polyacid, and thus enhancing the rate at which aluminum polyacrylate is formed in the cement [29]. These findings were confirmed by  $^{13}\text{C}$  NMR spectroscopy of the fluid cement pastes. TA also showed to react more readily than the polyacid with the glass, and hence suppressing the premature gelation of the cement [30].

Barry *et al.* [23] discovered that the thermal history of the G-200 glass have great influence on the two phases of the GIC: a continuous calcium aluminosilicate matrix and partly crystalline calcium fluoride-rich droplets. They showed by electron probe microanalysis that setting reactions are affected by the microstructure and microcomposition of the glass [23]. When analysed by transmission electron microscope, glass particles appeared surrounded by a siliceous layer set in a hydrogel matrix. The results of X-ray microanalysis (energy dispersive) supported the ultrastructural observations, proving the elemental composition of each region, with ions that originated from the glass particles being detected throughout the matrix of the set cement [31].

All of these techniques demonstrate that the setting of these cements involves neutralization of the polyacid by the basic glass, with the formation of metal polyacrylate units. Moreover, studies on the pH changes during setting reaction revealed that as the cements set, the pH rises from ca. 1.25 to ca. 3 when tartaric acid is fully complexed. As the polyacid reacts the pH rises further to ca. 5 [30, 32].

Young *et al.* [33] quantified by diamond ATR FTIR the polyacid neutralisation rates in different class of materials: glass ionomer cements (GIC), resin-modified GICs (RMGIC) and compomers. The results showed that the initial acid neutralisation rate in the RMGIC Vitremer and Fuji II LC were 0.16 and 0.09 times that of Fuji IX, a conventional GIC. Acid neutralisation in the RMGIC was not near completion even by 60 h and was very slow in compomers Compoglass and Dyract. This occurs due to the fact that the poly(acrylic acid) neutralisation reaction requires water. The poly(acrylic acid), as a weak acid, is probably to be partially ionised in water. This process is likely to be fast such that the early concentration of acidic protons in the GIC is determined mainly by the acid pKa, acid and water concentrations. Moreover, compomers, RMGIC and GIC absorb approximately 0.5, 5 and 3 wt% water, respectively, in the first 50,000 s of immersion. After this time water sorption continues with the compomers but to a much lesser extent with the cements. The combined lack of water in compomers and slow rate of water sorption explains the very slow acid neutralisation rates observed in this study. With the cements the acid neutralisation process is closer to the maximum possible levels by 50,000 s because of the greater water sorption rates combined with initial higher water content of the formulations. This process is important to application because diffusion of water through the cement provides a mechanism for fluoride release from the bulk of the

materials after attack of the glass by acid. The level of ions released would then be expected to be dependant upon the initial fluoride concentration in the glass and the rates of acid reaction and water diffusion in the material [33].

Recent study [34] observed the long term setting reaction in the glass ionomer restorative, Fuj IX, by monitoring the structural evolution of aluminium and fluorine species using  $^{27}\text{Al}$  and  $^{19}\text{F}$  MAS-NMR spectroscopy.  $^{27}\text{Al}$  MAS-NMR results show conversion of aluminium from the glass phase, where it has coordination number four, Al(IV), into the cement matrix where it has a coordination number of six, Al(VI). The majority of aluminium cations do not form tricarboxylates but are coordinated with one or two carboxylic groups and other ligands. The  $^{19}\text{F}$  MAS-NMR spectra are identical for the glass and cements at the early times and contain a dominant signal assigned to Al-F-Sr(n). The conversion of aluminium is confirmed to be a diffusion-controlled process at early stage less than 1 h and it is largely complete between 1 and 6 h. Again it was observed that insufficient amount of water and excess of glass in the cement formulation affect glass degradation mechanism [34].

#### *2.1.4. Classification and clinical application of GIC*

Glass-ionomers can be classified depending on their application as follow: luting cements (Type I), filling materials divided in esthetic restorative (Type IIa) and reinforced restorative (Type IIb), and lining or base cements (Type III) [26].

GIC bonds to tooth structure by hydrogen bonding provided by free carboxyl groups in the fresh paste with the calcium of the apatite of enamel and dentine. Wilson *et al.*

reported that mechanism of adhesion of the GIC is not one of simple ion exchange, since calcium ions are displaced by the phosphate ions. As the cement ages the hydrogen bonds formed between the cement and substrate will progressively converted to stronger ionic bonds as the hydrogens are displaced by calcium, aluminium or other metal ions supplied by either the cement or the substrate [35]. This leads to chemical bonding by a calcium phosphate-polyalkenoate crystalline structure acting as an interface between enamel or dentine and the set material [36].

The direct chemical bonding between glass-ionomers and the surface tooth structure (enamel and dentine) without any additional pre-treatment make this cement good for many clinical application:

- Restoration of deciduous teeth.
- Restoration of erosion and abrasion lesions without cavity preparation.
- Fissure and pits sealant material.
- Restoration of class III and V carious lesions.
- Core build up and repair of defective margins.
- Atraumatic restorative treatment.
- Fixation of orthodontic appliances.
- Cementation of crowns, inlays and bridges.
- Lining all types of cavities.
- Replacement of carious dentin in sandwich technique.
- Sealing the root surfaces of over dentures [26].

To achieve the long-term success of dental restorations, not only the professional carrying out the work, but also the different physical, chemical, and biological properties of

the materials play an important role. Different properties inherent to each class of materials, whether resin or glass-ionomer-based, have their advantages and disadvantages depending on the clinical application. The basis for the long-term success of dental restorations is the proper application of the dental practitioner knowledge about the chemistry, characteristics and handling features of the restorative material in clinical practice [37].

## **2.2. RESTORATIVE DENTISTRY**

### *2.2.1. Dental caries*

Dental caries is an acid-driven and localized de-mineralization of dental hard tissue caused by dental biofilm [38]. World Health Organization (WHO) reported that caries is still the most prevalent of the oral diseases worldwide and remarks it remain a problem despite the great improvement in dental public health [1]. In 2007, cross-sectional study among Brazilian preschoolers (0-to-5 years old) investigated the prevalence and severity of dental caries and their association with demographic and socio-economic variables. Forty per cent of the children (589/1487) presented dental caries. Age, educational level of mothers and low family income were determinant factors to the increase of caries experience [39].

Etiology of dental caries was first described by Miller in 1890 in his chemo-parasitic theory, which supports bacterial production of organic acids as metabolic products of dietary sugars, namely lactic, formic and acetic acids. Nowadays this theory is known as acidogenic theory [40]. Despite this simple cause in concept, dental caries is a multifactorial disease. The complex interplay between salivary composition combined with

diet, local immune response in the oral cavity and pH fluctuations influence the biofilm composition and metabolism, which will then, in concert with other factors such as fluoride ion concentrations in the oral fluids, determine the cyclical re- and de-mineralization process at any biofilm covered site [41].

The environmental process is a combined result of behavioural, social, cultural, dietary and biological risk factors, which in diverse levels ultimately influence the way the disease develops in individuals and in populations. Caries etiology is traditionally described by the Keyes diagram with the intersecting circles of ‘host’, ‘plaque/biofilm’, and ‘diet’ (Fig. 2.2). However, the occurrence of caries is thus an outcome of complex processes involving also secondary behaviour factors of individuals and societies [3, 38, 41].

The caries process may be detailed as follows:

1. Acidogenic biofilm ferments dietary carbohydrates and produces a variety of organic acids, which reduce the pH of the biofilm below 5 [42].
2. This acidic environment results in hydroxyapatite (HA) dissolution, thus calcium and phosphate ions start to diffuse out from tooth structure. This early sign of enamel caries is histopathologically featured by subsurface de-mineralization [43].

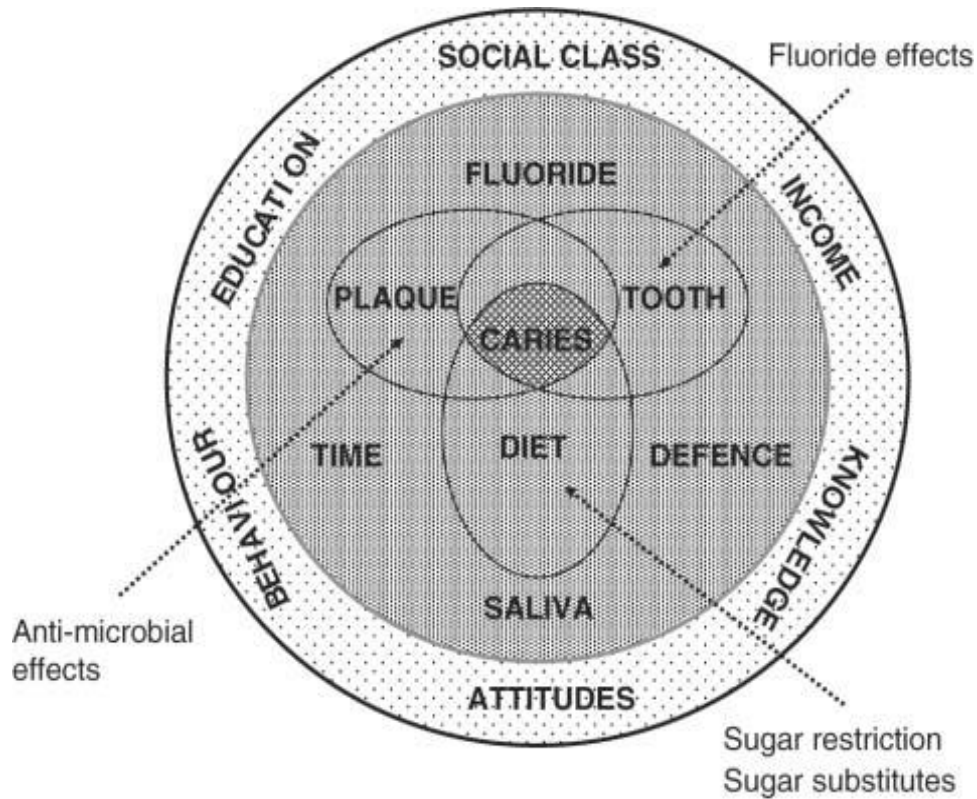


**Figure 2.2** Modified Keyes diagram of factors determining caries development [3].

3. The reversal process (re-mineralization) can be played if calcium, phosphate and/or fluoride ions are present in saliva to diffuse back to tooth structure, composing a new crystal structure. Apart from HA, mineral can be recovered as other apatite-like crystals on the surface, as such as fluorapatite (FA), which are more resistant to acid attack [44].
4. This dynamic physicochemical process can be controlled by the balance between the protective and pathological factors, and thus will determine whether de-mineralization will progress, be stopped, or be reversed in re-mineralization [45].



According to conventional modern dentistry, when caries progress and reach the dentino-enamel junction, the penetration of the lesion complex follows the direction of the dentinal tubules, and two demineralised layers can be identified on the caries focus: an outer infected and decomposed layer, that must be removed during restorative procedures; and other internal remineralizable layer, that might be spared [48]. This process is represented in Figure 2.4.

Cavities are restored in order to recover form, function and aesthetics. However, a major reason for restoring a tooth cavity, from a cariology and preventive point of view, is to seal it and facilitate mechanical removal of dental plaque from the restored surfaces of the tooth [37, 49].

One of the main requirements for the successful application of the MID concept is the selection of suitable preventive and restorative materials. Cariology and materials science have significantly contributed to support this approach. Therefore, the needs of the patients as well as the different clinical conditions dictate the choice among water based, resinous or hybrid materials. The biological and physical properties of the materials are important, as are other features such as their availability and costs, ease of use and tolerance to operator variability, storage conditions, shelf-life, and the operative equipment required [50].

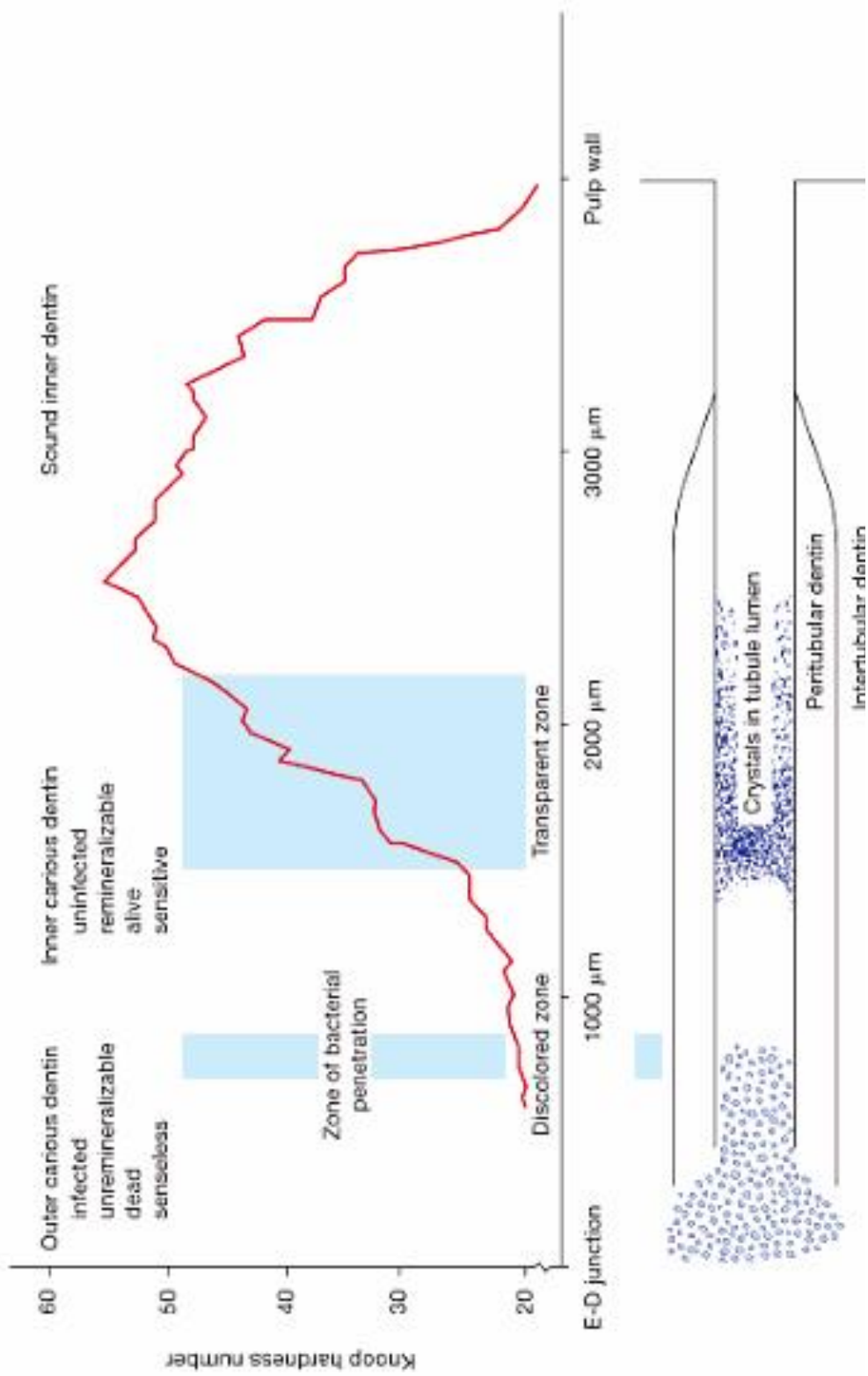


**Figure 2.4** Schematic diagram of the relationship between the hardness curve, the outer layer of dentin, the translucent portion and the inner layer of dentin. Shown below is the relationship between bacterial invasion and mineralization of dentinal tubules phenomenon [49].

In contrast to conventional stepwise excavation of carious lesions, Atraumatic Restorative Technique (ART) has been described as an one-session approach, where gross caries removal is done with manual instruments without anesthesia and cavity sealing with glass ionomer cement (GIC) is considered to be the final restoration. This approach is indicated to countries in which the oral healthcare system is usually insufficiently equipped to provide the needed care, and prevalence of dental caries is higher and its severity greater [49, 51, 52]. Although it was firstly considered a palliative treatment, systematic reviews have reported that sealed cavities have no further ability to drive the caries process once they are cut off from the oral cavity, thus depriving microorganisms of the source of metabolic nutrition required for their survival and for the production of acid that demineralises tooth surfaces [53, 54]. It means that a cavity skillfully restored with a well-manufactured restorative material, which seals the cavity, leads to the depletion of the cariogenic potential of those remnants of carious tissue. At this point, adhesion to dental structure and remineralization of the remnants dental tissues are important required material properties in order to stop the carious cavity progress and thus to stabilize the disease [55].

For this reason glass-ionomer cement (GIC) is an important tool in the fight against caries. It can be thought of as a reservoir of fluoride and other ions in the oral cavity, a mechanical barrier that protects the tooth surface against bacteria; most importantly, it can provide a long-lasting seal under the most challenging clinical circumstances. Recently, it was suggested that GIC also could be useful in the preventive arena as therapeutic coating. Moreover, the clinical application of the internal remineralization concept is extensively useful in pediatric clinics for management of early childhood rampant caries [38, 52, 56-58].

### *2.2.3. Biofilms, the environment and interfaces*

In 2002, Donlan and Costerton defined a biofilm as “a microbially derived sessile community characterized by cells that are irreversibly attached to a substratum or interface or to each other, are embedded in a matrix of extracellular polymeric substances that they have produced, and exhibit an altered phenotype with respect to growth rate and gene transcription.” [59].

Indeed, microorganisms accumulate within an extracellular polysaccharide matrix (EPS) to optimize, for example, the use of available nutritional resources [60]. The physiology of bacteria growing in biofilms is completely different from that of planktonic (i.e. freely suspended) bacteria, in a way that biofilm organisms confers especially favorable properties including resistance to antimicrobial agents [61]. Biofilm-related infections on medical devices and the high-level drug tolerance of bacteria living in such biofilm-associated state provide a starting point for the onset of chronic infections in humans. This has boosted the development of effective strategies to control or prevent biofilm-associated infections, which requires a thorough understanding of the biofilm development process [62].

Biofilm formation is a developmental process comprising of different stages including reversible adhesion, irreversible attachment possibly spreading, proliferation, maturation and dispersion (Fig. 2.5) [60, 63-65]. Firstly, bacterial motility associated to flagella or fluid stream deliver planktonic bacteria to solid surfaces. Extracellular organelles, such as flagella, curli, fimbriae (or pili), and outer membrane proteins, help bacteria to interact with surfaces [66]. In this first stage of biofilm formation, such

interactions depend on properties of both bacterial cells and the substrate surfaces (e.g., charge, hydrophobicity, and stiffness) [67, 68]. After this initial adhesion, attached cells start to produce extracellular polymeric substance (EPS), which may promote the transition of bacterial adhesion from reversible to irreversible attachment. In general, this transition varies depending on strain and physico-chemical interactions of outer membrane molecules with surface [69]. Secretion of EPS is stimulated by cell-to-cell communication, typically known as quorum-sensing system (QS), which regulates a variety of other cellular functions, such as motility and production of secondary metabolites [70]. As cells replicate and EPS accumulates, biofilm maturation takes place with microcolonies growing into three-dimensional (3D) structures. The next step in some mature biofilms, known as dispersion, is cells detachment and reattachment to surface in new environmental niches [65, 69].

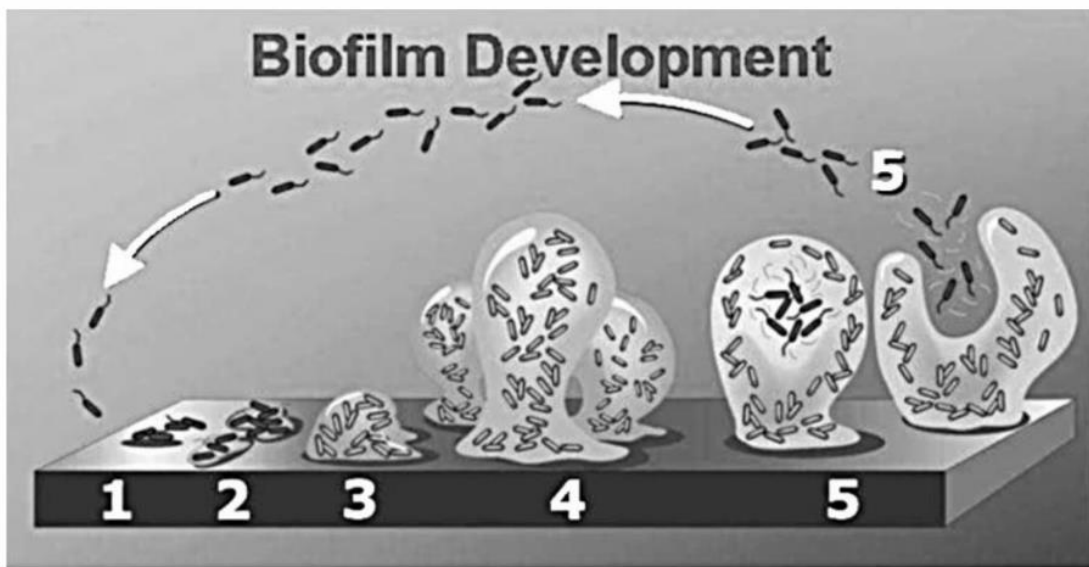


**Figure 2.5** Diagram showing the development of a biofilm as a five-stage process. Stage 1: initial attachment of cells to the surface. Stage 2: production of EPS resulting in more firmly adhered “irreversible attachment. Stage 3: early development of biofilm architecture. Stage 4: maturation of biofilm architecture. Stage 5: dispersion of single cells from the biofilm [65].

#### 2.2.4. Oral biofilms and ecological succession

Human oral microbiota, one of the most diverse human colonizing biofilms, is the habitat of around 700 individual taxa, in which 100 to 200 different species belong in the healthy mouth of any individual [65]. Half a century of traditional bacteriological investigation made oral microbial communities one of the best-described human microbial systems due to its accessibility. It is nowadays possible to identify novel microorganisms responsible for oral diseases [71]. However, analyzes of biofilm composition from diseased sites are difficult to interpret because biofilm-mediated diseases occur at sites with pre-existing resident microflora, in contrast to classical medical infections in which one single pathogen may be isolated from an infected site that is (a) normally sterile or (b) not usually colonized by that organism [72].

Establishment of oral biofilm architecture and microbial community interaction follows an ordered sequence of events that results in a well-organized and distinct architecture [71, 73]. For tooth surfaces, *acquired pellicle* formation is the preconditioning stage that defines the reversible–irreversible attachment of the colonizing bacteria [74]. If the environment provides essential nutrients and favorable conditions, early colonizers starts to divide. As soon as proliferation occurs and new species are recruited (late colonizers), local environmental conditions are modified by the presence of the sessile bacterial population, favouring additional diversity by making the site suitable for colonization by more fastidious species. These later colonizers bind to the already attached species via adhesin-receptor mechanisms (a process termed co-aggregation or coadhesion) [75, 76]. The first stage is dominated by Gram-positive cocci, especially streptococcal

species, while second and third stages respectively allows cross-linking via fusobacterium species, and predominant colonization by Gram-negative organisms (Fig. 2.6)[72].

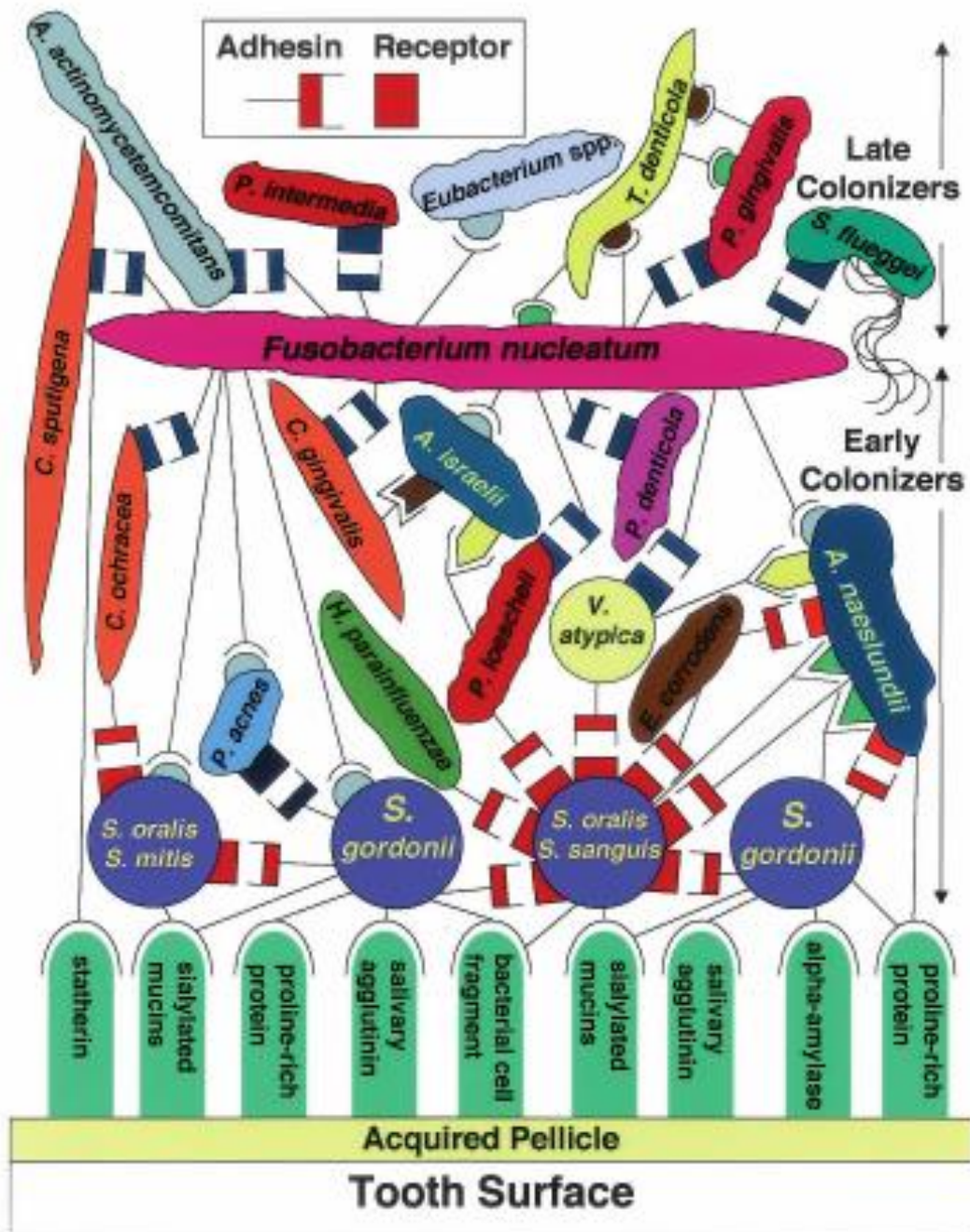


**Figure 2.6** Spatiotemporal model of oral bacterial colonization, showing recognition of salivary pellicle receptors by early colonizing bacteria and coaggregations between early colonizers, fusobacteria, and late colonizers of the tooth surface [75].

Once established, the composition of resident microflora remains stable over time. This stability, termed microbial homeostasis, stems not from low metabolism of the resident microflora but reflects a highly dynamic state in which the proportions of individual species are in balance due to the many interactions, both synergistic and antagonistic [72, 77]. Marsh proposed the ecological plaque hypothesis: a change in a key environmental factor (or factors) triggers a shift in the equilibrium of resident plaque microflora to disease-associated species composition [77].

In agreement with this hypothesis, some environmental conditions, including exposure to high-sugar-content foods and tobacco smoke, promote changes in biofilms, then favoring development of pathogenic dental plaque. Depending on the characteristics of diet as well as acidogenicity and aciduricity (acid tolerance) of the commensal oral bacteria, some factors lead to ecological shifts in the composition of plaque bacterial community and subsequently increase the risk of caries. Inefficient and insufficient oral hygiene practices, aging processes, genetic factors, and immune changes in the host also can generate conditions that encourage plaque microbiota to a disease-associated state [72, 74].

According to Loesche's 'specific plaque hypothesis', [78] *Streptococcus mutans* and *Streptococcus sobrinus* are important bacteria in the initiation of enamel demineralisation, while *Lactobacillus casei* is assumed to have greater importance after initial progression of the carious lesion. Nevertheless, such studies have shown that caries is associated with increases in proportions of acidogenic and aciduric bacteria, especially but not strictly

mutans streptococci (such as *Streptococcus mutans* and *Streptococcus sobrinus*) and lactobacilli, which demineralize enamel [72, 78].

It is now widely accepted that microbial etiology in relation to caries disease needs to be considered in terms of their activity rather than simply the specific name of species. Acid production (acidogenicity), acid tolerance (aciduricity), and extracellular and intracellular polysaccharide production are associated with cariogenic bacteria. Although other bacteria also display such activities to varying degrees, cariogenic traits are optimally expressed by mutans streptococci [38, 76, 79, 80]. Thus, the development of novel technologies in dissecting the physiology of *S. mutans* have placed this bacteria in an interesting position to further advance basic microbiology research, as a new Gram-positive model organism [81].

#### 2.2.5. Development of antibacterial dental materials

Dental materials have been found to accumulate more dental biofilm, when compared with enamel surfaces. There is strong evidence that biofilm formation contributes to the chemical and mechanical degradation of resin composites, i.e., the lack of inhibitory effect against cariogenic bacteria such as *Streptococci mutans*. Furthermore, adhered bacteria infect the neighboring soft and hard tissues, including the enamel, dentin and gingiva. Consequently, recurrent caries evolve around these restorations that, as a matter of course, are treated by restoration replacement, resulting in additional hard tissue loss. Therefore, one of the strategies to elongate the survival time of dental resin composites has been focused on antimicrobial treatment [82].

New paradigms on caries etiology have been focusing on ecological factors and multiple bacterial species, rather than just on the traditional caries pathogens. In 2009, ten Cate [3] have urged the necessity for antibacterial approaches to improve caries control, since effective antimicrobial therapies would broaden the arsenal of caries-preventive products, and make prevention less dependent on fluoride. The mechanism of this fluoride-antimicrobial approach may be effective due to the fact that fluoride affects the critical pH (at which dissolution starts to occur) and antimicrobials affect the depth of the Stephan curve [83]. Figure 2.7 represents the pH response of dental plaque following the consumption of fermentable carbohydrates (panel A), how this is affected by the use of fluoride (panel B) or by fluoride plus antimicrobial treatments (panel C). Therefore, reducing the amount and virulence of dental plaque could work synergistically with fluoride therapies. Also, findings on the development of biofilms and their reduction might be applicable to the development of oral biofilm remedies [3].

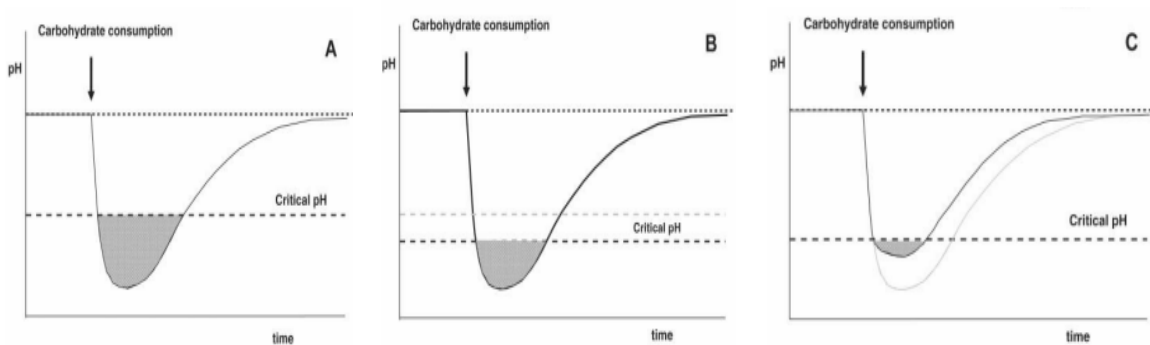


**Figure 2.7** Stephan curve. Schematic drawing of the pH of dental plaque following the consumption of fermentable carbohydrates (panel A). Panels B and C illustrate how the pH profile and critical pH are affected by the use of fluoride (panel B) or the combination of fluoride and antimicrobials (panel C) [3].

An antibacterial component may be incorporated to composite materials through modifications made to the filler particles or the resin matrix. These strategies can be divided into two groups: a released soluble antimicrobial agent, or a stationary non-released antibacterial agent [82].

Generally, dental composites consist of 70–90% (w/w) glass filler. Various modifications of the filler components have been reported to achieve antibacterial resin composites using soluble agents: strontium fluoride ( $\text{SrF}_2$ ) and ytterbium trifluoride ( $\text{YbF}_3$ ) [84, 85], silver ions [86], Ag–silica glass [87] and zinc oxide ( $\text{ZnO}$ ) [88].

Although a soluble agent may be gradually discharged from the bulk of the material over time, the agent's release has several disadvantages: an adverse influence on the mechanical properties of resin-based materials, the release of the agent possibly generating a porous structure, time-limited efficacy, and possible toxicity to the adjacent tissues given that the rate of diffusion can be difficult to monitor. The ability of the restorative dental material to withstand functional forces is an important requirement for their long-term clinical performance. To be clinically acceptable, modified materials must provide superior antimicrobial activity without compromising the mechanical properties. Soluble antibacterial agents that have been introduced are of low molecular weight, such as antibiotics, fluoride, chlorhexidine, silver ions, iodine and quaternary ammonium compounds [82, 89-91].

Non-released antibacterial agents were used to modify the filler particles in resin-based materials and to produce an antibacterial effect as well. For example, Yoshida *et al.* [92] report that an experimental resin composite containing silver-supported antibacterial

material (SSAM) into SiO<sub>2</sub> fillers inhibit the growth of *S. mutans*. Composites incorporating SSAM at 5 wt % or more of Novaron (N-5) and 7 wt % or more of Amenitop (AM-7) inhibited the growth of *S. mutans* after immersion in water for 6 months. There was no or extremely little release of silver ions from the N-5 and AM-7 composites after 1 day or after 6 months of immersion in water. According to the authors the antibacterial effect is achieved through direct contact of the bacteria with the silver-composites. However, it remained unclear whether the activity of resin composites incorporating SSAM used in this study can be attributed to the catalytic action of silver at the surface of the resin composite or to an anti-adhesion property of the surface.

An additional contact inhibition bactericide-immobilized filler contains 12-methacryloyloxydodecylpyridinium bromide (MDPB). The MDPB component, which maintains favorable mechanical properties in resin composites after aging, is more advantageous than agent releasing composites. Furthermore, MDPB is more preferable than immobilized silver agents regarding color stability, an important property for esthetic restorative materials [93].

However, matrix modification can be achieved by the addition of non-released antibacterial agents more readily than by filler modification. Non-released insoluble antibacterial agents can inactivate target microorganisms by contact without being released from the carrier material. This mechanism is based on immobilized bactericides, which have the advantage of being nonvolatile and chemically stable [82].

Antimicrobial approaches should ideally prevent plaque biofilm formation without affecting the biological equilibrium within the oral cavity. Use of nanotechnology offers the

possibility to control the formation of these and other oral biofilms through the use of nanoparticles with biocidal, anti-adhesive and delivery capabilities. When particles are reduced to nanometer size, the resultant properties such as hardness, active surface area, chemical reactivity, and biological activity are all altered [89, 94].

Since the bacterial cell surface is normally negatively charged, a structure-activity relationship analysis has revealed that antibacterial surfaces have to be hydrophobic (but not excessively so) and/or positively charged [95].

Metal and other nanoparticles have been combined with polymer or coated onto surfaces, which may have a variety of potential antimicrobial application within the oral cavity [96]. Zinc oxide (ZnO) nanoparticles have undergone testing using biofilm culture test systems. ZnO nanoparticles blended into a variety of resin-based dental composites were shown to significantly inhibit *S. sobrinus* biofilm growth at concentrations in excess of 10% (w/w) over a 3-day test period. However, the structural characteristics of such composites would need to be carefully assessed with a 10% ZnO loading [97].

Compared with free silver ions, reduced silver nanoparticles incorporated into a polymeric matrix provide a large reservoir of those ions that can be released in a more controlled manner at a steady rate, allowing for long-term antibacterial effects [98]. The direct incorporation of silver nanoparticles into a polymer matrix is a common strategy for preparing antibacterial resinous materials. However, silver nanoparticles are difficult to disperse, as nanosized particles tend to aggregate [99]. In 2011, a new technique for preparing dental polymers with evenly dispersed silver nanoparticles was described using coupling photo-initiated free radical polymerization of dimethacrylates with *in situ* silver

ion reduction. The experimental composites containing 0.08 % of silver nanoparticles exhibited a 30% reduction in bacterial coverage [4].

Ahn *et al.* demonstrated that incorporation of silver nanoparticles into bonding adhesives was successful on both physical and antimicrobial level. The experimental composite adhesives (ECAs) had rougher surfaces than conventional adhesives owing to the addition of silver nanoparticles, although bacterial adhesion to ECAs was shown to be less than that to conventional adhesives. As shown by the comparison of the effect of salivary pellicles on the adhesion, silver nanoparticles were capable of penetrating the saliva coating. The experimental material may be effective in preventing enamel demineralization around orthodontic brackets where most white spot lesions are present [100].

Studies from Cheng *et al.* [101, 102] characterized novel antibacterial dentin primers and adhesives (resin-based materials) containing quaternary ammonium dimethacrylate (QADM) and nanoparticles of silver (AgNP). Scotchbond Multi-Purpose bonding system (3M, St. Paul, MN), referred as “SBMP”, was used as base material for modification. According to the manufacturer SBMP etchant contains 37% phosphoric acid and SBMP primer contains 35–45% 2-hydroxyethylmethacrylate (HEMA), 10–20% copolymer of acrylic/itaconic acids, and 40–50% water. SBMP adhesive contains 60–70% BisGMA and 30–40% HEMA. The presence of those antibacterial agents proved not compromise the dentin shear bond strength of the material. Adding QADM or NAg markedly reduced the biofilm viability, compared to control, but both together had a much stronger antibacterial effect than using each agent alone ( $p$ -value < 0.05). Moreover, bonding agent with AgNP suppressed *gtfB*, *gtfC* and *gtfD* gene expressions of *S. mutans*

both on its surface and away from its surface. Also it did not adversely affect fibroblast cytotoxicity, compared to control ( $p$ -value < 0.01)[103].

If on one hand the research for anti-adhesive materials in resin-based restoratives has increased in the last 5 years, the development of aqueous cements with antibacterial activity receives little attention. The few attempts to modify glass ionomer cements was not directly addressed to water-based cements. Xie *et al.* [104] developed a newly synthesized poly (quaternary ammonium salt) (PQAS)-containing polyacid to formulate resin modified glass-ionomer cements (RMGIC) and study the effect of the PQAS on the compressive strength and antibacterial activity of the formed cements. The PQAS-containing cements showed a significant antibacterial activity, accompanying with an initial compressive strength reduction. The effects of the chain length, loading and grafting ratio of the QAS were significant. Increasing chain length, loading, grafting ratio significantly enhanced antibacterial activity but reduced the initial compressive strength.

In further study, Weng *et al.* [105] developed a polyacid constructed from a novel furanone derivative and formulated into experimental high strength cements (RMGIC). The results show that all the formulated furanone-containing cements showed antibacterial activity, with an initial reduction in compressive strength (CS). The effect of the furanone derivative loading showed antibacterial activity against both *S. mutans* and *Lactobacillus sp.* Increasing loading enhanced the antibacterial activity but reduced the initial CS of the formed cements. A 30-day aging study indicated that the cements may have long-lasting antibacterial activity.

### 2.2.6. Antibacterial activity of silver

By 1800, there was wide acceptance that wine, water, milk, and vinegar stayed pure for longer periods of time when stored in silver vessels. Privileged families used silver eating utensils and often developed a bluish-gray discoloration of the skin, thus becoming known as “blue bloods.” The prevalence of argyria prior to 1800 has not been documented, but it was reported to be associated with a reduced mortality rate during epidemics of plague and other infectious diseases. Silver nitrate also was used successfully to treat skin ulcers, compound fractures, and suppurating wounds. In the first half of the 20th century (until the introduction of antibiotics), silver was used in large extent as aqueous colloidal dispersion for oral consumption (also for the prevention of infection). Whereas such therapies generally were safe, it was shown that high doses of silver, when given parenterally, could cause convulsions or even death, and that oral administration of huge doses could cause gastrointestinal disturbances. The total dose of silver needed to cause argyria was approximately 0.9 g of metallic silver. In only 16 of the 239 cases where silver was given for medical indications had it been used for less than one year, and most of the patients with argyria had taken silver for a much longer time, as long as 20 years [106].

Studies have recently reported that macroscopic silver metal objects continuously release nanoparticles, a remarkable observation. Given this fact, it is important to notice that metallic silver is used in alloys, for example in dental alloys, that have been used for more than a century in dental practice [107].

As a noble metal ( $E^0 = + 0.80$  V), silver is not attacked by water or acids. However, silver metal continuously releases small amounts of ions, which act antibacterially at the

metal surface. As oxidizing agent, dissolved oxygen ( $O_2$ ) in particular comes into play ( $E^0 = + 1.23$  V), whereby the oxidation can be enhanced by complexation of the released silver ions by inorganic ions or organic molecules [108].

The bactericidal effect of silver ions (SI) on microorganisms is very well known; however, the bactericidal mechanism is only partially understood [89]. A silver cation is a soft Lewis acid that has an affinity to sulfur, but also to nitrogen. Studies have shown that the positive charge on the  $Ag^+$  ion is critical for antimicrobial activity, which allows the electrostatic attraction between the negative charge of the bacterial cell membrane and positively charged nanoparticles [109]. Thereby, it has many possibilities to disturb biochemical processes. Besides the formation of sparingly soluble silver salts ( $AgCl$ ,  $Ag_2S$ ), the adverse effect of silver ions is due to interactions with thiol and amino groups of proteins, with nucleic acids, and with cell membranes [108]. It has been proposed that ionic silver inactivates vital enzymes by strongly interacting with their thiol groups [110, 111]. It has been shown that the expression of ribosomal subunit proteins and other cellular proteins and enzymes necessary for ATP production becomes inactive [112]. Experimental evidence suggests DNA loses its replication ability once the bacteria have been treated with SI [113]. Still, structural changes in the cell membrane as well as the formation of small electron-dense granules formed by silver and sulfur were observed [113, 114].

Brett [115] conducted a literature review of six relevant and frequently discussed topics. Pre-clinical and clinical study data suggest that: a) bacterial resistance to silver may occur, b) silver dissociation is affected by the test medium used, c) bactericidal activity differences may be a function of the bacterial strain used for testing, d) higher rather than lower levels of silver may be needed because  $Ag^+$  binds to proteins and nucleic acids, e)

rapid delivery of silver (i.e., rate of kill) may be a positive factor when considering prevention of silver resistance and biofilm formation, and f) based on the vast majority of *in vivo* studies available, silver does not adversely effect mammalian viable cells; thus, is not cytotoxic. However, continued research into the implications of the data is warranted.

In biological environments, SI precipitate as silver chloride or form complexes with biomolecules. Silver nanoparticles will form a protein corona and change their properties, sometimes leading to agglomerates and precipitation. In this context, Teeguarden discussed the aspects of particle dosimetry *in vitro* [116].

The development of bacterial resistance against silver was extensively studied by Simon Silver [117]. Mechanistically, cells protect themselves by increasingly pumping out silver ions. The studies showed that the resistance against silver in *Salmonella* is coded by pMG101 plasmids, or more specifically plasmids with *sil* genes. Moreover, he also suggested that  $Ag^+$  resistance might exist widely but is not known in the absence of a ready means of testing [117-119]. Still, bacteria are far less likely to acquire resistance to metal nanoparticles than they are to other conventional and narrow-spectrum antibiotics. This is thought to occur because metals may act on a broad range of microbial targets, and many mutations would have to occur in order for the micro-organisms to resist their antimicrobial activity [120].

Silver ions have been demonstrated to be useful and effective in bactericidal applications, but the antimicrobial mechanism requires the continuous release of appropriate concentrations of silver ions. Moreover, silver ions might have only limited usefulness as an antimicrobial agent as they get inactivated easily upon reaction with

biofluids, such as saliva. For those reasons, the unique properties of nanoparticles, acting as reservoirs of ions, presents a reasonable alternative for development of new bactericides and more specifically anti-adhesive surfaces [121]. Allaker postulated that nanoparticles may be delivered in high concentrations in situations where antibacterial activity is needed, in contrast to general bactericidal applications, where the active typically gets bound to the EPS matrix of the biofilm or is otherwise de-activated [94].

With respect to metallic nanoparticles, the biocidal effectiveness has been suggested to be both due to their size and SI release (related to the high surface-to-volume ratio) [122]. At the nanoscale, Ag<sup>+</sup> ions are known to be released from the surface of base materials incorporating nanoparticles [122-124]. Sotiriou and Pratsinis proposed that the antimicrobial activity of small (<10 nm) nanosilver particles is dominated by Ag<sup>+</sup> ions, whilst for larger particles (>15 nm) the contributions of Ag<sup>+</sup> ions and particles to the antibacterial activity are comparable, with the Ag<sup>+</sup> ion release being proportional to the exposed nanosilver surface area [125]. It is suggested that a bacterial cell in contact with silver nanoparticles will take up Ag<sup>+</sup> ions, which possibly in turn will inhibit respiratory enzymes and so help to generate free radicals and subsequent free-radical-induced damage to the cell membrane. To determine the relationship between free radical formation and antimicrobial activity, the use of antioxidants does suggest that free radicals may be derived from the surface of silver nanoparticles [109].

Espinosa-Cristóbal *et al.* [126] evaluated three different sizes of AgNP (9.3, 21.3 and 98 nm) over adherence capacity of *S. mutans* on healthy human dental enamel (*ex vivo*). The results concluded that SI released from AgNP had adherence inhibition activity

as well as antimicrobial effect in *ex vivo* form. This anti-adherence property is associated with smaller particle size (9.3 and 21.3 nm), probably due to its potential of oxidation.

The use of medical devices containing silver must be undertaken with caution, since a concentration-dependent toxicity has been demonstrated. However, silver has been described as ‘oligodynamic’ due to its ability to exert bactericidal effect at very low concentrations. A systematic review pointed out the typical results of the action of silver on single-celled organisms. Although the results are not strictly comparable owing to different experimental conditions and different silver species, it can be concluded that the toxic concentrations and inhibitory concentrations are in the range of 0.1 to 20 mg. L<sup>-1</sup> [108]. However, there are studies with normalized amount of silver that analysed the effect of silver nanoparticle size on toxicity. It was indicated that smaller silver nanoparticles have a higher toxicity than larger silver nanoparticles or silver microparticles [127-130].

## **2.3. SILVER NANOPARTICLES**

### *2.3.1. Optical properties of AgNP*

The optical properties of small metal nanoparticles depend strongly upon the particle size and shape. These effects are due to the so-called localized surface plasmon resonance (LSPR), which is a coherent oscillation of the surface conduction electrons excited by electromagnetic (EM) radiation [131]. A schematic diagram is presented in Figure 2.9.

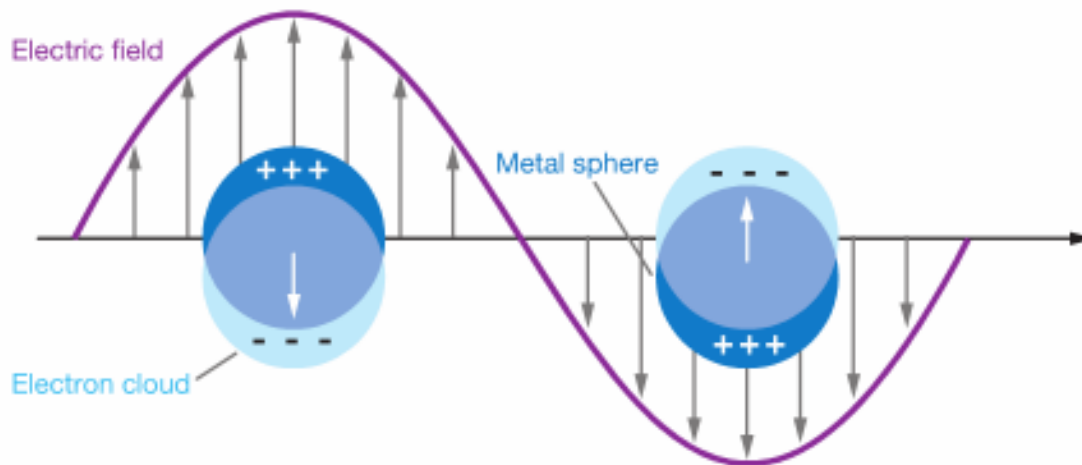


**Figure 2.9** Schematic diagram illustrating a localized surface plasmon resonance (LSPR)[131].

After EM excitation, the electrons are displaced from the equilibrium position, generating a dipole. If the field is later removed, they will oscillate with a certain frequency that is called plasmonic frequency. Although it is not possible to observe directly the electrons movement to determine their oscillating amplitude, this amplitude can be determined indirectly. The electronic oscillation implies an increase of kinetic and electrostatic energies associated to the electric fields of the dipole. As energy must be conserved, this increase of energy must be provided by the illuminating light. Therefore, light extinguishes partially when exciting surface plasmon (SP) inside the nanoparticle. The larger the electron oscillations, the larger the light extinction, so the optical absorption spectrum allows to detect the excitation of SP. The resonant frequency for these oscillations in metallic nanoparticles corresponds typically to UV-Vis light and consequently, the SP arise absorption bands in this region [132].

Besides surface plasmon, there are other possible electronic excitations in metallic NPs that may be analysed, for example, interband transitions. In the case of silver, both SP band and interband transition absorption edge are well resolved, as can be visualized in Figure 2.10. SP absorption is fairly larger than that of the interband transitions despite the fact that the absorbing centre is the same for both processes [132].

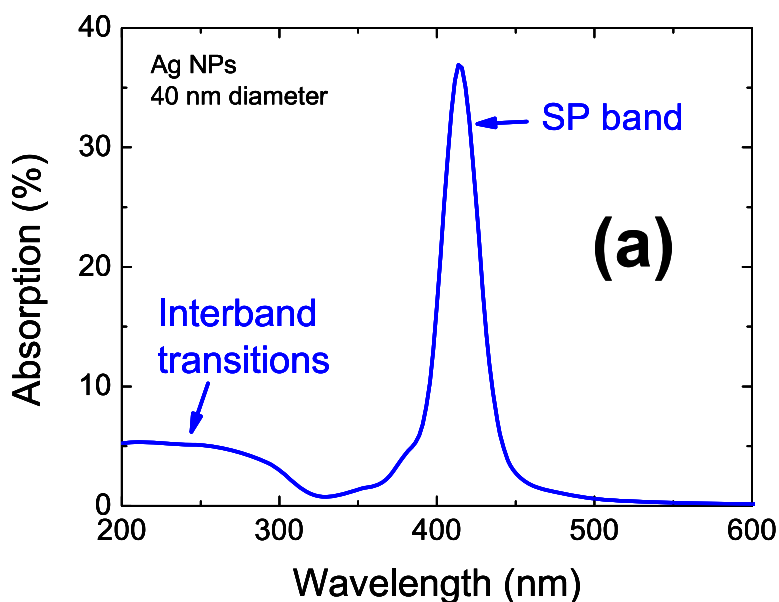


**Figure 2.10** Optical absorption spectra for AgNP with 40 nm size (embedded in a silica matrix)[132].

Only metals with free electrons (essentially Au, Ag, Cu, and the alkali metals) possess SP in the visible spectrum. The oscillation wavelength depends on a number of factors, among which particle size and shape, as well as the nature of the environment in which the metal particles are dispersed, are the most important. The refractive index of the

surrounding medium, as well as the average distance between neighboring metal nanoparticles, has been shown to influence the spectral features [131, 133, 134].

Aspects of SP properties can provide a clue of some characteristics of the nanoparticle population:

1. The predominant aspect will depend on the NP size range. As a general approach, for small size range ( $< 50$  nm), dependence of the SP affects mainly the width and the intensity of the resonance band. For size above 50 nm, the resonance band splits into several peaks: two peaks for quadrupole, three peaks for an octopole, etc.
2. Size dispersion induces a broadening of the absorption band. As Figure 2.11 illustrates, the larger the size dispersion, the wider the absorption band. Thus, it is not possible to determine the size of the NPs just from the FWHM of the absorption band, as it depends on two parameters: average size and size distribution width.
3. Interparticles interaction red-shift the resonance band increasing the FWHM, in general. The resulting spectra is composed by the intrinsic bands of the spherical nanoparticles and a new band, arising from interparticle plasmon coupling [132, 135].

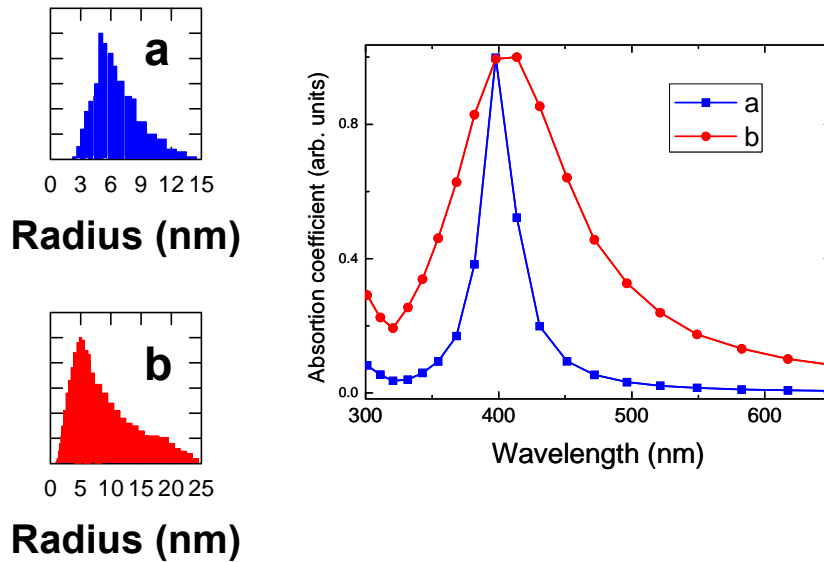


**Figure 2.11** (*left*) Size distributions and (*right*) optical absorption spectra for Ag NPs both with 10 nm average size but different size dispersion calculated according to the Mie theory and using  $n_m=1.5$  [132].

### 2.3.2. Synthesis of AgNP

Advances in the field of nanoscience and nanotechnology largely depend on the ability to synthesize nanoparticles of various different materials, sizes, and morphologies. Therefore, various approaches have been developed to control these parameters and, hence, meet the requirements for various applications. Though nanoparticles can be generated by physical approach (such as evaporation, arc discharge and laser ablation, etc.), chemical approach is one of the preferred methods for fabricating a wide variety of nanoparticles. Still, there are certain methodologies such as the preformed-seed-mediated growth approach, high-temperature polyol synthesis, template-based electrochemical synthesis,

photochemical techniques, etc., which are emerging as popular ways of developing anisometric nanoparticles [136].

Silver nanoparticles are prepared by the controlled reduction of silver salt solutions using appropriate reducing agents. These include strong chemical reducing agents such as sodium borohydride, weak reducing agents such as ascorbates, citrates, alcohol as well as polyols, by irradiation using gamma rays, ultra violet-visible (UV-Vis) rays, microwave as well as ultra sound [121, 137].

Generally, metal nanoparticles are formed from their ions in solutions through nucleation followed by growth. The nucleation process requires high activation energy where as the growth process is diffusion-controlled and requires low activation energy [138]. The size and distribution of the metal nanoparticles mainly depends on the relative rates of these two processes. In the case of AgNP, the relative rates of the nucleation and growth processes can be controlled by varying reaction parameters such as concentration of the reactants, potency of the reducing agent, pH and the reaction temperature [121].

The photo-induced synthetic strategies can be categorized into two distinct approaches, the photophysical and photochemical ones. The former prepares NP via the subdivision of bulk metals and the latter generates NPs from the zero-valent metal ( $M^0$ ) originated from molecular or ionic precursors. The essential of the photochemical approach is formation of  $M^0$  under the conditions that prevents their precipitation. Moreover, photochemical processes are classified in two methods: (a) direct electron transfer, which  $M^0$  is formed by the direct photoreduction of a metal source (metal salt or complex); (b) or by photosensitization, where reduction of metal ions takes place using the photochemically

generated intermediates, such as excited molecules and radicals. Those methods are illustrated in Figure 2.12 [139].

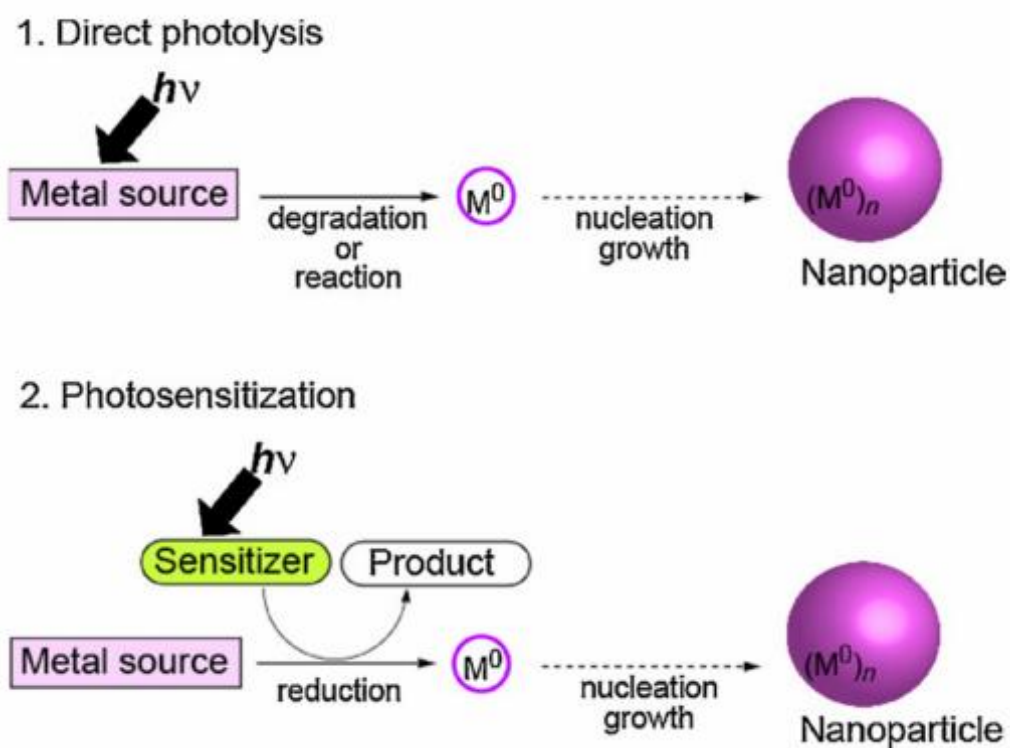


**Figure 2.12** Systematic scheme of photochemical synthesis of metal nanoparticles [139].

Under photochemical conditions, electron transfer becomes possible even when such a reaction is impossible in the ground state. In order to achieve exothermic electron transfer in the ground state, the energy of the highest occupied molecular orbital (HOMO) of the reductant must be superior to that of the lowest unoccupied molecular orbital (LUMO) of the oxidant. In the excited state, LUMO's (with respect to the ground state) are

occupied by one electron. Both frontier orbitals become singly occupied (SOMO). Electron transfer can occur from the higher SOMO of the excited donor molecule into the LUMO of the acceptor (a) or from the HOMO of the donor in its ground state to the lower SOMO of the excited acceptor molecule (b), which are represented in Figure 2.13. In the photoinduced electron transfer, the positive free enthalpy of the corresponding process in the ground state is compensated by the excitation energy [140, 141].

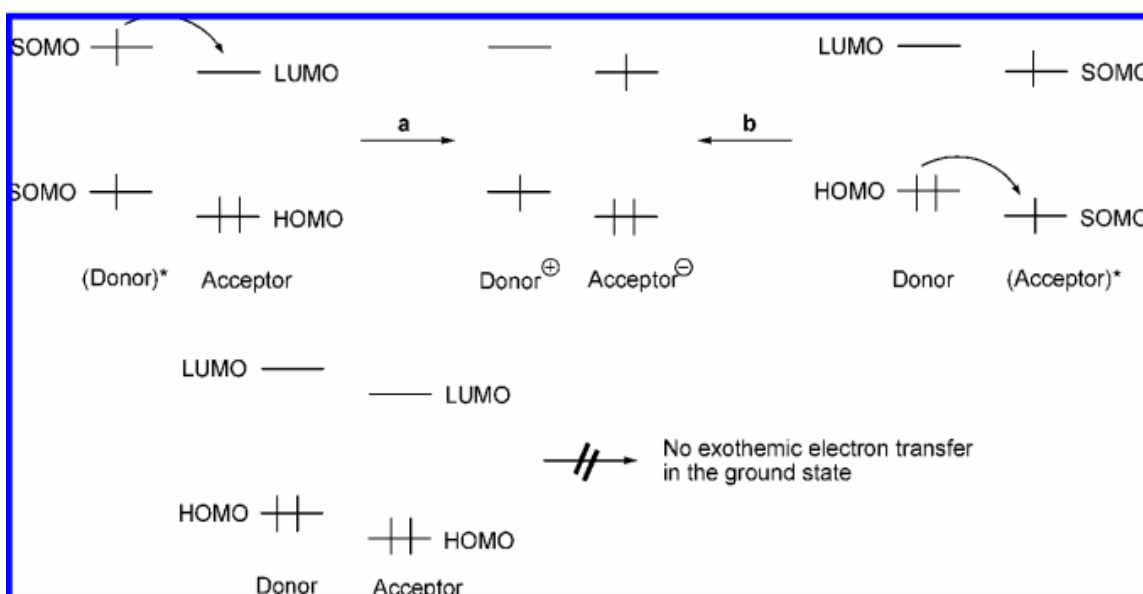


**Figure 2.13** Scheme of conditions for achieving electron transfer [140].

In photochemically sensitized reactions, light absorption not of the substrate but of the sensitizer leads to a chemical transformation. In the case of a photochemical electron transfer, the excited sensitizer can either abstract an electron or transfer an electron to one of the substrate molecules. The resulting radical ion of the substrate then undergoes

chemical transformations (e.g., deprotonation). In several of these reactions, the sensitizer is consumed and therefore used in large amounts. Currently, such processes are optimized in order to regenerate the sensitizer during the photochemical transformation. The sensitizing compound is then only needed in a catalytic amount and, in some cases, can be readily recovered after the reaction. Under these conditions, the sensitizer fulfills the criteria of a catalyst [140, 142].

The main advantages of the photochemical synthesis are as follows. (i) It provides the advantageous properties of the photoinduced processing, that is, clean process, high spatial resolution, and convenient useful, (ii) the controllable *in situ* generation of reducing agents; the formation of NP can be triggered by the photo irradiation, and (iii) it has great versatility; the photochemical synthesis enables one to fabricate NP in various mediums including emulsion, surfactant micelles, polymer films, glasses, cells, etc [139, 140].

The amount of energy conferred on a chemical system by using photons can be carefully controlled by the wavelength and intensity of the exciting light, in relation to the absorption spectrum of the targeted species. Such an energy can be transmitted to molecules without physically connecting them to the source (no 'wiring' is necessary), the only requirement being the transparency of the matrix at the excitation wavelength [143].

Aqueous solutions of silver nanoparticles are not stable due to the high reactivity of AgNP. In most of the preparation routes, irrespective of the reduction process the metal atoms coalesce into oligomers, clusters and eventually form precipitates upon storage [123, 144]. However, the precipitate formation can be significantly reduced if cluster stabilization is achieved using appropriate stabilizing agents [138, 145].

Essentially, nanoparticles stabilization is usually discussed in terms of two general categories of stabilization, electrostatic and steric. These include coating nanoparticles using thiol compounds, encapsulation of the particles in microemulsions, polymer assemblies or using dendritic structures [121]. The capping or protective agents not only protects the nanoparticles from precipitation but also play a critical role in the size, size distribution, morphology and the biocompatibility of the resulting silver nanoparticles. In certain cases the stabilizing agent itself acts as a reducing agent, resulting in a one step synthesis of AgNP [121].

Electrostatic stabilization is achieved by the coordination of anionic species, such as halides, carboxylates or polyoxoanions, to metal particles. This results in the formation of an electrical double layer (really a diffuse electrical multilayer), which causes coulombic repulsion between the nanoparticles. Steric stabilization is achieved by the presence of typically organic materials that, due to their bulk, impede the nanoparticles from diffusing together. Polymers and large cations such as alkylammonium are examples of steric stabilizers. The choice of stabilizer also allows one to tune the solubility of the nanoparticles [137, 146].

A wide range of polymers have also been investigated as stabilizing agents for silver nanoparticles. Poly(vinyl pyrrolidone) (PVP) is considered as one of the excellent polymeric stabilizing agents for AgNP. Apart from stabilization, PVP has an accelerating effect on the chemical reduction process during NP's formation. The mechanism of protection of AgNP by PVP is due to the coordinate bonds between nitrogen and silver to form the protection layer in the case of particles with diameter lower than 50 nm. Other

polymers investigated as stabilizing molecules for AgNP include polyacrylates, poly(vinyl alcohol) polyacrylonitrile and polyacrylamide [121].

Optical irradiation can provide a relatively easy, controlled reduction of metal salts. Photochemical reduction involves ultra-violet (UV) irradiation of the metal-precursor solution in the presence of an electron-donating reagent. UV irradiation has been successfully applied to develop shape-controlled synthesis of AgNP [136, 147, 148].

In 1990, Linnert *et al.* [149] described the best conditions for cluster formation in the reduction of silver ions. Radiation produces hydrated electrons in aqueous solutions, which are known to reduce silver ions:



It is also known that the atoms thus formed rapidly are complexed by  $Ag^+$  ions:



and that the  $Ag_2^+$  ions dimerize:



The absorption spectra of these species have also been observed (maxima at 360 nm ( $Ag^0$ ), 310 nm ( $Ag_2^+$ ), and 275 nm ( $Ag_4^{2+}$ )).

Silver clusters were reported to be formed as long-lived intermediates during the reduction of SI when the reduction is carried out in the presence of a polyanion. When the solution of clusters is illuminated with 308 nm light, where all the clusters have some

absorption, the cluster bands rapidly disappear and the PS absorption band of metallic silver appears. Light catalyses the conversion of small clusters into larger particles. The proposed mechanism contains the following elementary steps:



where  $(Ag)_n$  is the silver cluster containing  $n$  atoms of silver and  $e_{aq}^-$  is the electron in aqueous solutions [149].

Henglein *et al.* analysed the reactivity of the clusters towards nucleophilic reagents. They suggested that it is explained by the high coordinative unsaturation of the silver atoms in the clusters. This also explains the stabilization of the clusters by polyanionic polymers. Investigating the reactions of larger silver particles, which already have metallic properties, with complexing agents, also complemented these reactivity studies. The oxidative corrosion of such particles is strongly accelerated by the complexing agents. A mechanism for the catalysis of the oxidative corrosion was proposed, in which the main steps are the complexation of silver atoms on the surface with simultaneous electron transfer into the metal interior (“pre-complexation” or “pre-oxidation” of surface atoms) followed by capture of the electrons by oxygen [150].

Zhang *et al.* [151] prepared silver clusters and nanoparticles by reduction of silver nitrate by sodium borohydride in water, in the presence of polyacrylate ions, and in inverse

micellar solutions consisting of Laureth 4 and water. The formation of  $\text{Ag}_4^{2+}$  aggregates and  $\text{Ag}_9^+$  in the presence of polyacrylate ions was critically dependent on the manner in which reactants were combined. The procedure of adding aqueous sodium borohydride solution into the inverse micellar solution containing silver nitrate gave the most uniform spherical silver nanoparticles. The action kinetics of this procedure was investigated through UV-Vis spectra, which indicated that the generation of AgNP occurred in parallel with the disappearance of smaller clusters, and was characterized by a single exponential with a time constant of about 18 s, followed by aggregation into much larger particles. The formation of small silver clusters is found to be an extremely rapid process in aqueous solutions, in the presence of polyacrylate ion, and in microemulsion media. Following the initial burst of small clusters, the subsequent aggregation kinetics determines the size and distribution of final particles. Larger nanoparticles are stable for more than a month because of the protection of the surfactant molecules at the interface.

Mallick *et al.* [152] used methoxypolyethylene glycol (MPEG) to generate free radicals in the presence of UV radiation and acting as the reducing agent towards the silver ion. MPEG also served as a stabilizer of the silver particles formed. They described the mechanism as a two-step process, i.e., nucleation followed by successive growth of the particles, showed in Figure 2.14. In the first step, part of the metal ions in solution is reduced by a suitable reducing agent. The atoms thus produced act as nucleation centers and catalyze the reduction of the remaining metal ions present in the bulk solution. The atomic coalescence leads to the formation of metal clusters and can be controlled by ligands, surfactants or polymers.  $\text{OH}\cdot$  radicals can oxidize the ions or the atoms to the higher oxidation state and thus counter balance the reduction process. For this reason, the

solution generally contains a scavenger of OH· radicals. The preferred choice is solutes whose oxidation by OH· yields radicals that are unable to oxidize the metal ions but also have strong reducing properties.

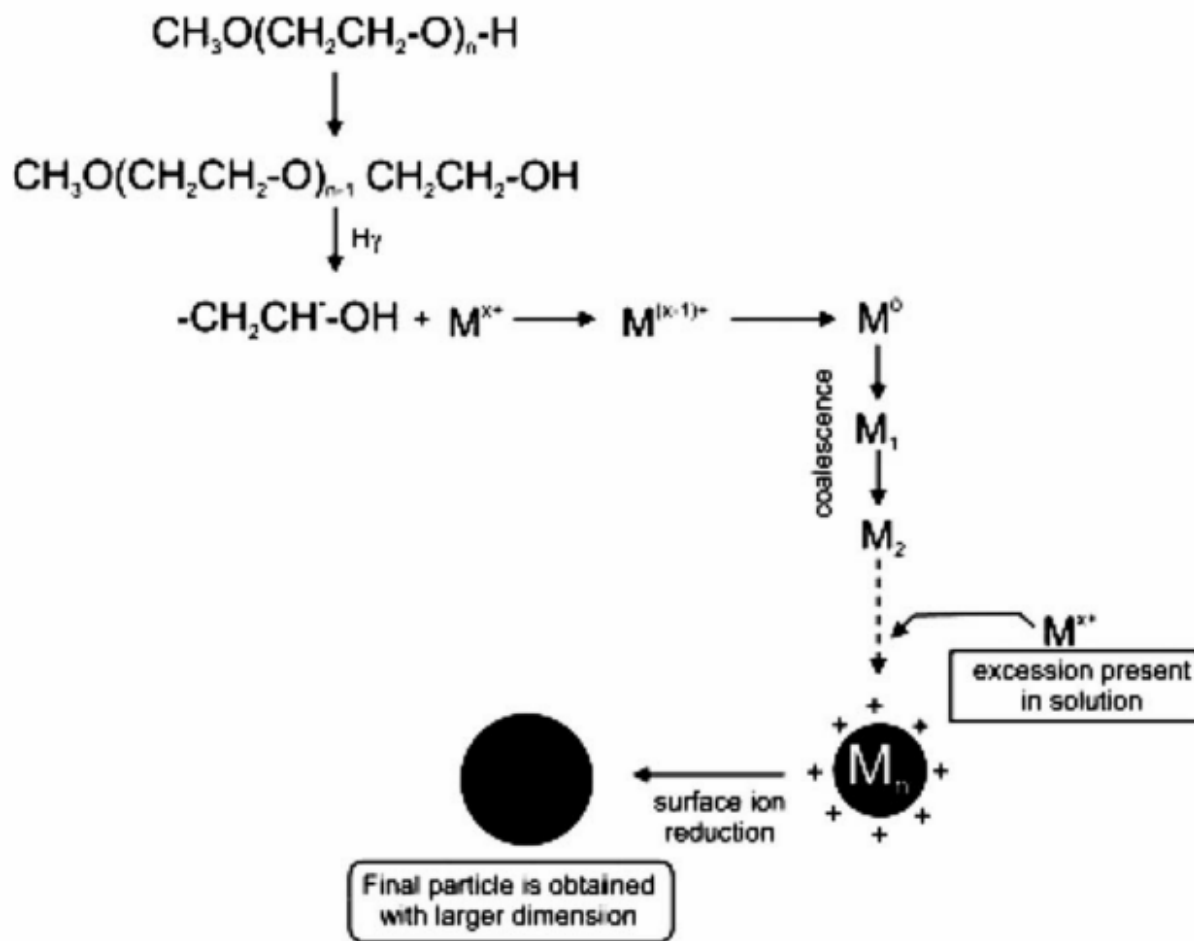


**Figure 2.14** Schematic representation for the nucleation and growth for the silver particles [152].

Hu *et al.* [153] described that the use of poly(acrylic acid) (PAA), in place of poly(vinyl pyrrolidone) (PVP) in the conventional polyol process, significantly limits the

growth of silver nanocrystals, prevents the interparticle aggregation and fusion, and leads to a uniform population of samples with high water solubility. The size of nanocrystals can be conveniently tuned by controlling the reaction time, the concentration and chain length of the polymeric surfactants, and the reaction temperature. The strong coordination of carboxylate groups to silver surface makes PAA an ideal surfactant for polyol process for the controlled synthesis of silver nanocrystals with sizes below 20 nm. An additional benefit of using PAA as surface ligand is that the uncoordinated carboxylate groups on the polymer chains provide the products excellent water solubility. Moreover, Zhang *et al.* [154] have also described that uncoordinated carboxylic groups from the PAA attribute to the nanoparticles a higher degree of dispersivity in water.

In 2008, Huang & Yang [155] developed a simple method for preparing silver nanoparticles via photoreduction of  $\text{AgNO}_3$  in layered laponite. The properties of silver nanoparticles were studied as a function of the UV irradiation time. A bimodal size distribution and relatively large silver nanoparticles were obtained when irradiated under UV for 3 h. Further irradiation disintegrated the silver nanoparticles into smaller size with a single mode distribution until a relatively stable size and size distribution were achieved. The synthesized laponite suspensions containing silver nanoparticles are stable over several months and have potential applications as antimicrobial ointments.

According to Balan *et al.* [156] three approaches have been developed for the preparation of nanocomposites. In the first and most common method, metal nanoparticles are mixed with or distributed in the matrix of a host polymer. However, due to the easy aggregation of the nanoparticles, it is difficult to disperse metal nanoparticles homogeneously into a polymer matrix by *ex situ* methods. In the second one, electronically

active polymers, generally PANI, are used to reduce the nanoparticles during the polymerization because of their ability to reduce noble metal salts into metal (0) nanoparticles. The latter and less commonly used approach requires the dispersion of the nanoparticles in the monomer. The polymerization is initiated in the presence of nanoparticles, which are simultaneously trapped in the polymer network.

The idea of *in situ* synthesis generating photopolymerizable metal-polymer nanocomposites have been described in the literature [156]. However, synthesizing and stabilizing AgNP *in situ* a polymeric aqueous solution that will further formulate composites polymerizable by chemical reaction have not been reported.

# III. Objectives

---

## 3.1. GENERAL

The main purpose of the present work was evaluating a new experimental glass ionomer cement containing silver nanoparticles (AgNP-GIC) with various silver contents.

## 3.2. SPECIFIC OBJECTIVES

- *In situ* synthesis of silver nanoparticles in the polymeric solution of glass ionomer cements;
- *In vitro* evaluation of mechanical, physico-chemical, antibacterial and toxicological properties of the AgNP-GIC to validate their applicability as water-based cements in dentistry practice.

# IV. Materials and Methods

---

## 4.1. GLASS IONOMER CEMENT COMPOSITION

The experimental GIC used in the present work is a composite constituted by agglutination of a polyelectrolyte matrix solution of poly (acrylic acid) (PAA) supplied by Sigma-Aldrich and an alumino-phospho-silicate ionomer glass powder (based on system  $\text{SiO}_2\text{-Al}_2\text{O}_3\text{-P}_2\text{O}_5\text{-CaO-CaF}_2$ ) produced in the Dental Physics Laboratory of the Queen Mary University of London (England).

The polyelectrolyte solution (ionomer liquid) used in all experiments was composed of a poly (acrylic acid) (PAA) ( $M_w \sim 100,000 \text{ g mol}^{-1}$ , 35 wt. % in  $\text{H}_2\text{O}$ ) and L-(+)- tartaric acid (TA) (99.5%) (Sigma-Aldrich). The former was selected taking into consideration the effect of concentration and average molecular weight of polymer solution on the viscosity and compressive strength values of GIC, as already evaluated by previous studies [157, 158]. Besides, TA (5 or 10 wt. %) was added to the 35 wt. % PAA aqueous solution under stirring at room temperature as chelating agent in order to control net setting reaction of GIC for clinical applications [2, 20].

## 4.2. SYNTHESIS OF SILVER NANOPARTICLES

A photochemical method by direct electron transfer was investigated in order to induce the formation of stable silver nanoparticles in a polyelectrolyte matrix solution of PAA and TA.

Silver nitrate ( $\text{AgNO}_3$ ) (99%) (Sigma-Aldrich) was added to the ionomer liquid formulation described above to configure silver polyacrylate solutions ( $[-\text{CH}_2-\text{CH}(\text{COOAg})-]_n$  or Ag-PA) containing increasing amount silver salt (0, 0.05, 0.10 or 0.50 wt. %) and tartaric acid (5 or 10 wt. %). These silver polyacrylate solutions containing tartaric acid (Ag-PA-TA) formulations were the basis for reduction to AgNP.

Ag-PA-TA solutions were submitted to direct UV-light exposure within a 10 cm distance from the source of light (254 nm, 2 x 30 W - Vilbert Lourmat). A quartz cell (1  $\mu\text{m}$ ) containing this formulation was gradually irradiated and monitored by UV-Vis spectroscopy (LAMBDA 750 UV/Vis/NIR Spectrophotometer, Perkin Elmer) under continuous UV irradiation in order to select the best configuration, based on intensity and full widths at half-maximum (FWHM) of the UV-Vis spectra band around 430 nm.

After different times of irradiation (0, 10, 30, 60 and 90 min) the laminated formulations were dried over a glass plate, and further analyzed by Attenuated Total Reflectance - Fourier transformed infrared spectroscopy (ATR-FTIR). The experiment was performed using a Perkin Elmer series 2000 FTIR spectrometer. With this technique the lower few microns of the sample in contact with the diamond is analysed. Resolution was set at  $8\text{ cm}^{-1}$  and wavelength range between  $800$  and  $4000\text{ cm}^{-1}$ .

After selection of the optimal parameters (time of irradiation and TA concentration) for each concentration of silver salt, syntheses were carried out in a vial ( $\varnothing$  20 mm) containing 3 mL of the formulation.

Colloidal stability was evaluated according to their visual aspect and followed by UV-Vis spectroscopy, since this characterization technique can provide information on whether nanoparticle populations are growing or aggregating over time.

Morphological analysis of AgNP was performed by transmission electron microscopy (TEM) (Philips CM200 instrument) with LaB6 cathode at accelerating voltage of 200 KV. AgNP containing solutions were directly dropped on 400 mesh Holey Carbon grids (Ted Pella Inc.). Size distribution of particle diameter was obtained using Image J image processing software [159].

### **4.3. PREPARATION OF THE IONOMER GLASS**

The experimental glass used in this study was comprised of silica ( $\text{SiO}_2$ ), alumina ( $\text{Al}_2\text{O}_3$ ), phosphorus pentoxide ( $\text{P}_2\text{O}_5$ ), calcium carbonate ( $\text{CaCO}_3$ ) and calcium fluoride ( $\text{CaF}_2$ ). The ratio for the glass composition is given in Table 4.1. This composition system was chosen based on previous chemical analyses by energy dispersive spectroscopy (EDS) of commercially available ionomer glasses, and the parameter of synthesis were previously studied [17, 160] at the Dental Physics Laboratory of the Queen Mary University of London (England).

**Table 4.1.** Ratio composition of the ionomer glass.

|               | SiO <sub>2</sub> | Al <sub>2</sub> O <sub>3</sub> | P <sub>2</sub> O <sub>5</sub> | CaO | CaF <sub>2</sub> |
|---------------|------------------|--------------------------------|-------------------------------|-----|------------------|
| Content ratio | 4.5              | 3                              | 1.25                          | 3   | 2                |

The glass was fired at 1440 °C for 1.5 hours. The crucible was removed from furnace and glass melt was quickly quenched into deionised water to produce glass frit. After drying, each 100 g of frit was ground in a Gyro mill (Glen Greston Wembley, London, UK) for two periods of 7 minutes. The resulting glass powder was passed through a 45 µm mesh sieve. The glass frit was further analysed by X-ray diffraction (XRD) to identify any phase separation.

#### **4.4. PREPARATION OF THE CEMENTS**

PAA-TA solutions containing synthesized silver nanoparticles (AgNP-PA-TA) were hand-mixed on a glass stab with the ionomer glass powder in a powder/liquid (P/L) ratio of 2.3 (w/w). Based on the amount of silver salt added in the polyelectrolyte formulations, AgNP-GIC samples were sorted in four groups: Without Ag (negative control); Low Ag (0.05 %); Medium Ag (0.10 %) and High Ag (0.50 %). Samples were freshly prepared for each of the following characterization assays.

## 4.5. CHARACTERIZATION OF THE GIC

### 4.5.1. Net Setting Time

Measurement of the net setting time were executed according to the *ISO 9917-1:2007* [161], for water based cements.

After the end of mixing, GIC samples were placed in a circular mould (10 mm x 2 mm). After pouring of the cement, this assembly - mould and cement specimen - was placed under the indenter of mass ( $400 \pm 5$ ) g, with a needle having a flat end of diameter ( $1.0 \pm 0.1$ ) mm. Sixty seconds after the beginning of mixing, the indenter was vertically loaded onto the surface of the cement and allowed to remain there for 5 s. The indentations were repeated at 30 s intervals. The net setting time was recorded as the time elapsed between the end of mixing and the time when the needle fails to make a complete circular indentation in the cement.

### 4.5.2. Compressive Strength (CS)

CS tests were carried out according to the *ISO 9917-1:2007* [161], for water based cements. AgNP-GIC groups (Without, Low, Medium and High Ag) were compared to Vitro Molar<sup>TM</sup> (Nova DFL, Rio de Janeiro, Brazil), as a reference of commercially available cement. Besides, in order to evaluate the effect of UV irradiation on mechanical properties of GIC, a formulation of PAA solution containing TA (5 wt. %) was irradiated with UV-light during 35 minutes without any silver salt added. The resulting solution was used to formulate the Without Ag I\* group.

Within 60 s after the end of mixing, specimens were packed to a slight excess in the PMMA mould with internal dimensions  $(6.0 \pm 0.1)$  mm high and  $(4.0 \pm 0.1)$  mm diameter. In order to consolidate the cement and avoid trapping air, after filling the mould to excess, polyester strips were placed on top, and then some pressure was applied on the bottom plate. One hour after the end of mixing, samples were removed from the moulds and immersed in milli-Q water at 37 °C.

Twenty four hours after incubation, the cylindrical specimens (n=8) of each group were slightly dried and placed with the flat ends between the plates of the mechanical tester and a compressive load along the long axis of the specimen was applied. A sheet of damp filter paper (e.g. Whatman N<sup>o</sup>. 1) was used in both top and bottom platens of the test machine to avoid contact with the specimens. The mechanical tester operated at a cross-head speed of  $(0.75 \pm 0.30)$  mm/min. The compressive strength,  $\sigma$ , in MPa of each specimen was determined using Eq. (1):

$$\sigma = \frac{4 F_f}{\pi d^2} \quad (1)$$

where  $F_f$  was the load at fracture (N) and  $d$  was the mean original specimen diameter (mm).

### *4.5.3. Analysis of the Silver Content*

GIC samples were ground into powder and submitted to Inductively Coupled Plasma - Optical Emission Spectrometry (ICP-OES), an analytical technique used for the detection of trace metals.

One hour after preparation, 3 samples of each group were immersed in deionized water and incubated for 24 h at 37 °C. Depending on having or not been previously incubated, samples were divided into “After-release” and “Pre-release”, respectively. 100 mg of the powdered GIC were diluted in 2.5 mL of aqueous solution of hydrochloric acid 20 % (v/v), shaken and allowed to stand for 16 h. After 10 min of centrifugation, 500 µL of clear solution was collected and further diluted in a 10 mL volumetric flask with 1.2 mL of aqueous solution of nitric acid 69 % (v/v). Flask volume was complemented with deionized water.

Analyzes were performed on a Perkin Elmer equipment, model Optima 2100DV, according to the operating conditions displayed on Table 4.2.

Silver standard for ICP-OES used in the curve was the Certified Reference Material (CRM) SPEX CertiPrep ASSURANCE<sup>®</sup> with certified concentration of 1001 mg L<sup>-1</sup>.

**Table 4.2** Operational conditions of the Optima 2100DV equipment from Perkin Elmer.

| Operational Conditions                         |                                    |                |              |            |            |            |            |                    |
|--|------------------------------------|----------------|--------------|------------|------------|------------|------------|--------------------|
| RF Power (W)                                   | <b>1300</b>                        |                |              |            |            |            |            |                    |
| Nebulizer gas flow rate (L min <sup>-1</sup> ) | <b>0.80</b>                        |                |              |            |            |            |            |                    |
| Plasma gas flow rate (L min <sup>-1</sup> )    | <b>15</b>                          |                |              |            |            |            |            |                    |
| Sample gas flow rate (L min <sup>-1</sup> )    | <b>1.50</b>                        |                |              |            |            |            |            |                    |
| Nebulizer                                      | <b>Concentric MEINHARD® Type C</b> |                |              |            |            |            |            |                    |
| Spray Chamber                                  | <b>Cyclonic (glass) MEINHARD®</b>  |                |              |            |            |            |            |                    |
| Element  | Wavelength (nm)                    | Plasma Viewing | Curve points |            |            |            |            | Units              |
|  |                                    |                | 00           | 01         | 02         | 03         | 04         |                    |
| <b>Ag</b>                                      | <b>328.068</b>                     | <b>Axial</b>   | <b>0.0</b>   | <b>0.1</b> | <b>0.5</b> | <b>1.0</b> | <b>3.0</b> | <b>mg/kg (ppm)</b> |

#### 4.5.4. Surface Chemical Composition

X-Ray Photoelectron Spectroscopy (XPS) investigated the chemical composition of the cement surfaces. Samples with increasing concentration of Ag were analysed by this method.

The XPS was measured with a VG Scienta FG30 spectrometer using a monochromatic Al K $\alpha$  source (1486.6 eV) - VG Scienta SAX100 (X-ray source) and XM780 (monochromator). The measurements were performed at normal incidence (the sample plane is perpendicular to the emission angle). The spectrometer resolution at the Fermi level is about 0.4 eV and the depth analyzed extends up to about 8 nm. All the peak shapes were limited to Gaussian ones. The peak assignments were referenced to the C1s aliphatic carbon set at 284.5 eV. A pass energy of 500 eV and a step size of 0.5 eV were

used for survey spectra. For high-energy resolution spectra, a pass energy of 100 eV and a step size of 0.1 eV were used. The size of the analysis area was  $0.4 \times 0.6 \text{ mm}^2$ .

#### **4.6. *IN VITRO* CYTOTOXICITY TEST (INDIRECT MTT ASSAY)**

MTT (3-(4,5-dimethylthiazol-2-yl)-2,5-diphenyltetrazolium bromide) is a colorimetric assay that measures the enzymatic reduction of MTT, a yellow tetrazole, to formazan. The viability of human gingival fibroblast cells (HGF-1) (ATCC<sup>®</sup> CRL-2014<sup>™</sup>) cells cultured in DMEM was determined using MTT (3--2,5-diphenyl-2H-tetrazolium-bromide; Sigma-Aldrich ref. M5655) indirect assay.

Disks (10 mm x 2 mm) of the Low, Medium and High AgNP-GIC samples, as well as of the negative control (Without Ag) were prepared under aseptic conditions. In order to prepare the extracts of AgNP-GIC, samples were incubated in Gibco<sup>®</sup> Dulbecco's Modified Eagle Medium (DMEM) without serum in a proportion of 0.1 g/mL for 24 h at 37°C. Because of alteration of the medium color to yellow, pH of the extracts were adjusted to 6.8 with NaOH (1M) and further passed through 45  $\mu\text{m}$  syringe filters for sterilization. In a 96-well plate, 2,000 cells/well were cultured for 24 h in DMEM medium with 10% of fetal bovine serum (FBS). Incubation of the cells using GIC extract (n=3) with DMEM medium as base with 10% of FBS was carried out for 24 h. Three different DMEM media without extract were used as negative control (NC): fresh DMEM, DMEM acidified with acetic acid (1 M) and adjusted to pH 6.8 using NaOH (1 M) and 24 h incubated DMEM; and several dilutions of phenol (1%, 10%, 15%, 25% and 50%) on DMEM as positive control (PC). FBS (10 v. %) were added to each well before incubation. MTT solution (0.5 mg/mL)

were added directly to the cells at 37°C in a humidified atmosphere containing 5% CO<sub>2</sub> for 3 h. After the complete withdrawal of MTT, 200 µl of acidic isopropanol (0.3% vol.) (Sigma-Aldrich W292907) was added to each well for 10 min. The optical density of the acidic isopropanol was read at 570 nm and 595 nm was used as reference wavelength for normalization on a microplate reader (ELX, 800UV, Biotec Instruments, INC).

#### **4.7. AGAR PLATE DIFFUSION TEST (*E. coli*)**

Susceptibility of *Escherichia coli* (*E.coli*) SCC1 strain [162], used as a model for Gram-negative bacteria, to the three diverse concentrations of silver ions released from Ag-GIC samples within the first 24 h of net setting reaction was analyzed by agar plate diffusion test.

Bacterial cultures were prepared by spreading bacteria with sterile loop from the stock solution (stored at -80°C) onto Petri dish containing agar-supplemented (15 g L<sup>-1</sup>) lysogeny broth (LB). After 24 h of incubation at 30°C, 1 to 3 colonies were inoculated in 10 mL of LB broth, resulting in a preculture that was further grown overnight (~ 16 h). A second preculture was prepared by inoculating 10 % (v/v) of the last preculture in fresh broth. After 4 h of incubation at 30 °C, bacterial suspension was adjusted to 10<sup>8</sup> cell mL<sup>-1</sup> and 100 µL was spread on agar-supplemented LB growth medium to form a thin bacterial film.

Disks (10 mm x 2 mm) of the Low, Medium and High AgNP-GIC samples, as well as of the negative control (Without Ag), were freshly prepared and sterilized by UV-light.

Samples were placed in contact with the previously inoculated agar plates, in triplicate. As positive controls, filter paper disks (10 mm of diameter) were also placed on the inoculated agar plates after dripping with 10 µL of 2 % vol. chlorhexidine digluconate (CHD). After 24 h of incubation at 30 °C, inhibition zones of bacterial growth potentially present around the samples were measured to evaluate the potential diffusion of silver ions from samples.

#### **4.8. SPECIFIC ANTIBACTERIAL ASSAYS (*S. mutans*)**

*Streptococcus mutans* Clarke 1924 strain (CIP 103220) isolated from carious dentine was used in order to understand the mechanisms of adhesion and biofilm formation on the surfaces of the AgNP-GIC. This strain is the most usual in literature to test antibacterial properties of dental materials.

##### *4.8.1. Bacterial adhesion and biofilm development*

Bacterial stock solution (stored at -80 °C) was scratched with sterile loop onto Petri dish containing Columbia agar base supplemented with 5% of defibrinated sheep blood, described here as Colombia Blood (CB) agar (enriched and selective medium). After 48 h of incubation at 37 °C, 3 to 5 colonies were inoculated in 5 mL of modified Basal Medium supplemented with mucine and glucose (MBMmg) broth, resulting in a preculture that was further grown overnight (~ 16 h). A second preculture was prepared by inoculating 10 % (v/v) of the last preculture in fresh broth. After 4 h of incubation, reaching the log phase at

37 °C, the inoculum was adjusted to  $10^7$  cell mL<sup>-1</sup>. Basal medium used in this protocol was based on Wong & Sissions [163] study and further description is detailed in Table 4.3.

Disks (10 mm x 2 mm) of material samples were freshly prepared, placed into small Petri dishes (ø 35 mm) and sterilized by UV irradiation for 15 min. Samples were further incubated in 3 mL of inoculum for 3 and 24h at 37 °C in order to analyze adhesion and biofilm formation, respectively. Samples were then carefully rinsed to eliminate non-adherent or loosely attached bacteria from substrate surfaces. For this purpose, 2 mL of incubated bacterial suspension were successively exchanged by NaCl solution (0.9 g L<sup>-1</sup>), kept for further bacterial concentration measurement and replaced by fresh NaCl solution (2 mL). The rinsing step was performed without direct flushing over material surfaces and by targeting with attention to force and content of the rinsing stream towards the walls of Petri dish. Material samples remained fully immersed in liquid during the rinsing steps, without creating any air-sample interface. Rinsing step was repeated until measurement of insignificant concentration of planktonic bacteria.

Material samples were kept from ambient light for 20 min in the last rinsing solution added by SYTO<sup>®</sup> 9 Green Fluorescent Nucleic Acid Stain (Life Technologies). They were then observed *in situ* by using an upright Confocal Laser Scanning Microscope (CLSM; Carl Zeiss, LSM700) equipped with a long working distance objective (LD EC Epiplan-Neofluar 50x/0.55 DIC M27; working distance of 9.1 mm). Three-dimensional images were taken of five different, randomly chosen locations on each sample. Image processing was performed using the ImageJ V.1.49b software with the LSM toolbox V4.0g plugin [159], allowing coverage area quantification of early adhered bacteria. Biofilm images were then analyzed with the COMSTAT2 software to quantify the biofilm

according to different parameters (Biomass, Mean Thickness, Roughness, Average Diffusion Distance and Surface to Volume Ratio)[164]. Confocal analyzes were conducted on AgNP-GIC samples, as well as on the bottom of a Petri dish (FB) as positive control. Two samples of each group were used for the experiment, which was repeated at least 3 times.

**Table 4.3.** Basal medium composition (Artificial Saliva)

| Modified Basal Medium supplemented with mucine and glucose (MBMmg), reagents per liter (L <sup>-1</sup> ): |        |
|--|--------|
| Partially purified pig gastric mucin* (type III)   | 2.5 g  |
| Glucose  | 2 g    |
| Proteose peptone   | 10 g   |
| Trypticase peptone   | 5 g    |
| Yeast extract  | 5 g    |
| Heamin   | 5 mg   |
| Menadione  | 1 mg   |
| Urea   | 1 mM   |
| L-Arginine   | 1 mM   |
| KCl  | 1.1 g  |
| CaCl <sub>2</sub>  | 110 mg |
| MgCl <sub>2</sub> .6 H <sub>2</sub> O  | 40 mg  |
| NaCl   | 0.6 g  |
| NH <sub>4</sub> Cl   | 0.1 g  |
| KH <sub>2</sub> PO <sub>4</sub>  | 0.5 g  |
| K <sub>2</sub> HPO <sub>4</sub> .3 H <sub>2</sub> O  | 0.7 g  |

\*Adjusted pH (7.0)

#### 4.8.2. MTT metabolic activity of *S. mutans*

Antibacterial tests described above were performed on AgNP-GIC shortly after synthesis. MTT assay was used as an accessory tool to evaluate differences in viability of 24 h biofilm between groups.

Following the same protocol as for biofilm growth of CLSM analyzes, groups of AgNP-GIC prepared with formulations after 7 days from AgNP synthesis were analyzed by this method. Disks containing 24 h biofilm grown on the surfaces were transferred to a 24-well plate, with 1 mL of MTT dye ( $0.5 \text{ mg mL}^{-1}$  in PBS) in each well and incubated at 37 °C. After 1 h, biofilm specimens were transferred to a new 24-well plate. Aliquot of 1 mL of dimethyl sulfoxide (DMSO) was added to solubilize the formazan crystals during incubation for 20 min in the dark. DMSO solution was transferred to a quartz cubet and the absorbance at 540 nm was measured [165].

### 4.8. STATISTICAL ANALYSES

Parametric analysis of variance techniques were used to quantify the results. Student's *t*-test was applied for statistical analysis and confidence intervals greater than 95 % ( $p$ -value  $< 0.05$ ) were considered to be significant.

# V. Results and Discussion

---

## 5.1. SYNTHESIS OF AgNP

Silver nanoparticles were synthesized by photochemically induced electron transfer from uncoordinated carboxylate groups of the polyelectrolyte to the  $\text{Ag}^+$  species [147]. Formulations of polyelectrolyte consisting of a silver polyacrylate ( $\text{Ag}^+$ -PA) solution were gradually converted into AgNP-PAA as irradiation progressed, and proportionally depending on the  $\text{Ag}^+/\text{COO}^-$  molar ratio.

Molecular structures of the polyelectrolyte formulations (PAA and PAA-TA aqueous solutions) were first analyzed by FTIR spectroscopy (Figure 5.1). The main vibrational bands related to carboxylic groups of the polyelectrolytes are at the range of 1800 to 800  $\text{cm}^{-1}$ : C=O stretch (1700  $\text{cm}^{-1}$ ), C-H scissor (1452  $\text{cm}^{-1}$ ), C-H bend (1412  $\text{cm}^{-1}$ ), C-O stretch (1235  $\text{cm}^{-1}$ ; 1128  $\text{cm}^{-1}$  e 1084  $\text{cm}^{-1}$ ). Figure 5.1 shows that absorption spectra of the PAA-TA solutions, differently from PAA, present peaks 1128 and 1084  $\text{cm}^{-1}$ , which are known to be typical interchain C-O stretch anhydride-like vibration bands [166, 167]. Also, these peaks seem to shift from 1109 and 1050  $\text{cm}^{-1}$  on PAA spectra, suggesting interaction of the PAA-TA composition.

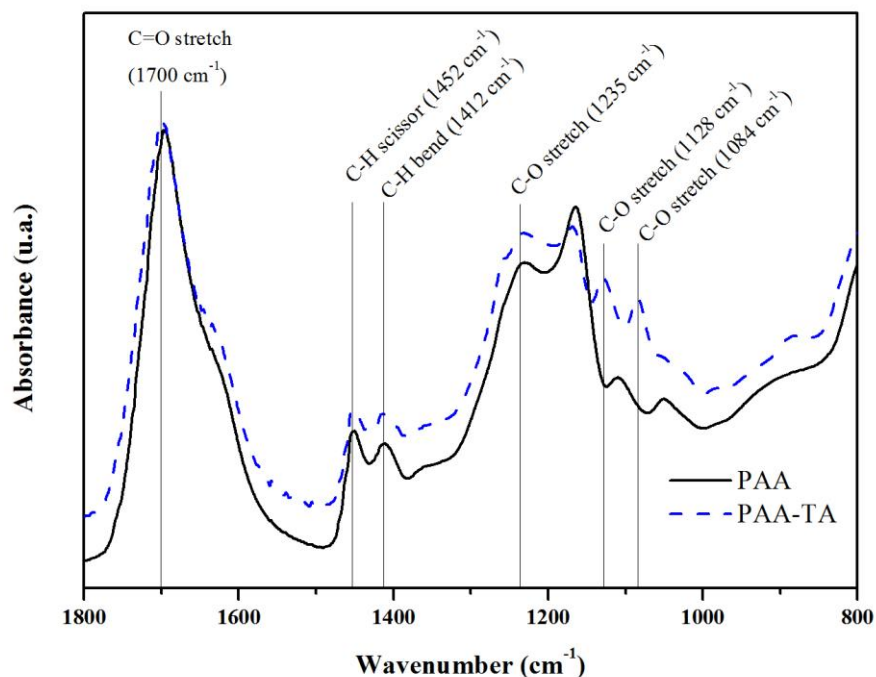


**Figure 5.1** Absorbance spectra of the polyelectrolyte formulations: PAA and PAA-TA (5 wt.%).

Formulations were submitted to UV-light irradiation with increasing exposure times in the presence of 0.1 wt. % of silver salt. As presented in Figure 5.2, analyses of PAA and Ag-PA after 0, 10, 30, 60 and 90 minutes of UV-light irradiation suggest that no significant modification occurs to the polymeric structure under such conditions. Despite the color of the solution have evolved from transparent to brownish (indicating the appearance of AgNP that will be further discussed in the next sections), FTIR absorption spectra showed that carboxylic groups from PAA are not significantly affected by UV-light, whether with or without silver added to the solution.

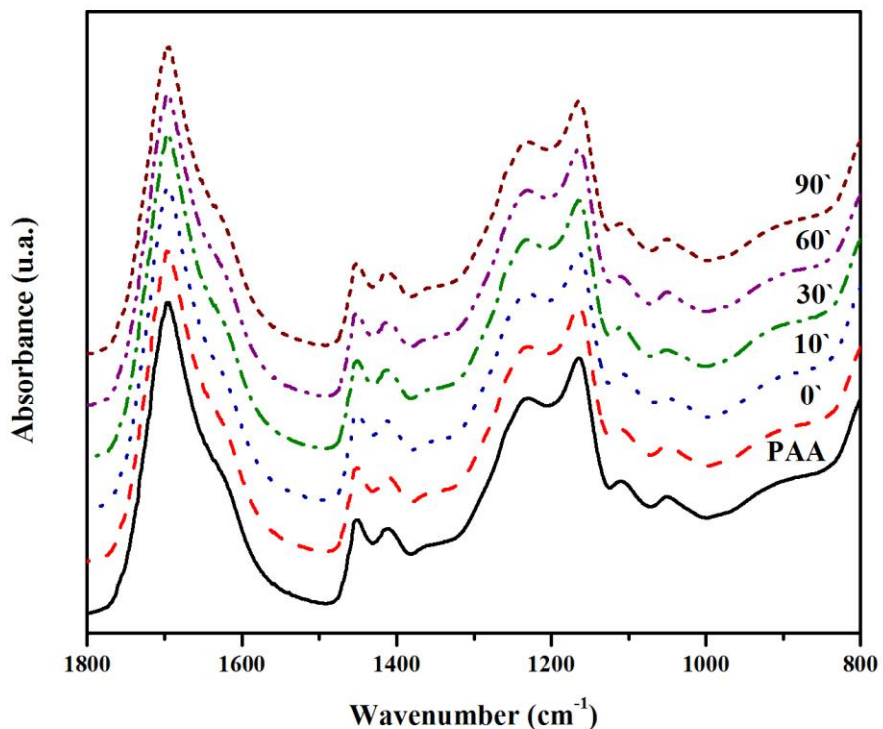


**Figure 5.2** FTIR spectra of the laminated PAA and Ag-PA after 0, 10, 30, 60 and 90 minutes of UV-light exposure.

Molecular structures of the polyelectrolyte formulations were affected by adding TA (5 wt. %) to the solutions. Figure 5.3 shows that peaks 1128 and 1084  $\text{cm}^{-1}$ , after 10 and 30 min of UV-light exposure, decreases as indicated in the chart by arrows. Possibly the absence of C-O stretching of anhydride-like vibration bands on the spectra of Ag-PA-TA is related to the process of AgNP synthesis, with C- O groups from TA molecules being involved in the process of stabilization of the NP. For this phenomenon to occur,  $\text{COO}^-$  is expected to form a layer of adsorbed TA molecules around AgNP. However, after 60 min of UV-light exposure, it was observed again a progressive increase of these vibration bands. This phenomenon may be attribute to two different reasons. Firstly, the kinetics of

AgNP generation, which occurs in parallel with the disappearance of smaller clusters, followed by aggregation into much larger particles [151]. Thus, as AgNP aggregates with the continuous UV irradiation, the amount of  $\text{COO}^-$  groups that are adsorbed to the surfaces of the NP progressively decreases, and becomes again free to form anhydride-like bonds.

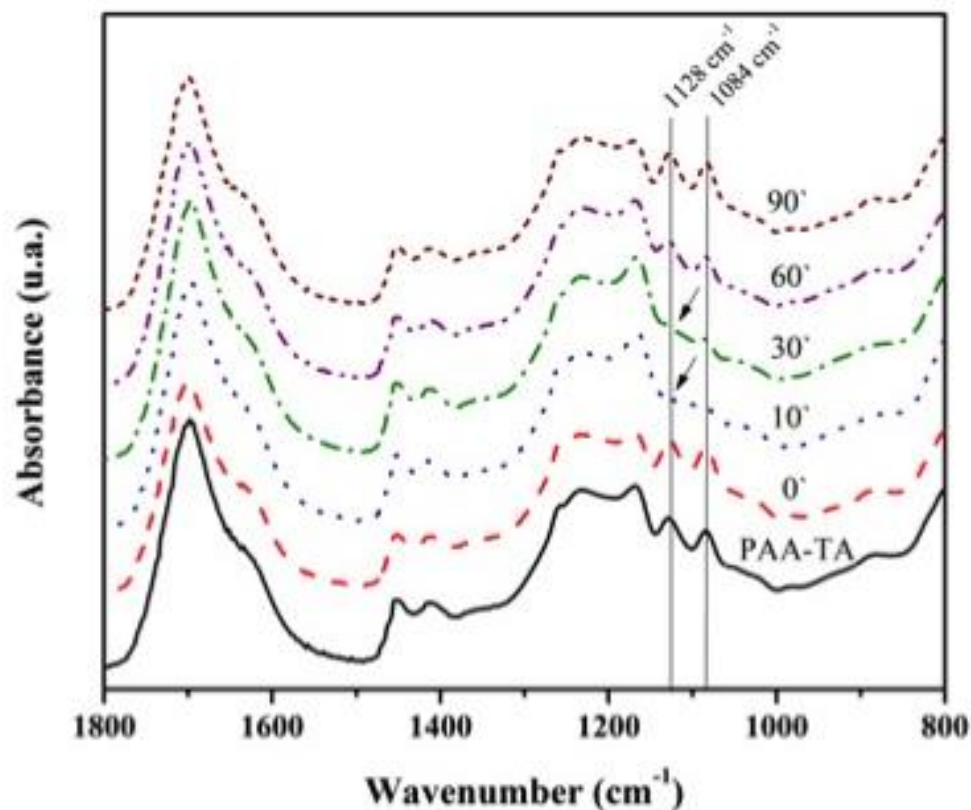


**Figure 5.3** FTIR spectra of PAA-TA and Ag-PAA-TA formulations after 0, 10, 30, 60, 90 minutes of UV-light exposure.

Henglein *et al.* [150] first showed the capability of PA- to stabilize intermediate  $\text{Ag}_n^{m+}$  clusters and described that electrosterically stabilized AgNP displays increased suspension stability in high ionic strength environments. This fact suggests that, under UV

irradiation, complexed carboxylic groups to  $\text{Ag}^+$  ions are gradually interacting to form AgNP.

Carboxylic groups from TA molecules are more likely to interact with silver ions than those from PAA. It can be explained by the fact that smaller molecules are expected to have higher functional reactivity than long chain polymeric molecules. Possibly because PAA have a coiled conformation inaccessible for steric reasons, i.e. with less access to  $\text{Ag}^+$  ions.

The second reason for the resurgence of anhydride bands may be considered if photo-degradation of polyacids in water is likely to occur. UV-irradiation of polyacids may cause cleavage of chemical bonds in main chains and in side groups. Evidence of occurrence of two opposite reactions in polyacrylic acids were already reported: abstraction (or destruction) of carboxylic groups and macro chain oxidation leading to the formation of a new type of carbonyl groups in the polymer [168]. Thus, cleavage of the polymer chains into smaller molecular structures may also contribute to an increased reactivity of the carboxylic groups. The photo-degradation of PAA was also examined in the presence of oxidizers. UV radiation was assumed to cause the decomposition of persulfate molecules into persulfate radicals, which generate the polymer radical. So in turn, PAA might be broken into much smaller species by the action of UV radiation [169].

Here, the proposed mechanism for AgNP synthesis is based on the one-electron transfer process proposed by Kéki *et al.* [147] to explain ionic silver undergoing photoreduction in the presence of carboxylate-terminated polymer (Figure 5.4).

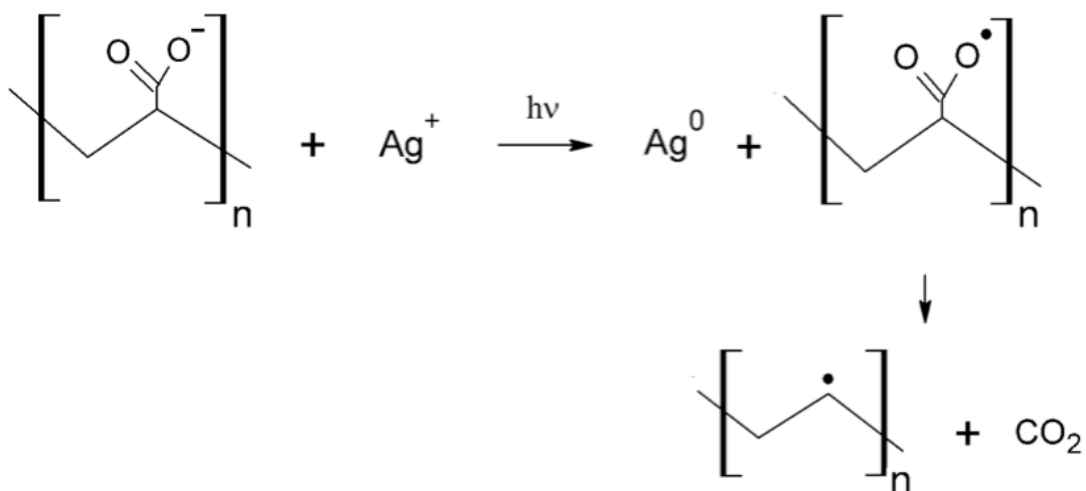


**Figure 5.4** Scheme of the photoreduction of Ag salt in the presence of PAA polyelectrolyte [147].

Therefore, considering free radical generation by UV irradiation in the presence of carboxylic groups, it becomes evident that photo-degradation of the PAA in such conditions is feasible. If generation of free radicals by irradiation of the polyelectrolytes exceeds the expected amount for nucleation of AgNP, the surplus of free radicals may degrade the polymer chains. Taking this fact into consideration, the phenomenon observed at the Figure 5.3 may be also influenced by degradation of the polymer chains.

#### 5.1.1. Synthesis by direct electron transfer method

*In situ* UV-Vis spectroscopy was used to follow up the kinetics of  $\text{Ag}^+$  photoreduction in PAA-TA formulation containing varying amounts of  $\text{AgNO}_3$  as a function of UV irradiation exposure time.

The optimal exposure times and TA concentrations to produce the set of formulations with the given  $\text{Ag}^+$  concentrations were determined by following this conversion kinetics. The intensity and FWHM of the Plasmon Surface (PS) absorption band of the AgNP-PA-TA solutions around 430 nm were used as the relevant criteria to optimize the parameters of synthesis. The formulations and parameters of synthesis of each group are gathered in Table 5.1.

**Table 5.1.** Formulations and parameters of synthesis of the AgNP-PAA-TA solutions.

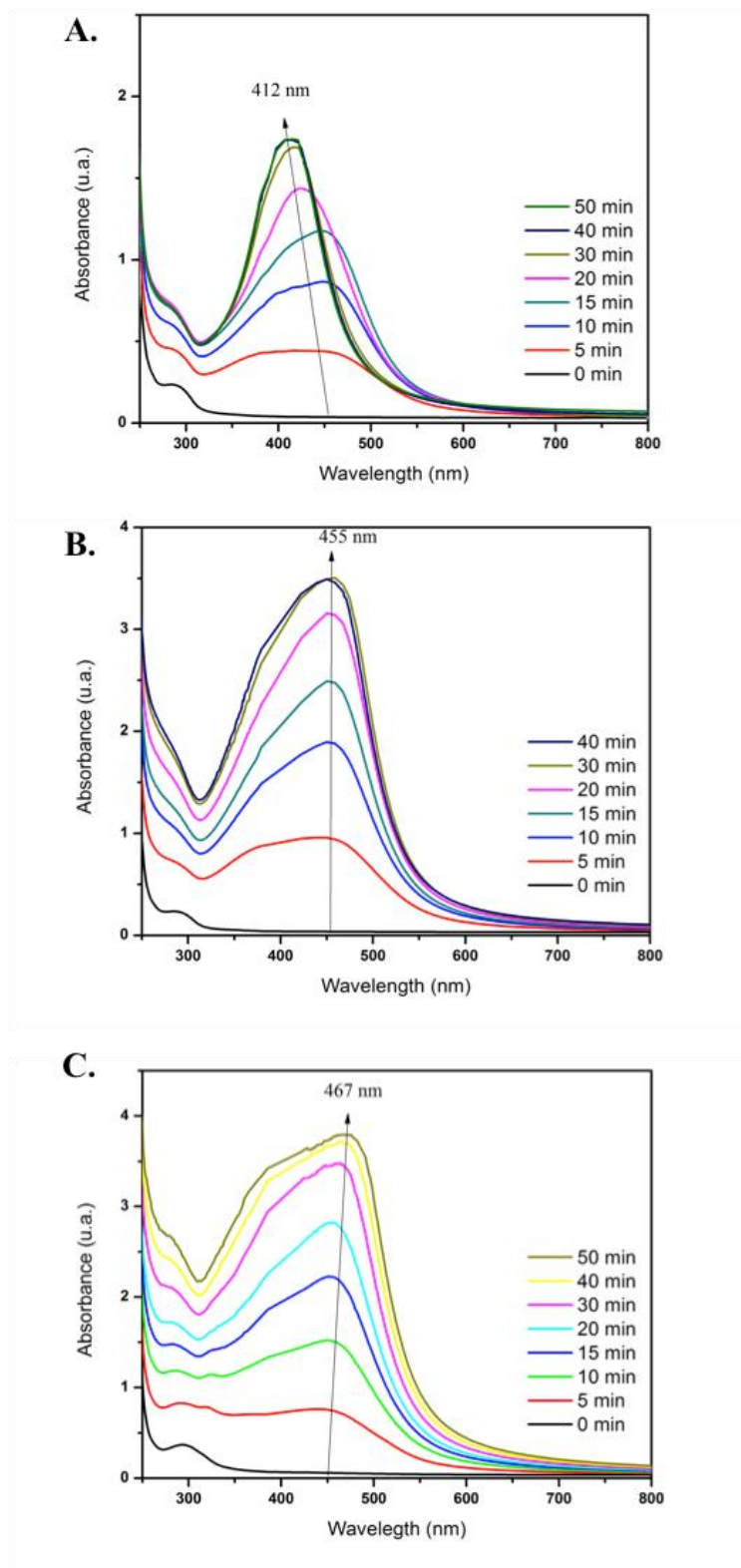
| <b>Formulation</b> | <b>AgNO<sub>3</sub><br/>concentration</b> | <b>TA<br/>concentration</b> | <b>AgNO<sub>3</sub>/TA<br/>molar</b> | <b>UV exposure<br/>time</b> |
|--------------------|---|-----------------------------|--------------------------------------|-----------------------------|
|                    | <b>(% wt.)</b>                            | <b>(% wt.)</b>              | <b>ratio (%)</b>                     | <b>(min)</b>                |
| <b>Without Ag</b>  | 0   | 5                           | 0                                    | 0                           |
| <b>Low Ag</b>      | 0.05                                      | 5                           | 0.009                                | 35                          |
| <b>Medium Ag</b>   | 0.10                                      | 10                          | 0.009                                | 35                          |
| <b>High Ag</b>     | 0.50                                      | 10                          | 0.044                                | 90                          |

Figure 5.5 present the kinetics of photoreduction in PAA formulation containing AgNO<sub>3</sub>/TA ratio (w/w): 0.05/5; 0.10/10 and 0.50/10. The absorption at 280 nm and around 430 nm were attributed to the presence of ions in solution, e.g. free  $\text{Ag}^+$  ions, or very small Ag clusters ( $\text{Ag}^0$  associated to ions), and spherical silver nanoparticles, respectively. The evolution of the PS absorption band in the region from 410 to 470 nm reflected the nano-sized character of the colloidal dispersion of metallic spheroidal silver particles produced by this method. An increase of the UV light-induced conversion was accompanied by cluster growth and formation of nanoparticles. The formation of a large number of small AgNP under continuous UV irradiation can lead to a change in the absorption band shape, represented by the decrease of the full widths at half-maximum (FWHM).

However, increasing concentration of  $\text{AgNO}_3$  red shifts the final PS absorbance bands in Figure 5.5 A, B and C (412, 455 and 467 nm, respectively). It is probably due to different size distributions of the AgNP population synthesized at each condition. Size dispersion induces a broadening of the absorption band, whereas growth and agglomeration of NP might red shift the PS band and increase the FWHM [132, 135]. As the percentage of PAA remains the same (35 wt. % in  $\text{H}_2\text{O}$ ) among the groups, one might assume it is due to the protective role of PAA that smaller NP are firstly induced at lower quantities of  $\text{AgNO}_3$ , as suggested by bands of Low Ag (Fig. 5.5A).

Absorption spectra of the four optimized formulations after 7 days from synthesis are reported in the Figure 5.6. Although the kinetics of irradiation depending on the initial formulation showed PS absorption bands ranging from 410 to 470 nm, when equilibrium of the colloidal system is achieved, nanoparticles tend to present absorption bands centered at 438 nm. Therefore, it can be assumed that the size and distribution of nanoparticles population are more likely to be dependent on the polyacid structures (average molecular weight and concentration) than directly depending on TA and  $\text{AgNO}_3$  concentration of the initial formulations.

The visual aspect of the synthesized AgNP-PAA-TA solutions with increasing  $\text{AgNO}_3$  concentrations shows that yellowish color intensity may be related to the concentration of AgNP. That would explain the reason PS bands increases in intensity.



**Figure 5.5** Kinetics of AgNP formation for PAA formulations: (A) Low Ag; (B) Medium Ag and (C) High Ag.

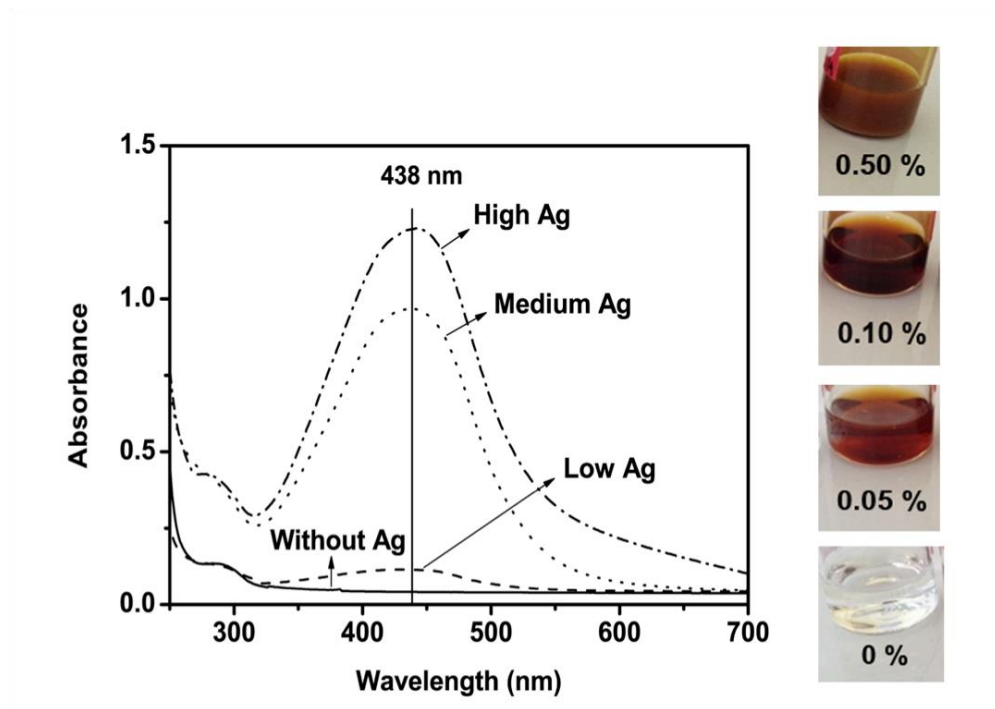


**Figure 5.6** Absorption spectra of synthesized solutions containing various  $\text{AgNO}_3$  concentrations and the visual aspect of the synthesized AgNP-PAA-TA solutions (wt. %).

It was observed sedimentation within 7 days after synthesis in the High Ag solutions, indicating agglomeration of nanoparticles probably because of saturation of the colloidal system. When high concentrations of silver salt are added to the current formulations, native particles tend to aggregate, and may introduce some instability into the system.

Shape and size distributions of AgNP measured by image analysis of the TEM micrographs are presented in Figure 5.7. AgNP exhibit size distributions centered around 5 to 6 nm, with an average diameter depending on the initial formulation ( $\text{Ag}^+/\text{COO}^-$  molar ratio) and UV exposure. High Ag presented tendency to form a bimodal distribution of the

AgNP population (centered at 6 and 11 nm). It also reflects the instability at this formulation because of the higher  $\text{Ag}^+/\text{COO}^-$  molar ratio.

Monitoring of the PS absorbance spectra and TEM images of the formulations over time confirmed the mechanism of colloidal stabilization of the solutions. Main differences on visual aspect and absorbance spectra occur at the first week (7 days from synthesis), when eventually solutions indicated colloidal stability. Absorbance spectra of the solutions after 180 days from synthesis show PS absorption bands with increased intensity, and centered around 420 nm (Figure 5.8).

Here, a phenomenon called Ostwald ripening (coarsening) can be assumed to occur observing the differences in the PS absorbance spectra of the analyzed AgNP systems over time. AgNP with radius larger or smaller than the critical radius grows or dissolves. Therefore, smaller particles with high energy disappear and lower energy regions of larger particles prevail. As a result of the material flux, the total free energy of the system decreases [170, 171].

This fact also matches with the hypothesis of agglomeration and sedimentation of the AgNP population that exceed the average size of colloidal stability. In other words, once PAA-TA system reaches the critical maximum  $\text{Ag}^+/\text{COO}^-$  molar ratio which it stands to stabilize, AgNP tend to agglomerate, grow and precipitate.

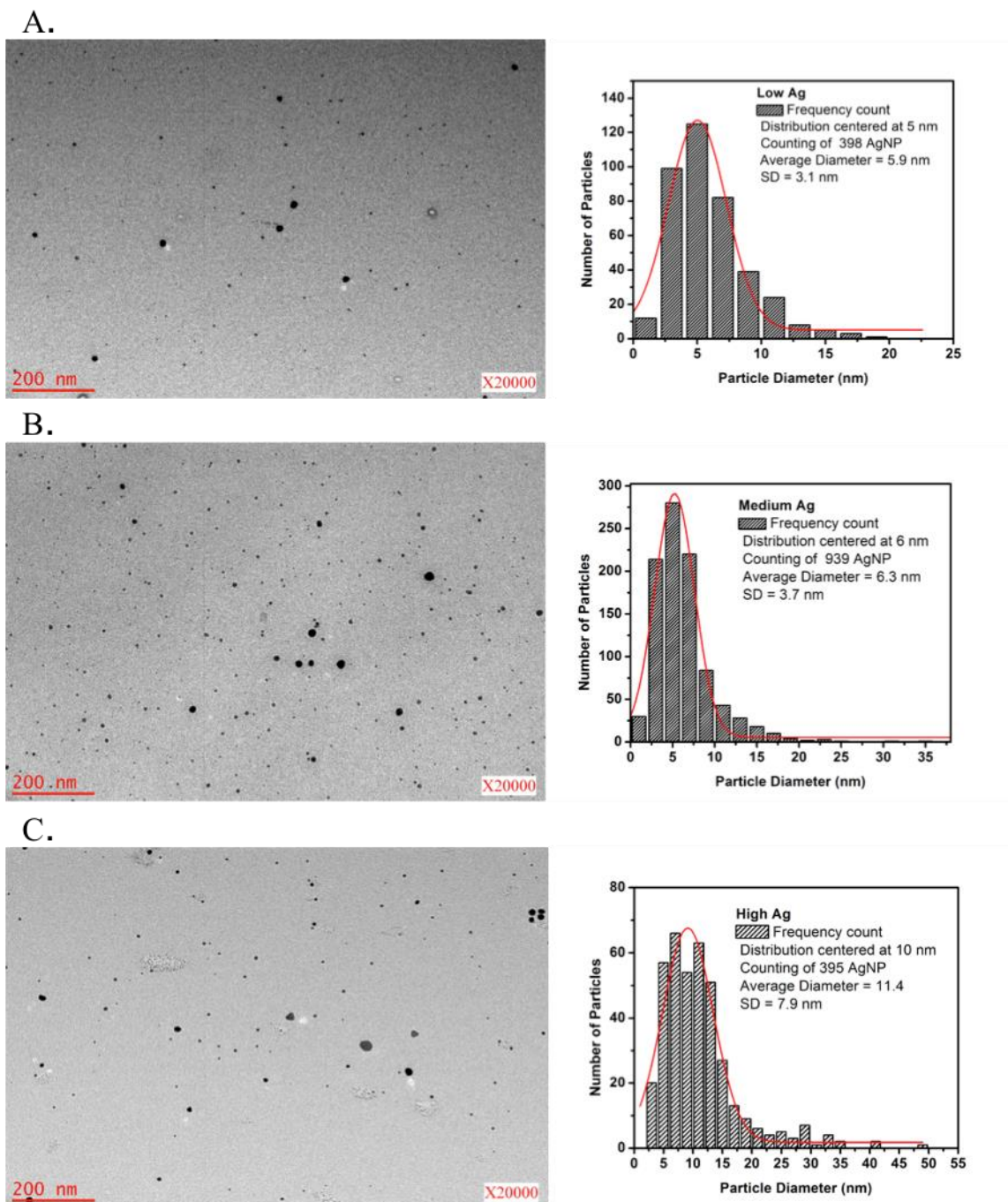


**Figure 5.7** TEM images and respective size distribution of nanoparticles in the various AgNP-PAA-TA solutions 7 days after synthesis. **A.** Low Ag **B.** Medium Ag **C.** High Ag.

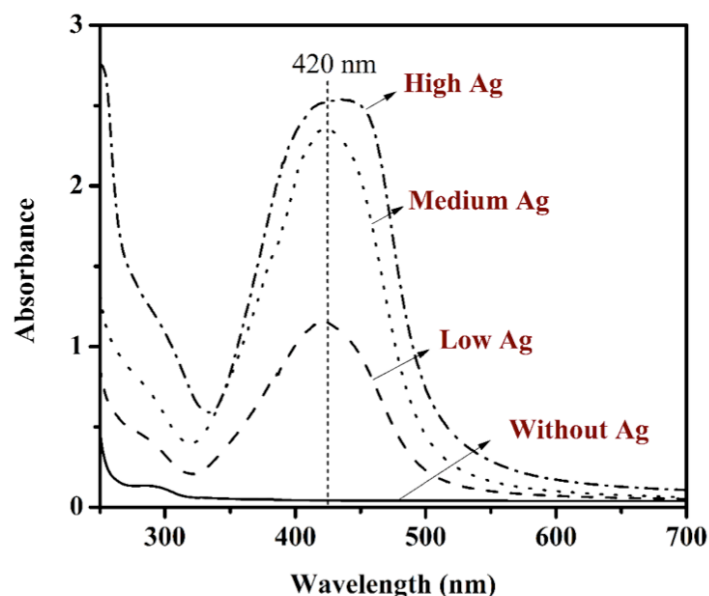


**Figure 5.8** Absorption spectra of synthesized solutions containing various  $\text{AgNO}_3$  concentrations 180 days from synthesis.

The particle size distribution after 180 days from synthesis, as observed by TEM analyses, also confirmed AgNP stability over time (Fig. 5.9). Although AgNP remained stable in the colloidal system, there were slight alterations on the center of the size distribution curve. Low Ag and Medium Ag suffered a small deviation, changing from 5 to 7 nm and 6 to 9 nm, respectively. High Ag, which presented instability and sedimentation in the first week after synthesis, remained with the center of size distribution curve at 10 nm, and narrowed the standard deviation (7.9 to 6.6). This phenomenon may be explained by a quantized Ostwald ripening, in which smaller sized particles from a bimodal size distribution of particles dissolve, and larger ones grow similarly to the regular Ostwald ripening, and results in focusing size distribution of larger particles. Indeed, a simulation study investigated the growth of colloidal semiconductor NP in the presence of two

distinctly sized NP in the so-called “bimodal growth regime”. Small particles with critical dissolution radius will act as sacrificial materials for a larger second size for the growth and size focusing, also called quantized Ostwald ripening technique. This slow growth condition could lead to a better reaction control over the NP synthesis. Also, the oversaturation of monomer over the growth could improve the overall quality of the NP [171, 172].

The phenomenon accounting for the stabilization of *in situ* produced AgNP is known as polyelectrolyte bridging interaction. It involves a charged PAA polymer chain and its adsorption to NP is mediated via coulombic interactions [173]. Generally dispersion stabilization is caused by two main mechanisms: charge or electrostatic stabilization and steric stabilization. DLVO theory can explain the electrostatic stabilization in an aqueous system involving adsorbed ions, which build up a charged layer around the nanoparticle, preventing aggregation by electrostatic repulsion. The use of ionic surfactants, usually anionic, to provide electrostatic stabilization is well established. Steric stabilization, on the other hand, is generally described to arise from two factors: a volume restriction component and an osmotic component involving change in matrices volume and thus causing an increase in polymer concentration. Those factors have been related as a function of pH and ionic strength of the polyacids [174]. Therefore, it is possible to combine chemical functionalities within the same polymer to provide both steric and electrostatic stabilization.

In the present formulations of polyelectrolyte, an electrosteric stabilization occurs if one considers that this effect is caused by steric as well as electrostatic repulsion as the polyelectrolyte adsorbs on a colloidal positively charged particle surface (Figure 5.10).

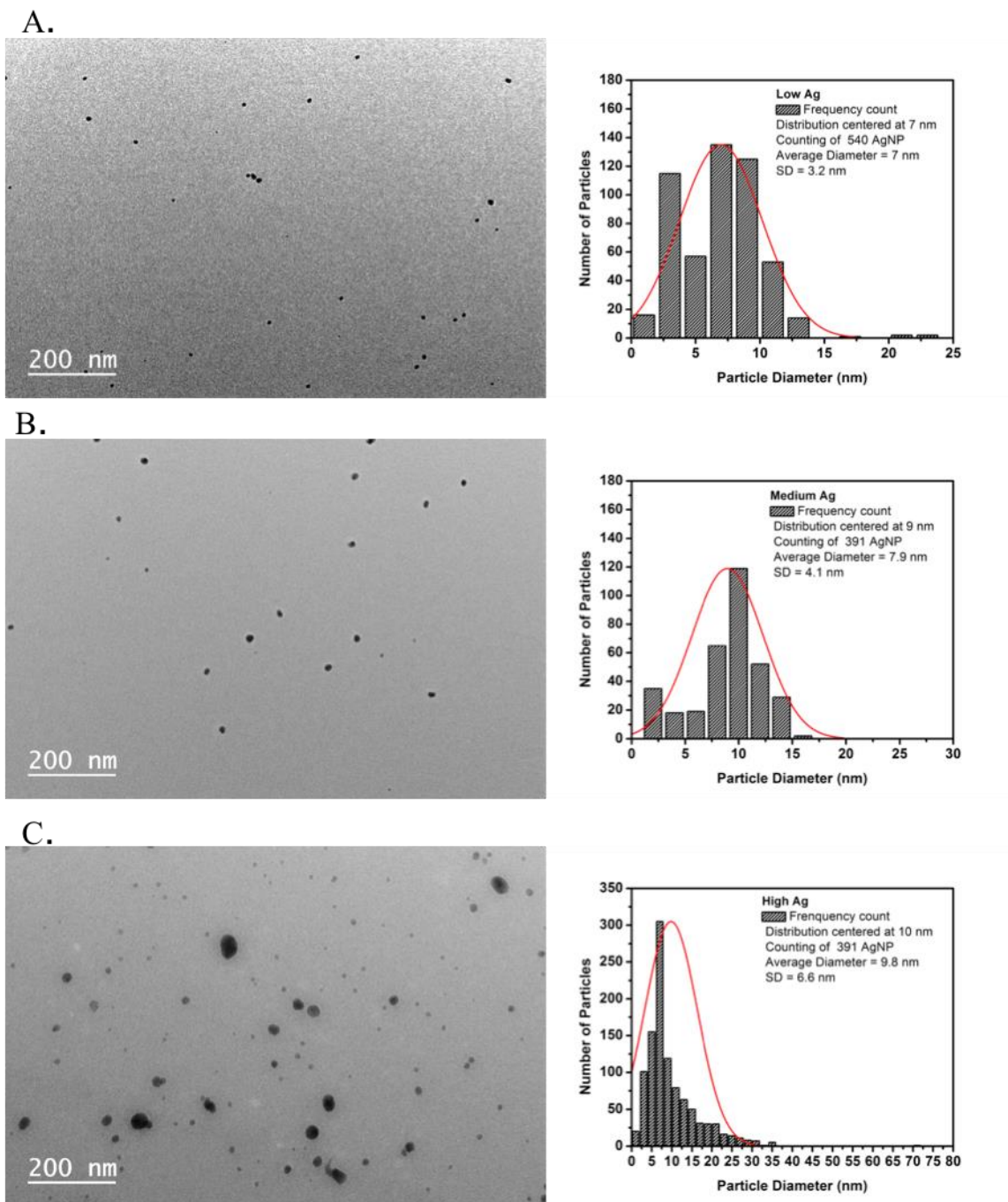


**Figure 5.9** TEM images and respective size distribution of nanoparticles in the various AgNP-PAA-TA solutions 180 days after synthesis **A.** Low Ag **B.** Medium Ag **C.** High Ag.

To assist dispersion properties, the effect of molecular weight [175, 176] and weight percentage [177] on the stabilizing action of polycarboxylic acid dispersant have been investigated previously. However, in the present study the criteria for choosing concentration and average molecular weight of PAA were based on previous studies of the effect of these parameters on the viscosity and compressive strength values of GIC [158].

GIC is the result of the hardening reaction between an ion-leachable glass and an aqueous solution of PAA, which is known as a polyelectrolyte and responsible for the rheology and the net setting time of cements [2]. During this reaction, the polymer chains cross-linking occurs as a result of polymeric acid attack on the glass surface, leading to dissolution and ions leaching. Changing polymeric concentration of the solution or exceedingly adding TA to the cement formulation may disable it for dental application, by interfering in the acid base setting reaction. Thus, *in situ* synthesis of AgNP in the ionomer solution was here achieved by using a suitable formulation and restricted by such conditions.

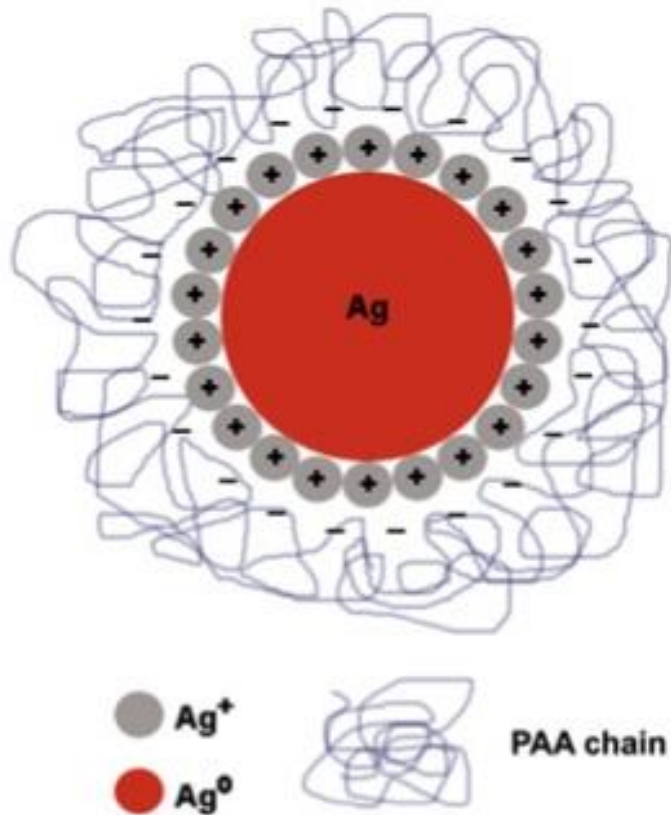


**Figure 5.10** Working model of the electrostatic stabilization of AgNP complexes (intermediate  $\text{Ag}_n^{m+}$  clusters) in the negatively charged PAA.[123, 150, 173]

## 5.2. THE IONOMER GLASS

The glass powder was analyzed by X-ray powder diffraction (XRD) to identify any crystal phases. The ionomer glass produced was optically clear and could therefore be assumed to be homogenous single-phase glass that has not undergone any amorphous phase separation. The typical amorphous diffraction pattern of the frit is shown in Figure 5.11.

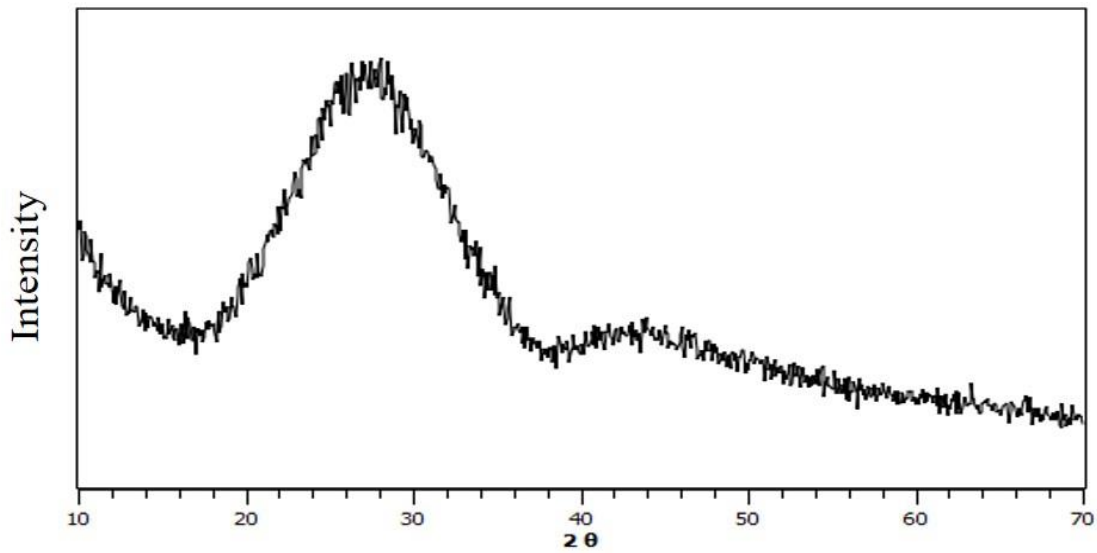


**Figure 5.11** X-ray diffraction pattern of the ionomer glass.

### 5.3. CHARACTERIZATION OF THE GIC

Evaluation of handling properties among the GIC groups showed a slight increase in the net setting time of the GIC, due to the presence of AgNP in the cement matrix. However, the analyzed groups fell within the range from 1.5 to 6.0 min, specified in the ISO 9917-1 (Table 5.2).

**Table 5.2** Net setting time values of the GIC.

|                  | Without Ag | Low Ag | Medium Ag | High Ag |
|------------------|------------|--------|-----------|---------|
| Net Setting Time | 3'05"      | 3'25"  | 3'55"     | 3'45"   |

Carboxylate groups have the ability of complexation to metal ions that are both present in the silver salt and at the outcoming ions from the ionomer glass. In the present work, UV exposure time and TA concentration were adequately adjusted in order to photoreduce different concentrations of silver salt without diminishing the availability of carboxylate groups for the setting reaction and therefore harming the final cement properties. Even though the complexation of metal ions to PAA is the basis of the setting reaction on the GIC, this reaction is not known to involve a net change in the charge of the polyelectrolyte in the presence of sub-stoichiometric concentration of cations [178, 179]. Thus, when very low concentrations of  $\text{Ag}^+$  are dispersed in the solution, only few carboxylic groups in the polyelectrolyte act as reducing agents under UV irradiation. Since the neutralization reactions that occurs during hardening of the cements is directly dependent on the  $\text{COO}^-/\text{M}^+$  ratio, it can be assumed that no significant change in the polyelectrolyte took place as it was revealed by the registration of the net setting time of the AgNP-GIC.

Considering the presence of the AgNP in the cement, the handling properties of the AgNP-GIC were not drastically influenced by variation of Ag concentration neither by UV-irradiation exposure among the diverse formulations.

The compressive strength (CS) of the AgNP-GIC groups and one commercially available GIC (Vitro Molar<sup>TM</sup> - Nova DFL, Brazil) was analyzed by a mechanical assay. As shown in Figure 5.12, strength values of the experimental groups in MPa were in a decreasing order: High Ag ( $55.5 \pm 3.0$ ) > Without Ag ( $50.8 \pm 1.8$ ) ~ Medium Ag ( $49.3 \pm 6.5$ ) ~ Low Ag ( $48.6 \pm 5.4$ ) > Without Ag I\* ( $41.9 \pm 4.7$ ). Presence of AgNP in the matrix

increased the compressive strength of the cements. High Ag showed to be more resistant to compression than Without Ag and Vitro Molar<sup>TM</sup> within a confidence interval of 95 %. However, Low and Medium Ag showed no statistical difference from Without Ag group.

Moreover, it was observed that UV-light exposure have affected the CS of cements formulated with irradiated PAA-TA solution (Without Ag I\*). Compressive strength values are known to vary depending on polymer properties (average molecular weight and viscosity) [157, 158], with CS values decreasing as a function of  $M_w$ . The chain length of the polyacid was found to be an important parameter in formulation of a cement. Thus, the higher the molecular weight, the better the properties. However, in practice the molecular weight is limited by viscosity, and some balance has to be achieved among concentration, molecular weight, and viscosity [158]. Although liquid to powder ratio and ionomer glass composition are major variables on mechanical properties of GIC [180], in the absence of cations consuming enthalpy energy to reduce metallic silver, one may hypothesize that generated free radicals by UV-light might induce polymer chain degradation. This fact confirms the hypothesis made during the interpretation of FTIR data in the previous section (Figure 5.3).

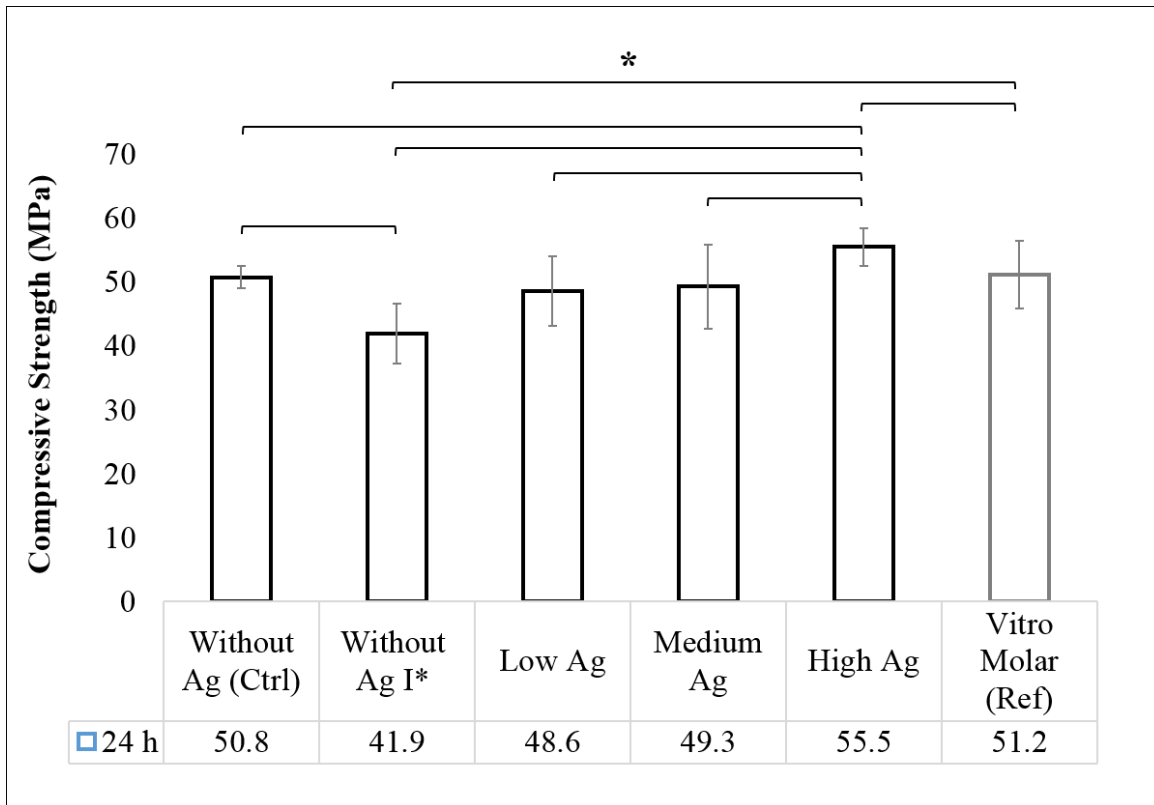


**Figure 5.12** Compressive strength values (MPa) of the experimental AgNP-GIC and a commercial GIC (Vitro Molar™, Nova DFL). \* ( $p$ -value < 0.05)

Metal-reinforced glass ionomer cements, also called Cermets, were once commercially available because of their increased mechanical strength and radiopacity. Silver particles were sintered onto the glass, and a number of products then appeared where the amalgam alloy content had been fixed at a level claimed to produce optimum mechanical properties for a glass cermet cement [13]. However, clinical trials discouraged their application in clinics, because the conventional glass ionomer cements had better physical properties and because mechanical properties were not shown to be effectively enhanced [181]. Moreover, if one consider that glass ionomer cements were used as

aesthetic materials, there was no reason to sustain their application. That is the reason why cermets were finally put out of the market.

Nonetheless, introducing AgNP in the polymer matrix to obtain anti-adherent or antibacterial properties has quite different results from sintering silver alloy particles onto the ionomer glasses. Firstly, silver alloy particles tend to be more stable than metallic nanoparticles immobilized by polyacids. Either the amount of silver, and their ability to be oxidized to silver ions influence the final properties of the cements. For a fixed filler content the rate of the silver ion release from nanocomposites is about one order of magnitude higher in comparison to microcomposites, because of the much larger specific surface area of the nanoparticles [182]. Due to the high surface-area-to-volume ratio of nanoparticles, it should be possible to impart significant antibacterial properties to the cement only by adding little amounts of silver salts to the PAA aqueous solution originally used to formulate the product, without damage to the GIC properties.

Mechanical property of the AgNP-GIC groups was reinforced, considering that the highest silver content presented an increase in the compressive strength of the cements ( $p$ -value  $< 0.05$ ). It can be inferred that anchoring of AgNP homogeneously distributed in the matrix helped to increase cohesive strength among the polymers chains, since the polymeric matrix is usually the preferential phase for crack propagation in composites. Furthermore, the proximity of Vitro Molar<sup>TM</sup> values, a commercially available GIC, indicates the potential use of the experimental groups for dental application.

There may be other strategies to increase the absolute values of CS obtained for the experimental GIC, despite being within the range expected by the ISO 9917:1 standard and

might be comparable to national products. Considering that the formulation chosen in the present work was the most simple as possible, in order to evaluate the contribution of each basic component of the GIC in the synthesis of AgNP, it is possible now to further evaluate other variables that can improve the mechanical properties of GIC in general, such as the use of PAA copolymers or resinous bases for formulating a RMGIC containing AgNP.

The most important issue though is that the photochemical route for AgNP production *in situ* the polyacid of an experimental GIC did not harm their compression resistance, as it was observed for other biocides when added to the matrix of dental materials [82, 89-91]. Withstanding functional forces is an important requirement for clinically acceptable materials, which must also provide superior antimicrobial activity.

Evaluation of the release of silver ions from AgNP-GIC is another important point to be discussed. The affinity for complexation onto negatively-charged surfaces of the positively-charged silver clusters in the polyelectrolyte solutions should drastically inhibit transport and mobility of the AgNP [183]. However, in the particular case of the AgNP-GIC, the colloidal stability of the AgNP synthesized for this purpose is pursued until the mixing of the cement.

ICP-OES analyses quantified the amount of Ag (ppm) present before and after immersion of the samples into deionized water for 24 h at 37 °C. These values and standard deviations are gathered in the Table 5.3. The immersion time (24 h) was chosen according to the end of net setting reaction of GIC.

The concentrations of Ag released in water were estimated by calculating the difference among the values before and after immersion. The estimated values of Ag

release (ppm) are presented in Figure 5.13. High Ag is presumed to release ca. 100 ppm in water, which is equivalent to ca.  $1 \times 10^{-3}$  M of Ag.

**Table 5.3** Concentrations of Ag (ppm) in the AgNP-GIC before and after release in water for 24 h.

|                  | <b>Before Release</b>                 | <b>After Release</b>                  |
|------------------|---------------------------------------|---------------------------------------|
|                  | <i>Ag (ppm) (<math>\pm</math> SD)</i> | <i>Ag (ppm) (<math>\pm</math> SD)</i> |
| <b>Low Ag</b>    | <b>174.09</b> ( $\pm$ 0.95)           | <b>130.90</b> ( $\pm$ 0.36)           |
| <b>Medium Ag</b> | <b>283.69</b> ( $\pm$ 0.26)           | <b>261.94</b> ( $\pm$ 0.44)           |
| <b>High Ag</b>   | <b>1019.04</b> ( $\pm$ 7.52)          | <b>920.83</b> ( $\pm$ 18.83)          |

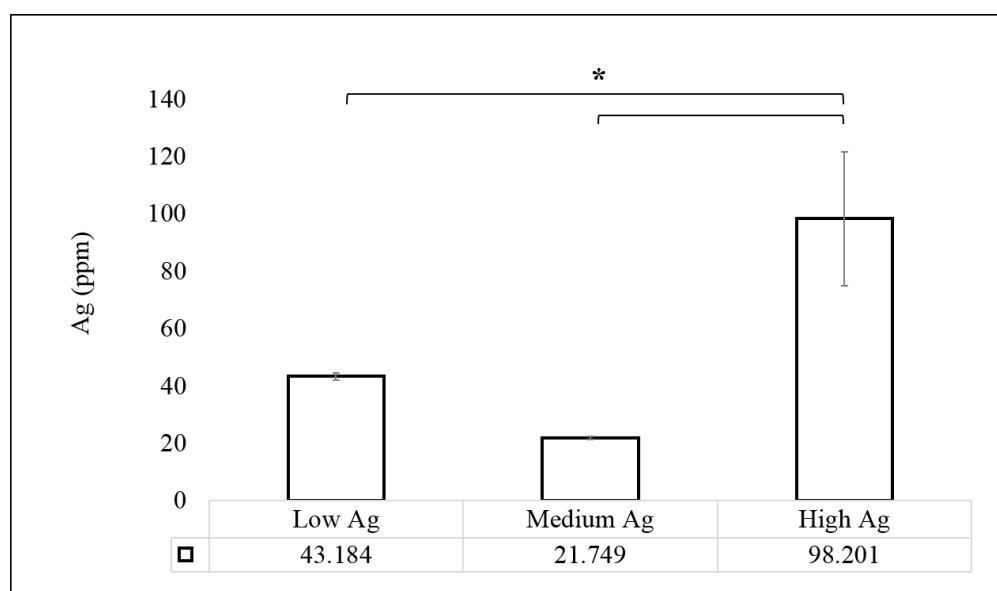


**Figure 5.13** Estimated values of Ag concentration (ppm) released from the AgNP-GIC in water after 24 h.

$\text{Ag}^+$  ions are likely to be released from the materials incorporating nanoparticles. Damm *et al.* [184] observed that the absolute amount of the long-term SI release increases exponentially with the maximum water absorption of the polymers used as matrix materials, because SI are formed from elemental silver particles in the presence of water, only. It was also found that the long-term silver ion release increases with a growing diffusion coefficient of water in the polymer. Liu *et al.*[124] applied elements of the drug delivery paradigm to nanosilver dissolution and presented a systematic study of competing chemical concepts for controlled release. Because the major ion source is oxidation, it was hypothesized that ion release can be controlled through manipulation of the oxidation pathways, involving surface area (size), ligand binding, polymeric coatings, sulfidic films, scavenging of peroxy-intermediates, and preoxidation treatments. Moreover, Martin *et al.* [123] showed that the main factor in the colloidal stabilization of AgNP is the disruption of stable polyelectrolyte coating molecules, followed by the oxidative dissolution (e.g., AgNP transformation into  $\text{Ag}^+$ ) and hence the silver ions release to the environment. Thus, during the setting reaction of the AgNP-GIC, when polyacids are neutralized by basic ionomer glasses, their colloidal stability is likely to be affected and would enable further release of  $\text{Ag}^+$  to the surroundings of the cement. As the cement completes the setting reaction, we speculate that the stable nanoparticles should be dispersed and entrapped in the GIC matrix, and should not be expected to readily release from the AgNP-GIC.

Since these AgNP are dispersed within the material, as already hypothesized by Cheng *et al.* [4] when analyzing resin-based dental composites, it is further expected that the surface of the composite suffers mechanical erosion during mastication, exposing the underlying particles, which should allow the antibacterial activity to be maintained. In the

present study, water-based cements containing AgNP are expected to provide higher antibacterial efficiency, since GIC are known to have higher levels of metallic ions diffusion than resin based composites [33, 160]. This is attributed to the greater amount of water that remains present in these materials. Indeed, although it was established that water-based cements continues to undergo reaction as they age, which is accompanied by an increase in the ratio of bound to unbound water [15], the amount of unbound water in GIC remains higher than in resin composites [33]. This may favor water flow and reactive metal ion release (dissolution) between cements and surrounding aqueous media, such as saliva and other biological fluids, thus facilitating the release of Ag<sup>+</sup> ions from the material.

Furthermore, the advantage of *in situ* formed over pre-formed AgNP plays an important role on this process, because it facilitates AgNP destabilization, and silver ions release to the environment [154].

On the other hand, several publications suggested that proteins adsorbed from physiological fluids, such as saliva-derived protein films, are able to attenuate the antibacterial properties of the underlying surfaces significantly [93, 185, 186].

The silver atomic concentration at AgNP-GIC surfaces was determined by XPS within a range of depth of 8 nm. The values are displayed as a function of the total amount of silver (% wt.) added to the cement (Figure 5.14). The amount of Ag (% wt.) added to each group was: 0.009 (Low Ag); 0.019 (Medium Ag) and 0.095 (High Ag).

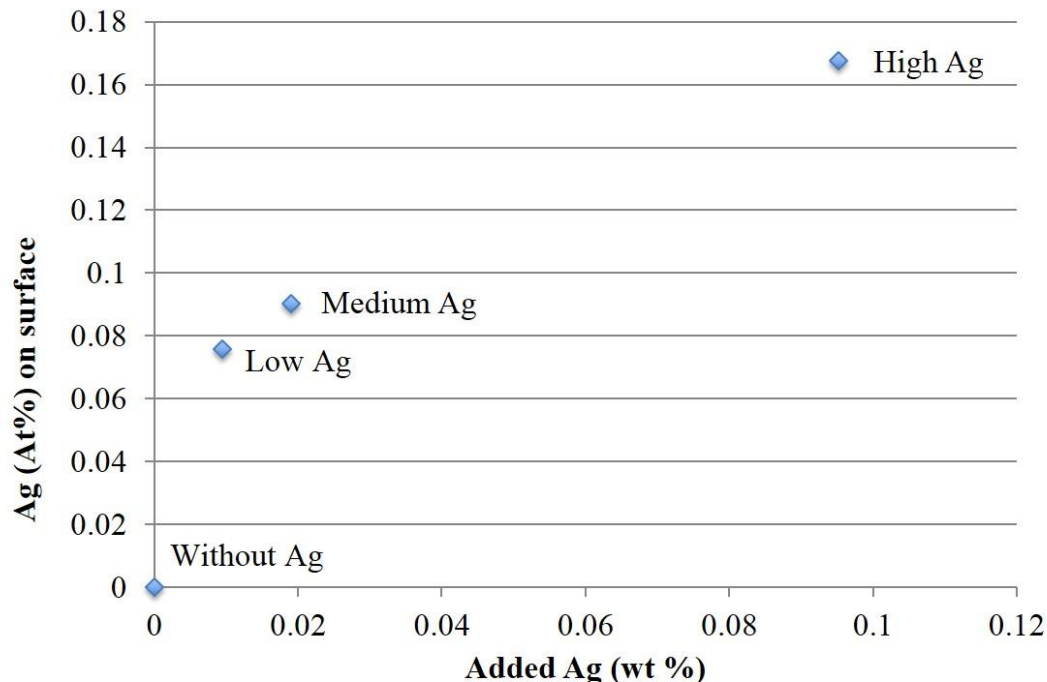


**Figure 5.14** The atomic concentration of silver at the surface of AgNP-GIC measured by XPS.

Cheng *et al.* [4], assuming a uniform distribution of the total amount of silver salt added to a resin composite, observed that the surface silver concentration as determined by XPS exceeded the expected concentration calculated from the compositions of the formulations. They attributed the preferential adsorption of silver species onto the surface due to the affinity (electrostatic and/or hydrogen bonding interactions) between the silver salt complex and glass slide surface used during preparation of the samples. Thus, the same phenomenon is expected to occur in the present study. Comparing the amount of silver (At. %) measured on the surface of the resin-based composite to the values here obtained by XPS, it is possible to assume that water-based cements (GIC) are more prone to have silver species preferentially adsorbed onto their surfaces. High Ag groups, which have 0.15 wt. %

of silver salt added to the formulation, presented 0.17 against 0.08 atomic silver (%) of the equivalent resin-based composite on the analyzed surfaces.

#### **5.4. *IN VITRO* CYTOTOXICITY (INDIRECT MTT ASSAY)**

The results of metabolic activity of HGF-1 cells comparing AgNP-GIC with increasing concentrations of silver are shown in the Figure 5.15. In an indirect contact assay using eluates of AgNP-GIC, cell metabolism of Without Ag, Low Ag and High Ag decreased for a 24 h incubation period. Cytotoxic effect on cells was significant for Without Ag and High Ag ( $p$ -value < 0.01). Considering ICP-OES analyses on High Ag samples (Fig. 5.13), higher concentrations of silver ions released (~100 ppm) caused a cytotoxic effect on HGF-1 cells. However, the low rates of cell survival in Without Ag can be attributed to other fact than silver concentration, and might be associated to residual impurities from polymerization process of PAA solution.

A number of different polyacid grades are commercially available that vary in their chemical structure, degree of crosslinking, and residual components. Solution polymerization is an industrial process used for synthesis via conventional free-radical polymerization of the polyacids and copolymers used in GIC formulations [187]. During solution polymerization a monomer is dissolved in a non-reactive solvent that contains a catalyst. One of the most used solvents in this process is benzene, a highly cytotoxic molecule, because it is cost effective for producing on an industrial scale. One may attempt to the fact that cytotoxic molecules (e.g. benzene) might be used in the process of solution polymerization of PAA, since the solutions used in this study are not guaranteed to have

pharmaceutical grade (i.e., have been purified after polymerization process) by the suppliers (Sigma Aldrich). For biomedical application some treatments must be done to avoid cytotoxicity. Dissolution in anhydrous methanol and precipitation from ethyl acetate, followed by freeze-drying to remove residual monomers and thus no leachable should be expected [188-190]. This may be the reason of cytotoxic tendency in absence of silver. Moreover, it can be hypothesized that the photochemical process of reduction of silver ions may have contributed to increasing of PAA biocompatibility, although the molecules and the exact mechanism this phenomenon took place must be further investigated.

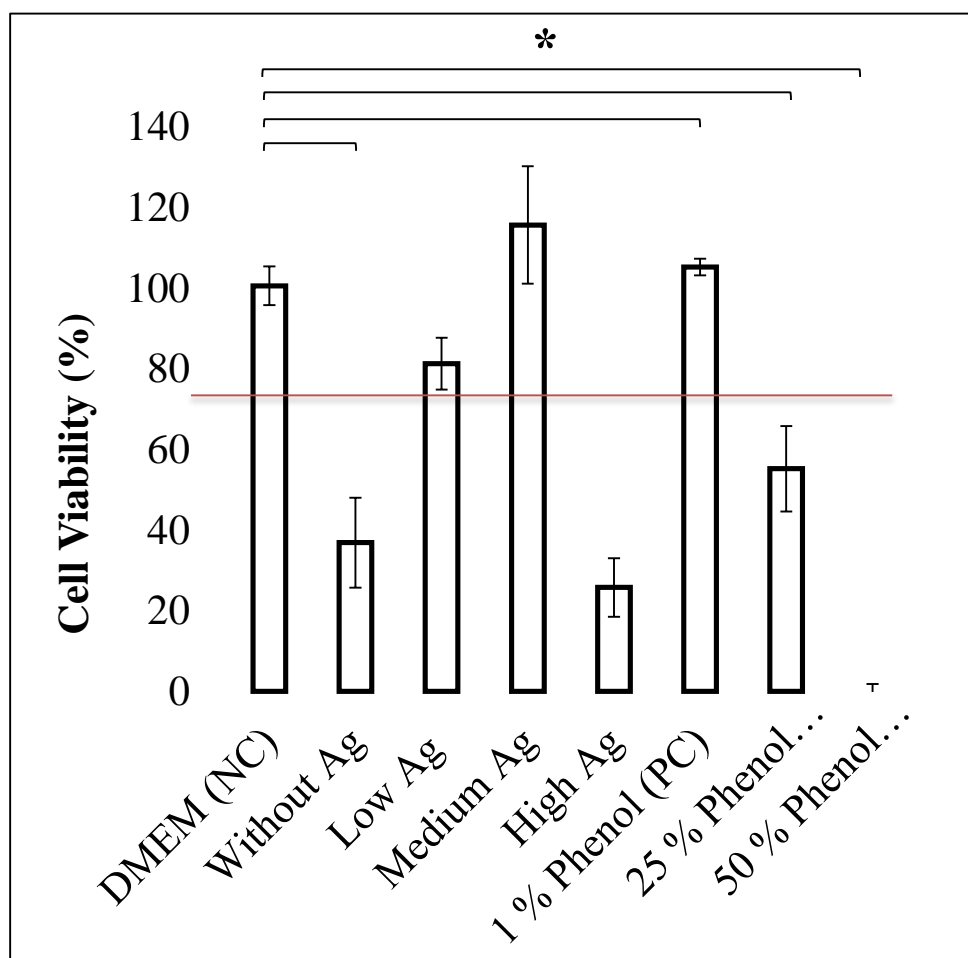


**Figure 5.15** Metabolic activity of HGF-1 cells over eluates of the AgNP-GIC, DMEM as negative control (NC) and Phenol as positive control (PC). \*( $p$ -value < 0.01)

## 5.5. AGAR PLATE DIFFUSION TEST (GENERAL ANTIBACTERIAL TEST)

Diffusion test with *E. coli* strain, here used as a bacterial model, was pursued for general antibacterial validation, but also as screening parameter for the concentration range of AgNP to be further analyzed by specific anti-biofilm test.

Antibacterial efficacy that is expected from the silver nanoparticles was assessed by measuring diameter and calculating area of the zone of bacterial inhibition growth around GIC samples, which resulted from diffusion of Ag<sup>+</sup> ions in agar medium. As shown in Figure 5.16, AgNP-GIC samples were all surrounded by inhibition zones of bacterial growth on agar plate.

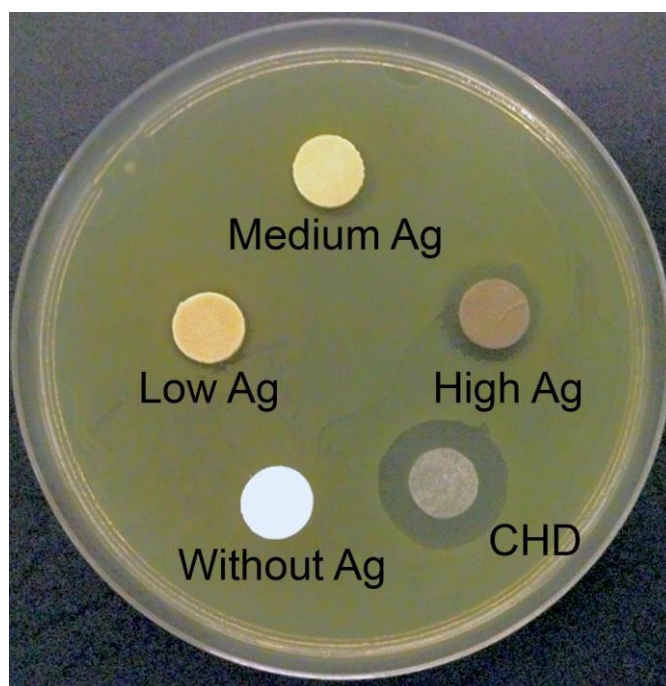


**Figure 5.16** Agar diffusion test performed with *E. coli*: Image of the bacterial growth inhibition zones in the LB agar plate. Chorhexidine digluconate (CHD) as positive control.

Measurements of the inhibition zones and standard deviations are presented in the Table 5.4. All of the AgNP-GIC groups exhibited statistically significant difference compared to negative control group (Without Ag) ( $p$ -value  $< 0.05$ ). On the other hand, there was no significant difference between Low Ag and Medium Ag groups ( $p$ -value  $> 0.05$ ).

**Table 5.4** Values of the inhibition zones (mm<sup>2</sup>) and associated standard deviation (SD).

| <i>Samples</i>                       | <b>Inhibition Zone</b>                      |
|--------------------------------------|---|
|                                      | <b>(mm<sup>2</sup>) <math>\pm</math> SD</b> |
| <b>Without Ag (Negative control)</b> | <b>0</b>                                    |
| <b>Low Ag</b>                        | <b>32.8 <math>\pm</math> 3.4*</b>           |
| <b>Medium Ag</b>                     | <b>32.8 <math>\pm</math> 5.6*</b>           |
| <b>High Ag</b>                       | <b>76.1 <math>\pm</math> 6.9*</b>           |
| <b>CHD (Positive control)</b>        | <b>178.5 <math>\pm</math> 1.73*</b>         |

\* ( $p$ -value  $< 0.05$  for comparison to negative control).

Bacterial growth inhibition observed on the surrounding of AgNP-GIC suggests that nanoparticles act as a reservoir of silver, promoting liberation of SI from cement matrix to environment by diffusion. The present range of silver salt concentrations in GIC (from 0.015 to 0.150 wt. %) was here shown to provide significant antibacterial effect on *E. coli* species, whose sensibility to low material-related Ag concentrations has already been reported [182]. It is possible to correlate inhibition growth by SI diffusion in agar plate with

results of estimated SI release from the AgNP-GIC in previous section (Fig. 5.13), in decreasing order High Ag ( $1 \times 10^{-3}$  M), Low Ag ( $4.3 \times 10^{-4}$  M) and Medium Ag ( $2.2 \times 10^{-4}$  M). Low Ag and Medium Ag present SI release within the same order of magnitude, thus the results in inhibition of bacterial growth were not significantly different.

If one considers bioactivity of matrices in which AgNP are entrapped, it is of great importance to observe that GIC offers high SI diffusion considering the amount of silver salt added to the former material. Fan *et al.* [191] used resin-based polymers to synthesize AgNP using different concentrations of Ag benzoate (AgBz). Light-cure (LC; bisphenol A glycidyl methacrylate, tetraethyleneglycol dimethacrylate, bisphenol A ethoxylate dimethacrylate blend) and chemical-cure systems (CC; orthodontic denture resin) were used as matrices. LC resins only released Ag<sup>+</sup> ions when AgBz concentration was greater than 0.1 wt. %, while CC specimens showed release with as low as 0.002 wt. % AgBz. AgNP-loaded CC resins made with 0.2 and 0.5 wt. % AgBz were tested *in vitro* for antibacterial activity against *Streptococcus mutans*, and results showed 52.4% and 97.5% of bacterial inhibition, respectively. However, the area considered for the evaluation of bacterial growth was not the inhibition zone on the surroundings of resin disks. Instead, the authors measured transparency of the area under the disks on agar plate, and correlated to none, half or total growth inhibition. Therefore, results are not directly comparable with the present study, since bacteria strains and test protocols were not equivalents. Nevertheless, one might observe that the matrices' properties are of great importance for the releasing process of SI from AgNP. Even though there was release of SI from resin-based silver nanocomposites, *S. mutans* inhibition zone were not observed on the surroundings of the disks, even for the greater amount (0.5 wt. %) of silver salt added to the resin.

## 5.6. SPECIFIC ANTIBACTERIAL ASSAYS

From CLSM analyses, LSM images acquired after 3 h of incubation were processed using “Make Composite” and “Z-project (Max Intensity)” ImageJ functions to create 2D images of the analyzed groups. Representative images of each group are gathered in Figure 5.17. Percentage areas of adhered bacteria covering surfaces were quantified after binarization of those 2D images. These results are shown in the Figure 5.18. At early stages, bacteria adhered to Petri dish control (FB) group were significantly more dispersed on the surface than those attached to the GIC ( $p$ -value < 0.05), which showed tendency to form microcolonies of agglomerated bacteria. Nonetheless, differences among GIC groups were not remarkable.

Representative images (2D) of *S. mutans* biofilms (i.e., after 24 h of incubation) of each group are presented in Figure 5.19. It is possible to observe a tendency of microcolonies to agglomerate on GIC. The covered area is progressively sparser (i.e., less continuous) and size of microcolonies over the GIC decreases with the increasing of silver salt content (Figure 5.19 C, D and E).

The previous qualitative remarks were quantified by using COMSTAT2 analysis features. Several variables were used to describe and quantify shape and three-dimensional structure of biofilms, as described in this section.

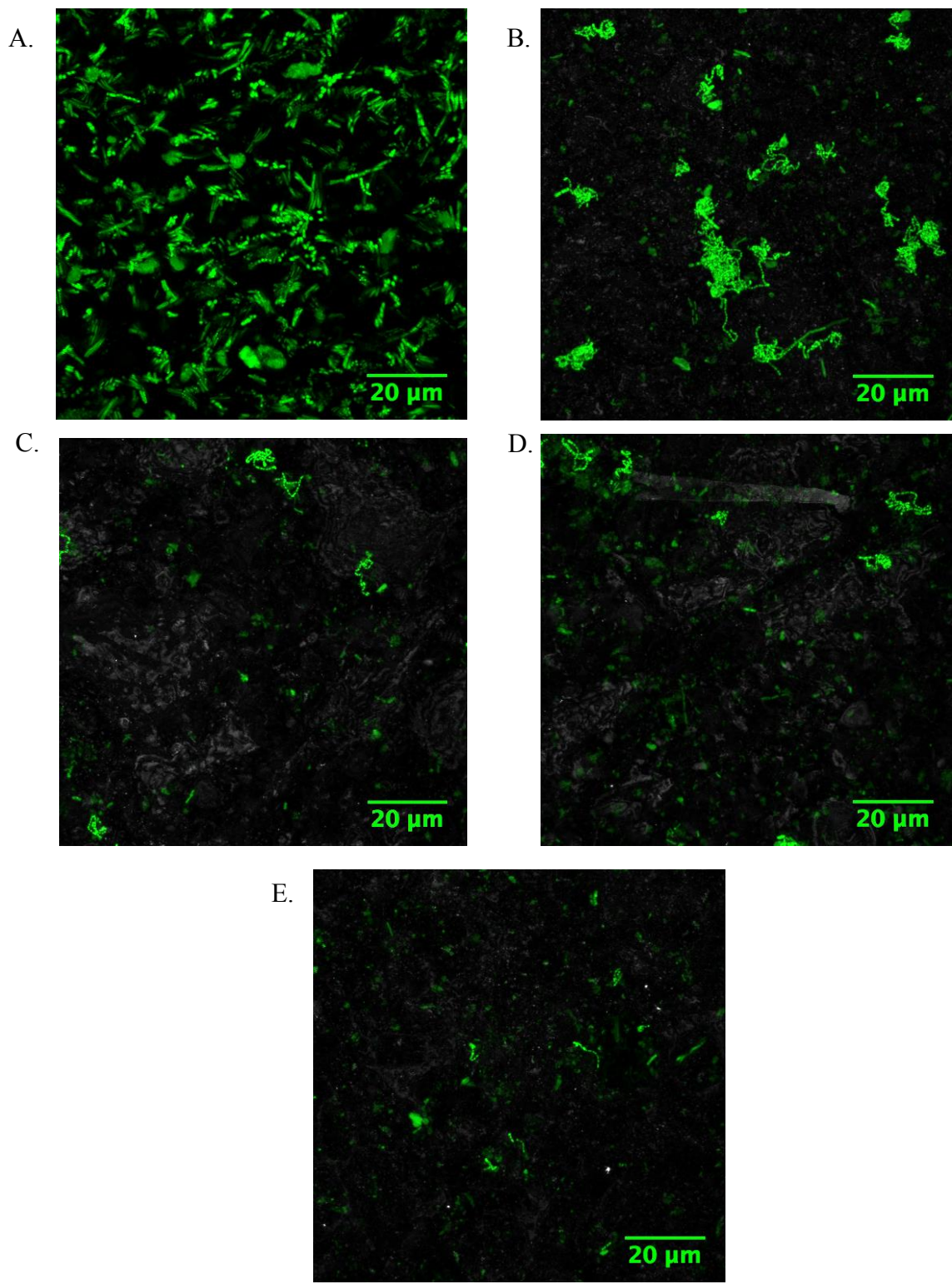


**Figure 5.17** 2D representative images of early adhered bacteria (3 h) on surfaces of the samples. **A.** Control (FB) **B.** Without Ag **C.** Low Ag **D.** Medium Ag **E.** High Ag.

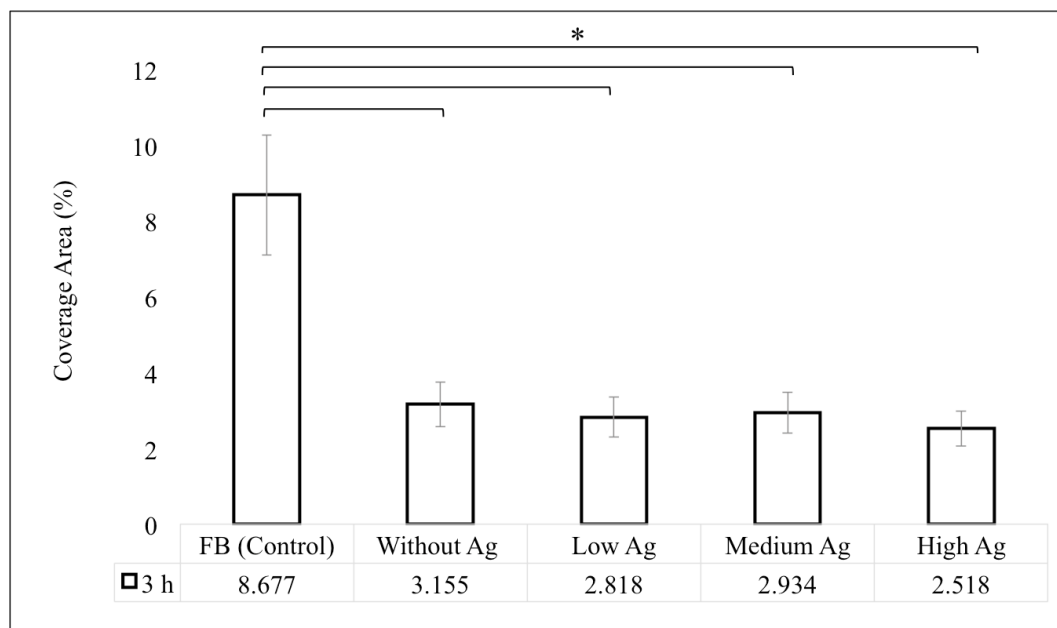


**Figure 5.18** Percentage area of surfaces covered by *S. mutans* adhered at early stages (3 h) and standard errors. \* ( $p$ -value < 0.05)

Bio-volume is defined as the number of biomass pixels in all images of a stack multiplied by the voxel size [(pixel size)<sub>x</sub> x (pixel size)<sub>y</sub> x (pixel size)<sub>z</sub>] and divided by the substratum area of the image stack. It represents the overall volume of the biofilm, and also provides an estimate of the biomass [159]. Biomass of early-adhered bacteria was plotted as a function of the coverage area (%) in Figure 5.20. All of the GIC groups presented significant difference from FB (control) group ( $p$ -value < 0.01). Although bacteria are similarly distributed on the surfaces of the GIC groups, biomass values reveal a significant difference between Without Ag ( $0.315 \mu\text{m}^3/\mu\text{m}^2$ ) and other AgNP-GIC ( $p$ -value < 0.05), namely Low Ag ( $0.177 \mu\text{m}^3/\mu\text{m}^2$ ), Medium Ag ( $0.210 \mu\text{m}^3/\mu\text{m}^2$ ) and High Ag ( $0.171 \mu\text{m}^3/\mu\text{m}^2$ ). These values represent the agglomeration suffered by bacteria, as qualitatively displayed in the Figure 5.17.

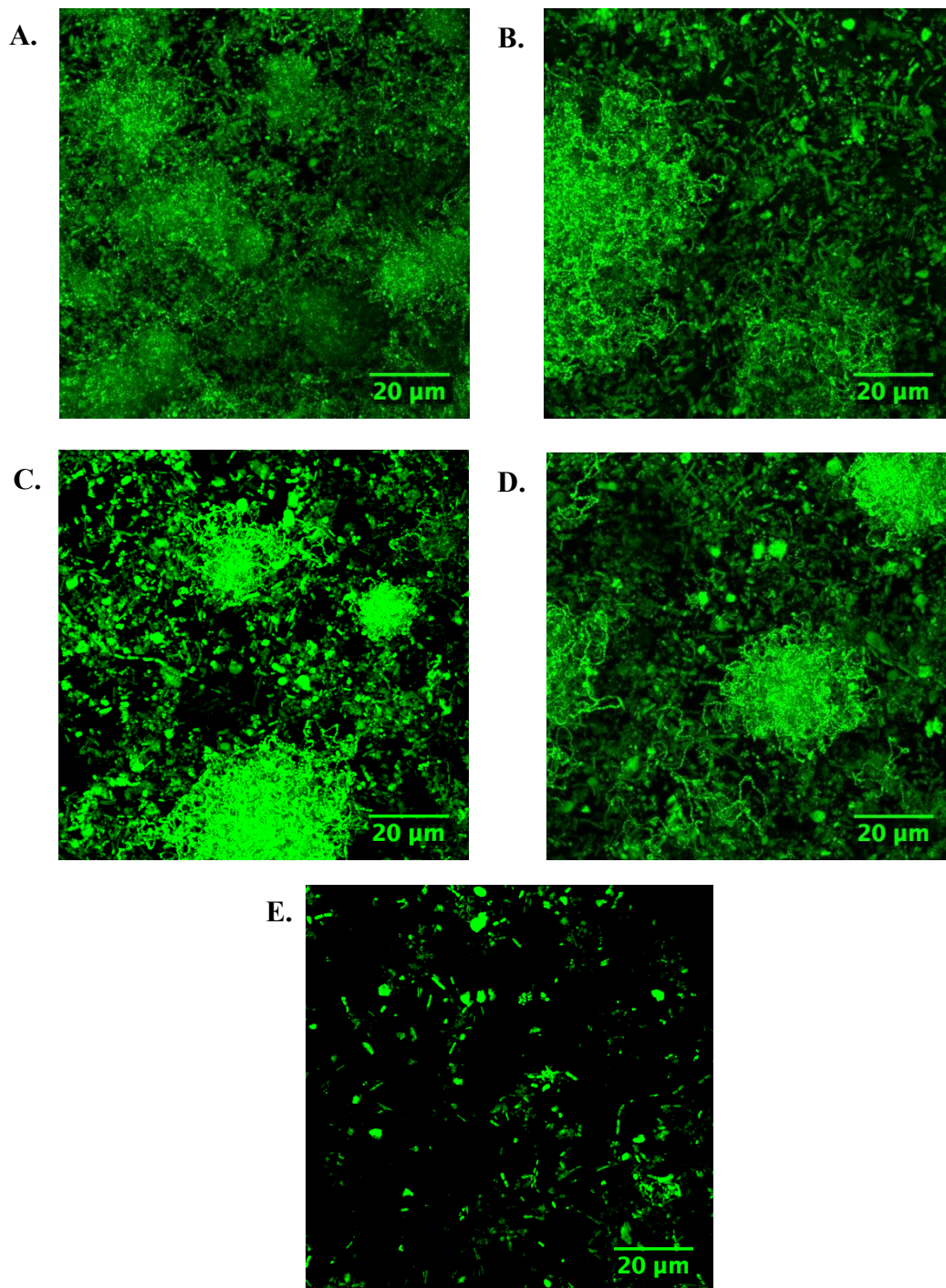


**Figure 5.19** 2D representative images of biofilm structure (24 h) on surfaces of the samples. **A.** Control (FB) **B.** Without Ag **C.** Low Ag **D.** Medium Ag **E.** High Ag.

It is interesting to observe that even though no significant difference is observed among AgNP-GIC, average biomass values of early adhered bacteria are inversely related to the amount of SI released in water in the previous ICP analyses, respectively High Ag, Low Ag and Medium Ag.

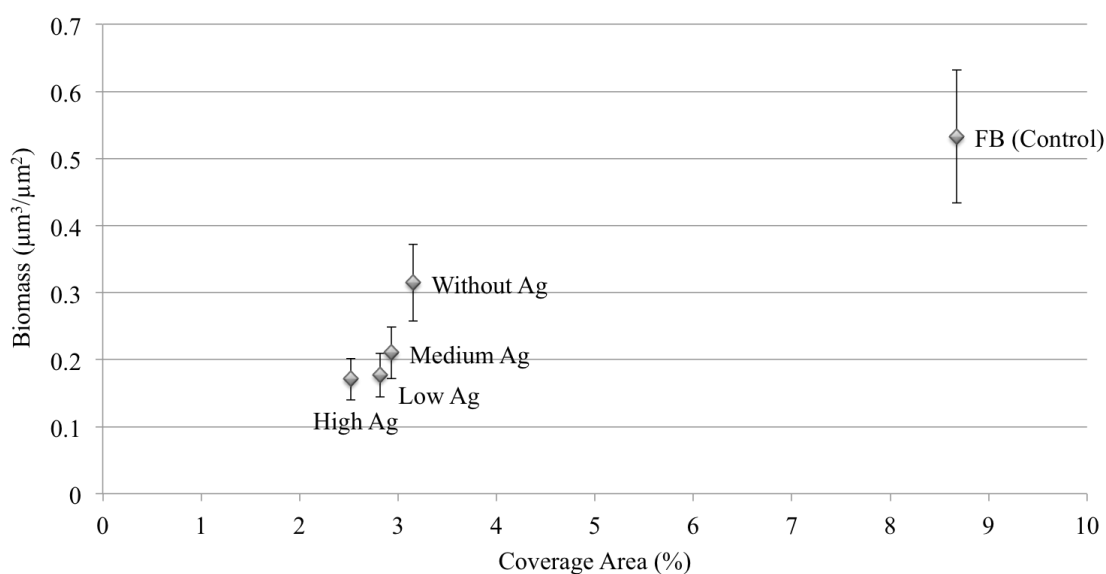


**Figure 5.20** Bio-volume values ( $\mu\text{m}^3/\mu\text{m}^2$ ) and standard errors as a function of *S. mutans* area (%) covering the surfaces at early stages (3 h).

As shown in the Figure 5.21, biomass value of 24 h biofilms decreases with increasing the amount of silver salt added to AgNP-GIC. Medium Ag and High Ag showed statistical significant difference from FB (control), as well as from Without Ag ( $p$ -value < 0.05) materials. Considering FB (control) as a standard biomass value for 24 h *S. mutans* biofilm grown in the given conditions, High Ag presented more than 50 % of bio-volume reduction. Biomass percentages for the GIC groups are in the following decreasing ranking:

Without Ag (101 %) > Low Ag (84 %) > Medium Ag (71 %) > High Ag (44 %). It is important to highlight that biofilm formation (24 h) is mainly related to increasing amount of AgNP that remained exposed on the surface of the GIC, as observed by XPS, and then are further oxidized to release SI; whereas early adhered bacteria (3h) also suffer additional influence of SI diffusion from AgNP-GIC in the early stages of net setting reaction, when the greater amount of unbound water and thus the water flux through the cements are expected to assign higher bioactivity [15, 160].

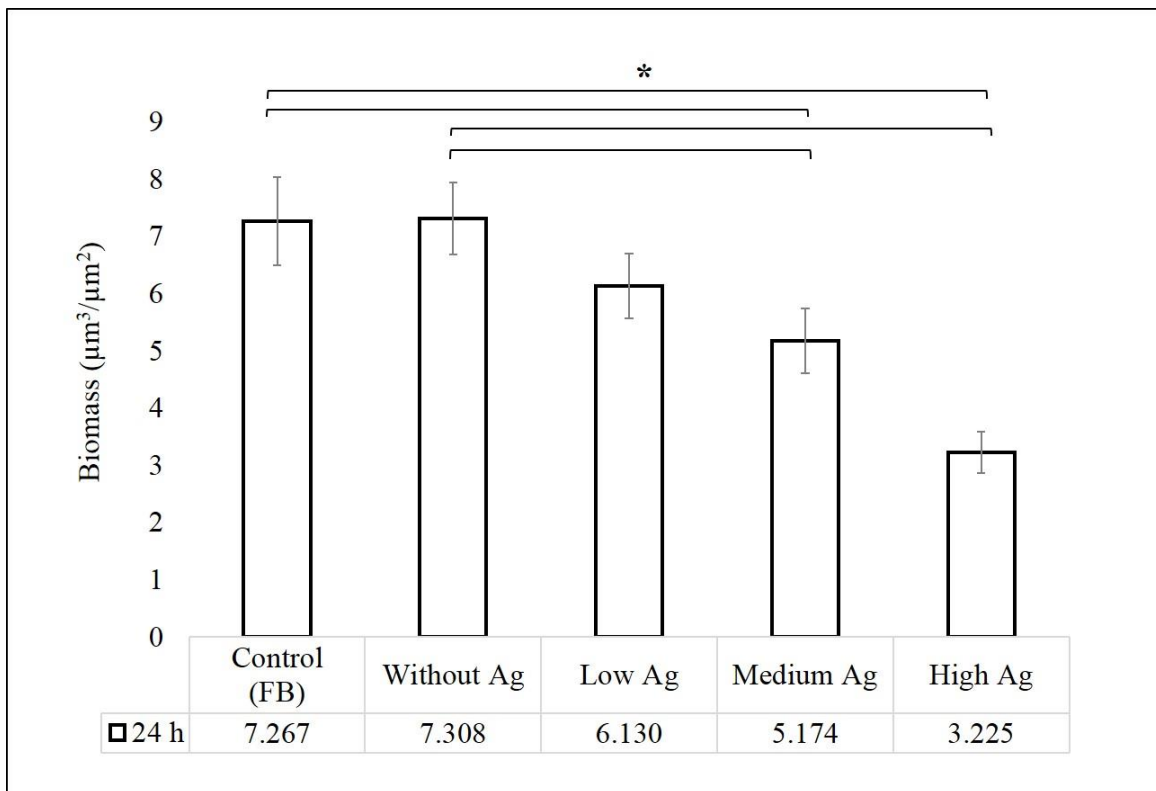


**Figure 5.21** Bio-volume values and standard errors of 24 h biofilms on the AgNP-GIC surfaces. \*( $p$ -value < 0.05)

Another parameter used to quantify biofilm is its thickness that is calculated ignoring pores and voids inside biofilm, over a given location. Thickness distribution can be used to further calculate biofilm roughness and mean biofilm thickness, which values are presented in the Figure 5.22 and 5.23, respectively.

Biofilm roughness is calculated by a dimensionless roughness coefficient ( $R_a$ ), which indicates how much the thickness of biofilm varies over the location, and is therefore an indicator of biofilm heterogeneity.  $R_a$  biofilm values for Low Ag and Medium Ag were significantly greater than Without Ag ( $p$ -value  $< 0.05$ ), while High Ag showed statistical significant difference from the control and Without Ag ( $p$ -value  $< 0.01$ ). It is important to remark that biofilm over GIC without any bactericidal activity promoted by silver (Without Ag) tends to have significant lower  $R_a$  coefficient value than control ( $p$ -value  $< 0.01$ ). Assuming that homogeneity is related to the development of mature and structured biofilms, this results corroborates a study [192] that affirms the formation of biofilms to be increased on surfaces of GIC. Biofilms over AgNP-GIC can be assumed as more heterogeneous on the basis of the  $R_a$  values, then suggesting a delay in maturity.

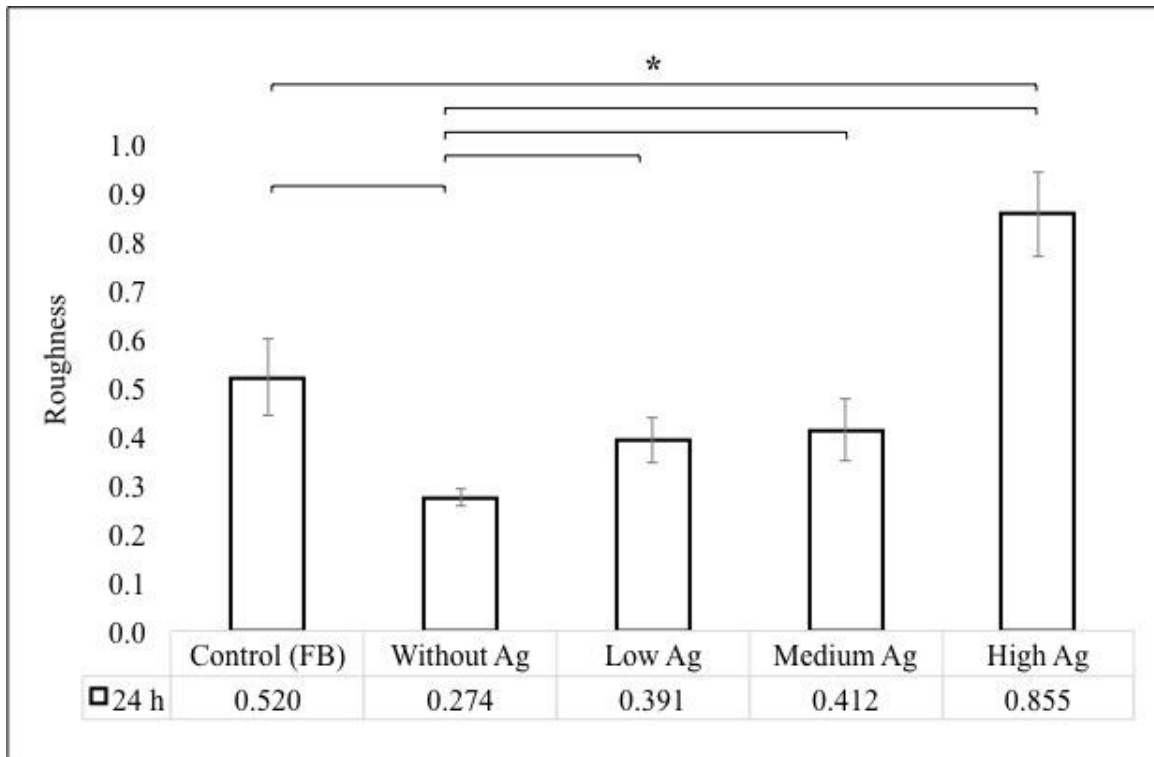


**Figure 5.22** Biofilm roughness coefficient ( $R_a$ ) of the AgNP-GIC. \*( $p$ -value < 0.05)

Mean biofilm thickness values indicate that Medium Ag ( $p$ -value < 0.05) and High Ag ( $p$ -value < 0.01) samples have substantially thinner biofilms than Without Ag and than FB groups ( $p$ -value < 0.01). High Ag showed to be 50% thinner than control group. In turn, Low Ag presented statistical difference from Without Ag ( $p$ -value = 0.01). As the amount of silver increases, biofilms get less structured in a 24 h period. The thinner the biofilm is, probably the easier it gets to be removed or displaced by mechanical forces.

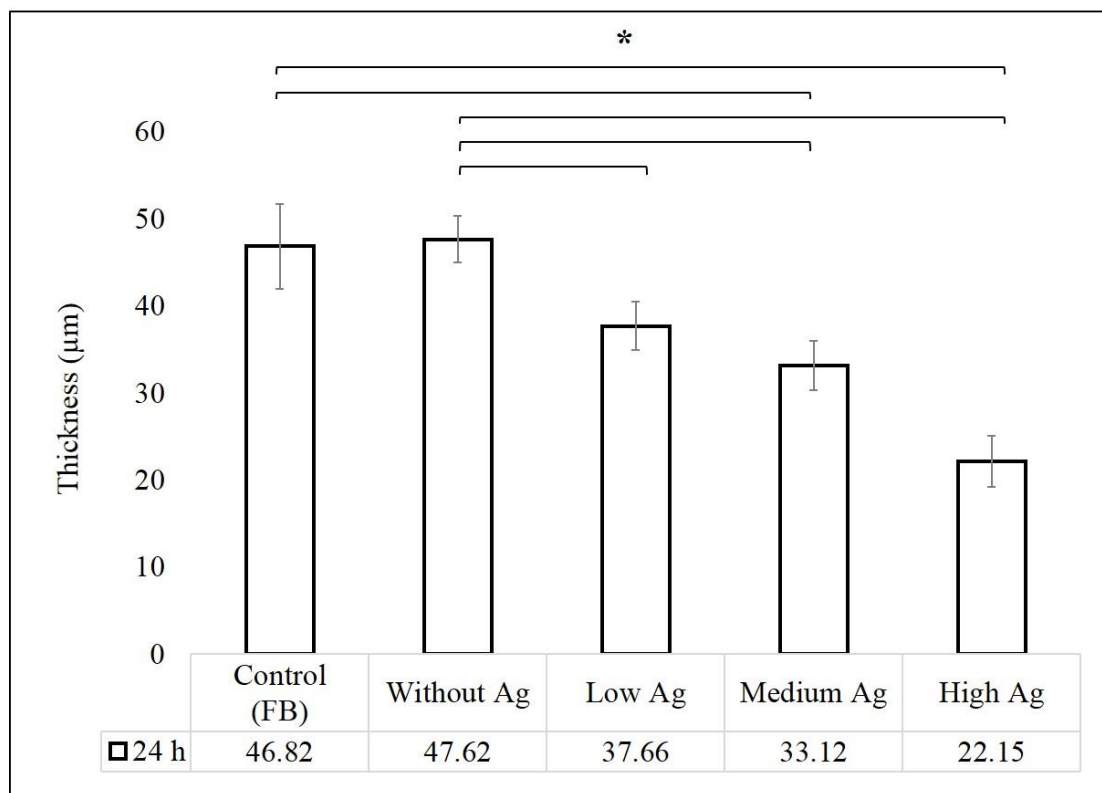


**Figure 5.23** Mean biofilm thickness ( $\mu\text{m}$ ) values of the AgNP-GIC.  $*(p\text{-value} < 0.05)$

Average diffusion distance is a biofilm description parameter that provides measures of the distances over which nutrients and other components have to diffuse from the void to bacteria included in micro-colonies. In other words, it estimates whether bacteria are organized to access or to hide from their environment. Average diffusion distance values ( $\mu\text{m}$ ) for biofilms developed on AgNP-GIC are gathered in Figure 5.24. Again, High Ag biofilms are statistically different from Without Ag and control ( $p\text{-value} < 0.01$ ). Medium Ag also showed lower average diffusion distance than control groups ( $p\text{-value} < 0.05$ ). In this case however, differences on average diffusion distance may be related to bio-volume of biofilms. Bacteria are more exposed to medium nutrients or

biocides when biomass is comparatively reduced than control. Therefore, increasing the amount of silver in the AgNP-GIC helps the biofilm to be more susceptible to biocides and/or antibacterial treatment that might be used.

Another parameter associated to this biofilm structure is the surface to bio-volume ratio, which is defined as the surface area divided by the bio-volume, where the surface area is the area of all biomass voxel surfaces exposed to the background. This parameter reflects the fraction of biofilm that is directly exposed to the nutrient flow and to silver ions released from the material. Thus, it may indicate how the biofilm adapts to its environment.

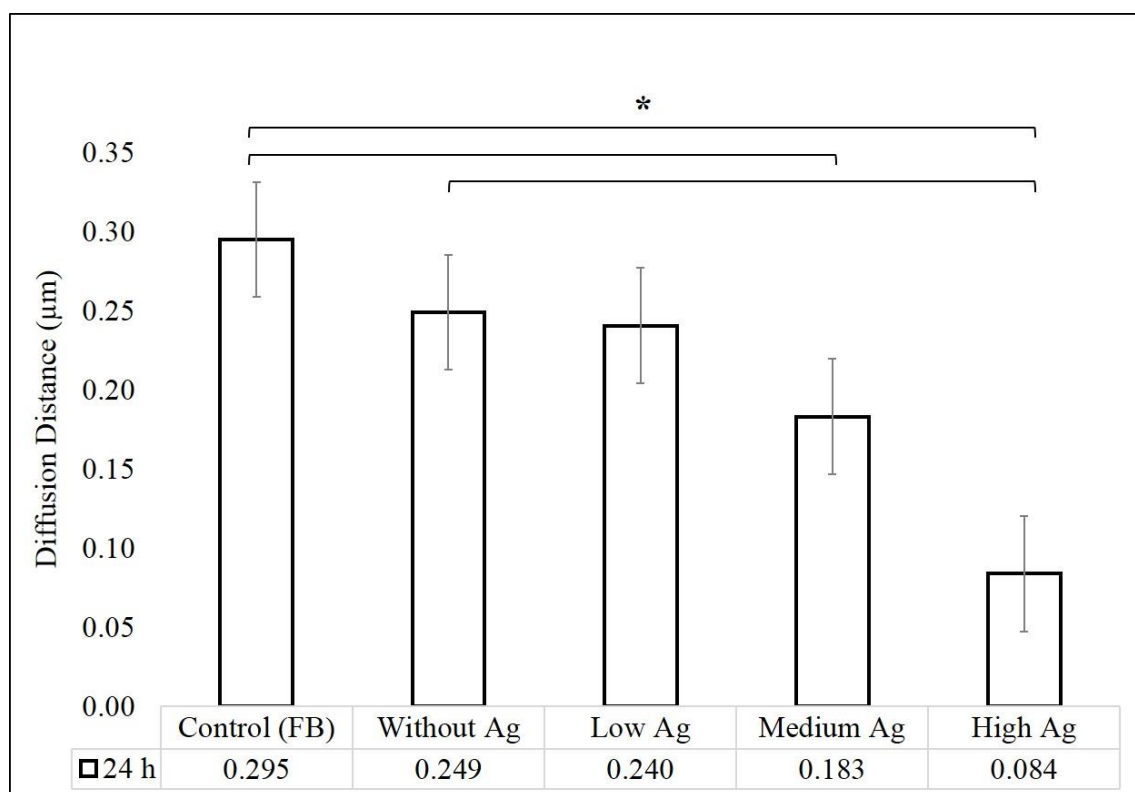


**Figure 5.24** Average diffusion distance (µm) values of 24 h biofilms on the AgNP-GIC. \*(*p*-value < 0.05)

Surface to bio-volume ( $\mu\text{m}^2/\mu\text{m}^3$ ) values of 24 h biofilms developed on AgNP-GIC are presented in Figure 5.25. In this context, biofilm over High Ag samples shows to be significantly different from the control and Without Ag ( $p$ -value  $< 0.01$ ), while Medium Ag is more likely to have bacteria directly in contact to environment than Without Ag ( $p$ -value  $< 0.01$ ). One might assume that bacteria are more and more exposed to nutrients and biocide (silver ions) as the silver concentration in environment increases. The most important fact is that such an undifferentiated biofilm may be more susceptible to treatment by antimicrobial agents [105], like those present in dentifrices, or may be easily removed from material surfaces by mechanical activity, such as tooth brushing or tongue movements.

Metabolic activity of the 24 h biofilms over GIC samples was assessed by MTT assay. Results are presented in Figure 5.26. High Ag biofilms evinces statistical difference from those formed on Without Ag, Low Ag and Medium Ag groups ( $p$ -value  $< 0.01$ ). High Ag materials caused a reduction of bacteria viability of 99% compared to values obtained with Without Ag. What should be remarked though is the fact that even with Medium Ag having statistically different biomass, mean thickness and surface to volume ratio from the Without Ag group, their viability as measured by MTT activity remained unaffected. The amount of SI released by diffusion from High Ag ( $\sim 1 \times 10^{-3}$  M), together with oxidation of AgNP exposed on the surface of cements inactivated the growth of the population of sessile bacteria and affected the biofilm structure. Although the results are not strictly comparable owing to different experimental conditions, it had been already remarked that the inhibitory concentrations and toxic concentrations are in the range of 0.1 to 20 mg. L<sup>-1</sup> ( $\sim 1 \times 10^{-6}$  to 2

x 10<sup>-4</sup> M for SI). Therefore, the total amount of SI have exceeded the minimal inhibitory concentration (MIC) at these conditions, and reduced viability of bacteria on the surface of the High Ag. Furthermore, lower concentrations of SI, which were not able to reduce bacteria viability, such as Medium Ag, may still affect important parameters of the biofilm structure.

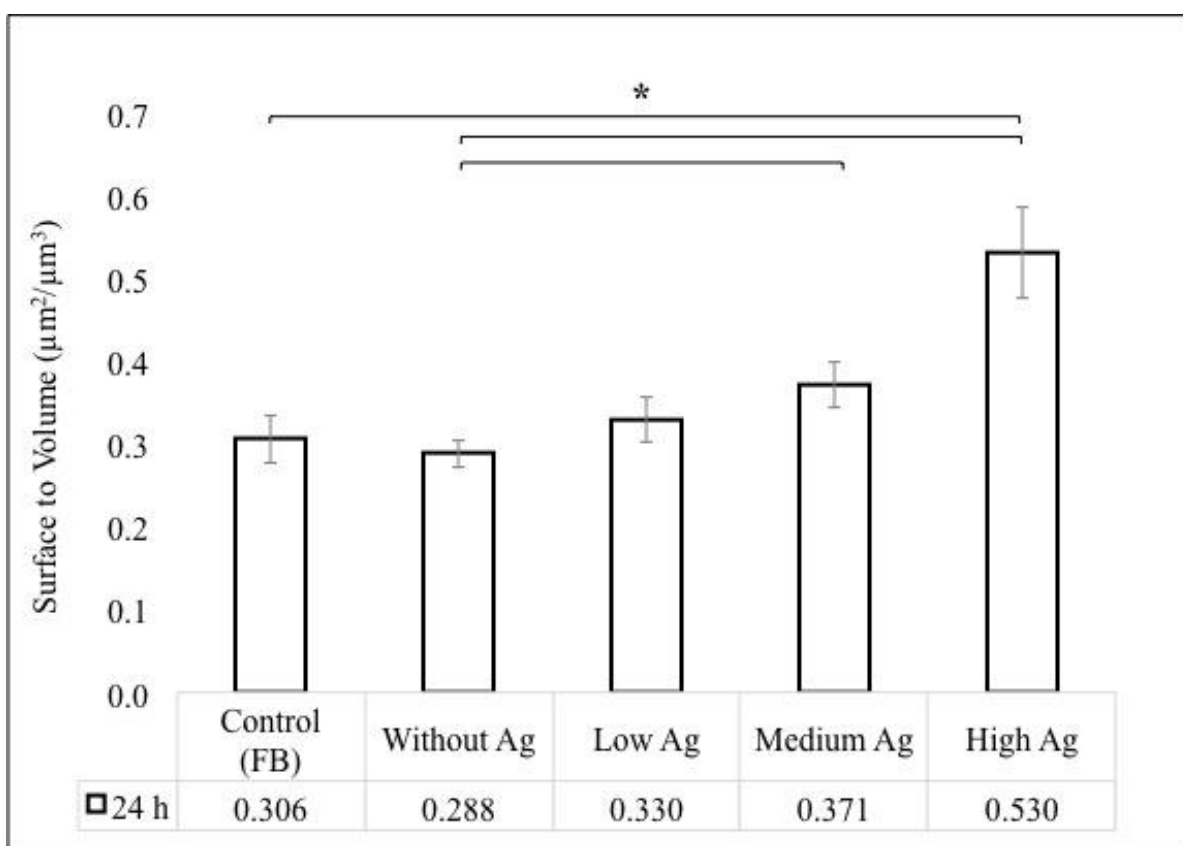


**Figure 5.25** Surface to Bio-volume values (µm<sup>2</sup>/µm<sup>3</sup>) of 24 h biofilms on the AgNP-GIC. \*(*p*-value < 0.05)

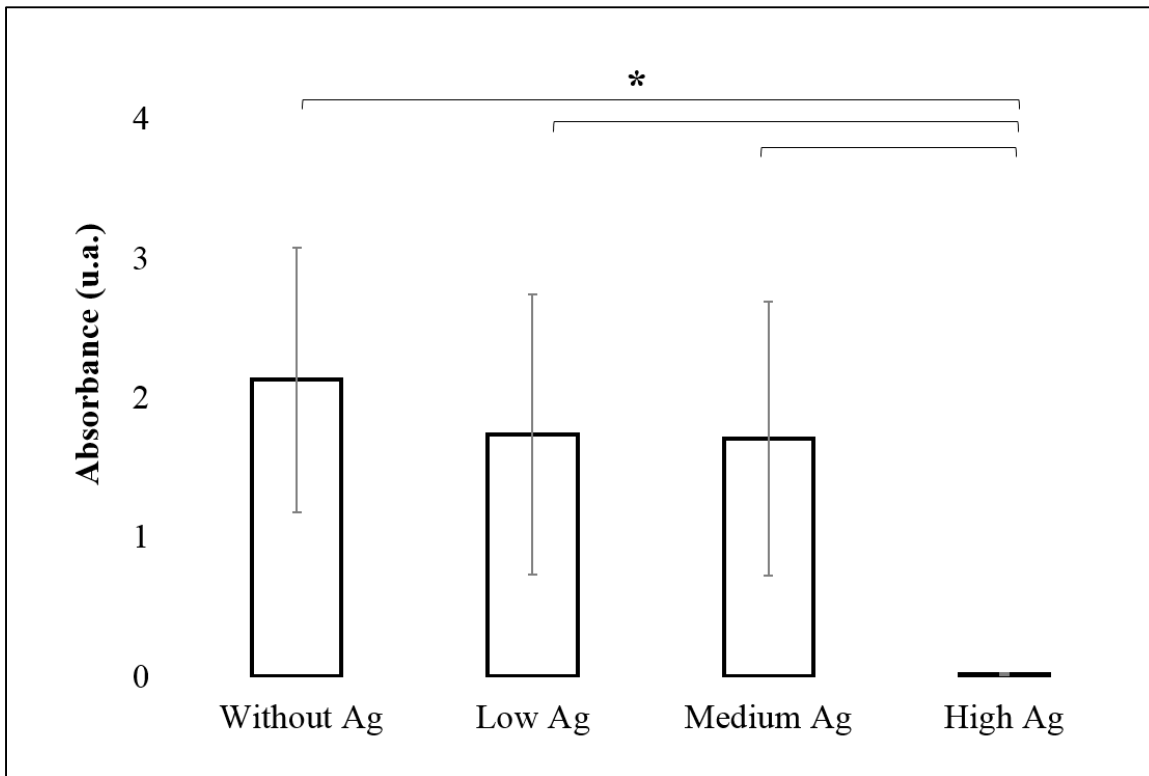


**Figure 5.26** Absorbance values from MTT assay of 24 h biofilm viability on the AgNP-GIC. \*( $p$ -value < 0.01)

An important issue was observed in evaluating salivary microcosm biofilm during different stages at the presence of a biocide, namely *Gala chinensis* extract (GCE) [193]. It was possible to detect reduced metabolism of bacteria in biofilms at lower concentrations of GCE than those inhibiting bacterial growth. The dose-response data for 48 h biofilms reveal a concentration dependency of the GCE effect, reaching significance with treatments above 1,000 ppm. In our study, dose-response for 24 h biofilm proved effective above 100 ppm ( $\sim 1 \times 10^{-3}$  M) of released SI. However, if biocide is bound to biofilms and slowly

released, as it is expected for SI released from AgNP, this could be disrupting biofilm formation. Inhibition of lactic acid production was observed with low levels of GCE present during the acid formation phase of the experiment, but did not caused bacterial killing. Even when a biocide penetrates slowly through a biofilm, it may inhibit acid formation at concentrations 10-fold lower than those inhibiting bacterial growth. This indicates the potential of subcritical doses of biocides as caries-preventive strategies, which affects biofilm growth and acid production.

Moreover, analyzing the presence of AgNP as potential biocide in other dental materials, a study [4] evaluated the antibacterial efficacy of AgNP formed *in situ* a photocrosslinking resin-based polymer. It was assessed by measuring three parameters (fraction of total surface area covered by bacteria; object density; and individual object area) of the initial bacterial colonization on composite disks with different silver salt concentrations. The results show that the concentration of SI released from the 0.03 wt. % silver salt substrates, the lowest concentration tested with the bacteria, was sufficient to reduce in 30 % *S. mutans* colonization. For the given concentration, ~ 0.05 atomic Ag (%) was detected by XPS on the surfaces of the resin-based polymer. Whereas, comparing AgNP-GIC data for the same concentration of silver salt added (Medium Ag), the percentage of reduction in early adhered bacteria (3h) on AgNP-GIC were ca. 70% compared to control and atomic Ag (%) analyzed by XPS was approximately twice the observed for resin-based polymers. The presence of additional silver nanoparticles (by higher silver salt concentrations) did not further enhance the antibacterial activity for resin-based polymers. The lack of a trend in antibacterial activity as a function of silver salt concentration was attributed to a reduction in activity when the silver nanoparticles are

aggregated. Maximum atomic silver value on the surfaces of resin-based polymers was ca. 0.10 % for 0.08 wt. % of silver salt added to the material. Different tendency was observed on AgNP-GIC, where atomic silver (%) was found to increase progressively with the percentage of silver salt added to the material, reaching 0.17 % for High Ag (0.15 wt. % of silver salt). Supporting this observation, it was already remarked that AgNP are more likely to be homogeneously dispersed and have higher water solubility when in a polyanion matrix (as for PAA-TA solution, and thus AgNP-GIC) than in resin-based systems [153, 154]. Thus, it is possible to assume that water-based cements like GIC, supporting AgNP as biocides, have increased bioactivity when compared to resin-based material.

Still comparing AgNP incorporated in resin-based polymers, another study [104] tested antibacterial activity against plaque microcosm biofilm of AgNP incorporated in a resin-based bonding agent. For a range of silver salt similar to that on AgNP-GIC, concentrations of 0.05 and 0.1 wt. % of nanoparticles added to the resin greatly decreased the biofilm viability, CFU counting and lactic acid production, compared to commercial adhesive control. Although the results are promising for application in terms of reduced viability and acid production, biofilm structures were not evaluated quantitatively.

In order to understand how bacteria respond to biocides when structured as biofilms, further evaluation is necessary than only analyzing viability, metabolism and CFU counting. Bacteria from plaque can communicate with one another in a cell density-dependent manner via small diffusible molecules (quorum sensing), using strategies similar to those described for other biofilms. In *S. mutans*, quorum sensing is known to be mediated by a competence-stimulating peptide (CSP), which increases the transformation frequency of biofilm-grown *S. mutans* from 10 to 600-fold [194].

Important mechanisms of cariogenic plaque, like acidogenicity and aciduricity (acid tolerance), may be as well related to cell-to-cell communication and its ability to form mature biofilms. As caries develops in an intermittently acidic environment, one of the most significant virulence properties of cariogenic bacteria like *S. mutans* is their aciduricity, which is also known to be involved with the CSP. Cell density and biofilm growth mode modulated acid adaptation in *S. mutans*, suggesting that optimal development of aciduricity in this organism involves both low pH induction and cell-to-cell communication [195]. Environmental cues, such as nutrient and biocide concentrations, pH, and adherence to a surface, are also known to modulate the level of the CSP or the effectiveness of CSP interaction with the receptors [195, 196]. For example, SI have been suggested to oxidize thiol groups and, therefore, reduce acidogenicity of dental plaque [197].

Demonstrating how architecture of biofilms may influence bacteria communication, and thus its metabolism, Li *et al.* [196] essayed *S. mutans* wild-type NG8 and mutant strains for their ability to initiate biofilm formation. The spatial distribution and architecture of the biofilms were evaluated by CSLM. The results showed that inactivation of any of the individual genes under study resulted in the formation of an abnormal biofilm. The *comC* mutant, unable to produce or secrete a CSP, formed biofilms with altered architecture, with extremely long chains, resulting in the formation of large aggregates or web-like biofilms, as it was observed for biofilms grown on AgNP-GIC. The *comD* and *comE* mutants, which were defective in sensing and responding to the CSP, formed biofilms with reduced biomass. It is important to remark that at least some bacteria must not only be able to sense surfaces and nutritional conditions for the transition to biofilm life but also apparently

require cell-to-cell signaling and other coordinated activities to form differentiated, mature communities [196]. These results affirm the idea that viable bacteria with difficulty concerning cell-to-cell communication tend to form undifferentiated biofilms due to interference in the quorum sensing system. Although not being conclusive, this may provide an insight of the observed fact that subcritical concentrations of biocides are influencing architecture of viable biofilms.

Still, *S. mutans* uses quorum-sensing signal transduction system to stimulate the uptake and incorporation of foreign DNA. Dental biofilm may provide streptococci with a vast reservoir of genetic information which can be readily incorporated outside of their species boundaries [198]. Considering the potential for transferring of antibiotic resistance to pathogens that may transiently reside in biofilm, disruption of cell-to-cell communication system might have important implications.

Interaction with surfaces containing AgNP reduced homogeneity and biomass of the 24 h *S. mutans* biofilm. Thus, SI concentrations lower than MIC released by oxidation of AgNP-GIC surfaces, as observed for Low Ag and Medium Ag, may be leading to the formation of unstructured *S. mutans* biofilms. The mechanism of interfering in cell density, and thus in cell-to-cell communication, might be the explanation for the young architecture of 24 h biofilms formed over AgNP-GIC. It may be hypothesized that SI are binding to CPS receptors in cell membrane and/or contributing to defective gene expression of adhered-bacteria. However, more specific studies of molecular biology should be carried out in order to affirm that SI are directly affecting quorum-sensing system.

The rapid suppression of the resident oral microflora by administration of antibiotics can result in overgrowth by previously minor components of the microflora, or colonization by exogenously acquired (and often pathogenic) microorganisms. Thus, the resident microflora acts directly as an important component of the host defenses by forming a significant barrier against exogenous populations, termed “colonization resistance” [194]. That’s one reason why SI might be a strategic antibacterial agent in the oral environment. These ions are not expected to have long distance interaction with oral microflora due to their great affinity to abundant chloride ions in saliva (tending to form sparingly soluble silver salts) or to adhered pellicle [116]. Thus, microbial homeostasis of biofilms formed away from Ag-containing surfaces is not likely to be disrupted, whereas biofilms formed onto these surfaces may be easily removed.

## VI. Final Considerations

---

Silver compounds have been used in dental pediatric clinics for more than a decade as the silver diamine fluoride (SDF) treatment. It is a cost-effective agent and appears to conform to the World Health Organization's Millennium Goals and the US Institute of Medicine's criteria for 21<sup>st</sup> century medical care [199]. Arrest and prevention of active caries have been proved effective under SDF treatment [200, 201]. A literature search indicates that there were no reported cases about acute toxicity or significant adverse effects after professional application of SDF. Even though SDF solution concentrations used for treating caries range from 12 to 38 %, it is considered a minimal chance of excess silver accumulation causing toxicity, since only a minute amount of SDF is applied to the dental tissue semi-annually or annually [202]. Previous studies suggest that SDF did not cause severe pulpal reactions, and no severe pulpal damages have been reported [200, 201, 203]. An *ex vivo* study shows that over 90% of the deep carious primary teeth treated with SDF showed favorable pulpal response histologically, which was evidenced by the presence of abundant reparative dentine and a wide odontoblast layer [203]. Although indirect cytotoxicity test on HGF-1 reduced cell viability of High Ag groups, these clinical studies indicate that greater amounts of SI delivered by ordinary caries stopping treatments on clinical practice are not likely to cause severe pulpal damages.

Moreover, the choice of GIC as matrix for supporting AgNP concerning their use in dental practice can be sustained by bioactivity of the given cements and their specific role

on fighting dental caries. It is worth to highlight that release of fluoride and exchange of metal ions with tooth structure are remarkable properties that make GIC important materials in the fight against caries. Such materials have the potential for ‘smart’ behavior, i.e. they can react to changes in the environment to bring about advantageous changes in properties. The controlled movement of water or aqueous media through the material may be the carrier for various dissolved species, and may influence the potential for the formation of biofilms at the surface. Clearly, materials that do not have the capacity for water transport or storage do not have the potential for this sort of behavior [181, 204]. Thus, due to these specific properties of water-based GIC, the presence of silver and fluoride ions being released by AgNP-GIC would impart anti-adherent and cariostatic properties. Demineralized dentin disks treated with silver fluoride (AgF) showed to prevent formation of an *S. mutans* biofilm and were significantly more resistant to further demineralization than the control disks. The presence of silver and fluoride in the outer layers of the disks treated with AgF was the likely cause of prevention of biofilm formation [205].

During the first phase of the setting reaction when GIC are exchanging ions with tooth structure of their surroundings, and therefore in direct contact with decayed dental tissue, the arresting of active caries with direct uptake of silver and fluoride is targeted. In addition, the surfaces that are going to host the formation of biofilms are expected to have anti-adherent and/or antibacterial features. This would enable AgNP-GIC to provide a suitable caries management treatment together with reduced biofilm accumulation on the restoratives.

In this context, indication of AgNP-GIC in the treatment of active and rampant caries, or more specifically, early childhood caries (ECC) might be of major importance. ECC has been regarded as one of the most prevalent chronic diseases in early childhood. Advanced and severe rampant caries affects multiple teeth, and is typically seen in children with neglected oral care, frequent sugar or syrup medicine intake, individuals with decreased salivary flow, and those with poor oral hygiene and drug addiction. Patients with rampant caries are very challenging to manage and the prognosis is not often satisfactory [202]. SDF treatment usually is the elected treatment for rampant caries [206], or more traditionally the surgical removal of all the infected and softened dental tissue followed by the filling of the cavity to restore the function and aesthetics of the tooth. In addition, conventional restorative method alone is insufficient at tackling this prevalent disease [202]. Therefore, AgNP-GIC would assemble restorative characteristics from Atraumatic Restorative Technique (ART) approach and cariostatic activity attributed to release of silver and fluoride ions coupled with a low cost production and an easy application procedure at once.

Other strategies to produce anti-adhesive surfaces have been used to reduce biofilm viability and formation over resin modified glass ionomer cements (RMGIC), which is a composite that are supposed to have both GIC and resin-based polymers properties, like bioactivity and stability, respectively. However biocompatibility to human cells was not proved [104, 105]. Further elaboration of RMGIC containing AgNP-GIC would be possible, since conventional GIC composition is the basis of the RMGIC formulation. This would broaden their range of application in dental practice.

Another issue to be remarked here is the necessity of achieving aesthetical results. In SDF treatment, although the dental aesthetics is not pleasing, it is considered that children with arrested caries will at least be less susceptible to suffer from pain and infection. Although AgNP-GIC initially presents yellowish/brown coloration due to the presence of silver nanoparticles, it is far more aesthetically acceptable than the results of SDF treatment. Or, at least, the same argument should be applied to AgNP-GIC color. Moreover, as observed for the AgNP solutions after synthesis, the color intensity of the material is directly related to the presence of high concentrations of AgNP due to their optical Plasmon Resonance properties. One might assume that once silver ions starts to be released in the saliva medium during the first 24 h (i.e., first phase of setting reaction), coloration of AgNP-GIC are likely to be more and more reduced in intensity, thus rising its acceptability. Using silver concentrations lower than the MIC should also diminish color intensity, and still contribute for biofilm formation disruption, as observed in Medium Ag groups.

If aesthetics is of major importance, this treatment might be followed by the sandwich technique [47]. This would imply an initial caries management control, by placing AgNP-GIC at once in all decayed teeth. In following sessions each restoration could be replaced by wearing the material surface to the bottom and complement with a suitable material for long-term restorations, such as composite resins or ceramics.

## VII. Conclusions

---

- Silver nanoparticles were synthesized *in situ* in the poly(acrylic acid) solutions containing tartaric acid by UV irradiation inducing an electron transfer from uncoordinated carboxylate groups of the polyelectrolyte to the Ag<sup>+</sup> specie.
- Spheroidal silver nanoparticles with size distribution centered at 7 to 10 nm, depending on the initial formulation, remained stable in the polyelectrolyte matrix up to a monitoring of 180 days.
- The colloidal system was sustained via electrosteric stabilization by regulating initial tartaric acid concentration (Ag<sup>+</sup>/COO<sup>-</sup> molar ratio) and UV exposure time of each formulation.
- Despite net setting time have increased with addition of AgNP, the setting reaction remained acceptable according to the ISO requirements.
- Compression strength of the analysed GIC were not damaged by in situ synthesis of AgNP, and assigning increased CS values for High Ag when compared to control. Medium Ag and Low Ag had similar values to that of reference material (Vitro Molar<sup>TM</sup>), indicating the potential use of the AgNP-GIC for dental application.
- High Ag proved to release a significant larger amount of silver content when incubated in deionized water for 24 h compared to Medium Ag and Low Ag.
- After adsoption of salivary protein on the surface of the cements, the quantity of silver directly exposed for bacterial adhesion is diminished.

- HGF-1 viability decreased significantly in High Ag group because of the great amount of silver ions released from these cements.
- All silver containing groups showed significant differences of inhibition of *E. coli* growth by diffusion on agar plates, suggesting bioactivity of the AgNP-GIC.
- Early-adhered bacteria (3 h) showed tendency to form microcolonies of agglomerated bacteria on the surfaces of the AgNP-GIC compared to FB (control) ( $p < 0.05$ ), and biomass values were significant different from the Without Ag ( $p < 0.05$ ).
- Biomass values of 24 h biofilm on Medium Ag and High Ag groups showed statistical significant difference from FB (control) ( $p < 0.05$ ), as well as from Without Ag ( $p < 0.05$ ).
- Medium Ag affected important parameters of the biofilm structure, like biomass, mean thickness and surface to volume ratio compared to Without Ag, but viability as measured by MTT activity was not significantly changed for bacteria on biofilms, neither for HGF-1 cells.
- The amount of SI originated from High Ag was effective in inactivating the growth of the population of sessile bacteria and affected the biofilm structure, reducing viability of bacteria, but also of HGF-1 cells.
- It can be stated that the new AgNP-GIC developed in this work proved biocidal effect against 24 h *S. mutans* biofilms, suggesting the oxidative dissolution of silver ions from the cement matrix, without necessarily causing cytotoxic effect on HGF-1 cells or reducing compression strength of the final cement.

## VIII. Proposal Of Future Studies

---

- Synthesis of AgNP by in situ photoreduction in PAA solution of a commercially available GIC;
- Synthesis of AgNP by in situ photoreduction in different PAA homopolymers and copolymers solutions;
- Study of the influence of different ionomer glass compositions on the bioactivity and biocidal activities of AgNP-GIC;
- Investigation of the mechanism of purification process in PAA solution by in situ photochemical synthesis of AgNP;
- Study of the mechanism by which subcritical amount of silver ions are disrupting biofilm formation, and whether it may be related to interfering in quorum sensing system of cariogenic bacteria, its acid production, acid tolerance and/or bacterial resistance;
- *Ex vivo* evaluation of ions exchange of AgNP-GIC with dental tissue and *in vitro* caries inhibition;
- Evaluation of the cytotoxic response of AgNP-GIC on odontoblasts and histological response of pulpal tissues through a dentin barrier.

## IX. References

---

1. POUL ERIK, P. "The World Oral Health Report 2003: continuous improvement of oral health in the 21st century – the approach of the WHO Global Oral Health Programme." **Community Dentistry and Oral Epidemiology**, 2003.
2. WILSON, A.D. and KENT, B.E. "The glass-ionomer cement, a new translucent dental filling material." **Journal of Applied Chemistry and Biotechnology**, v. 21, n. 11, p. 313, 1971.
3. TEN CATE, J.M. The need for antibacterial approaches to improve caries control. **Advances in Dental Research**, v. 21, n. 1, p. 8-12, 2009.
4. CHENG, Y.-J.J.; ZEIGER; D.N.; HOWARTER, J.A.; ZHANG, X.; LIN, N.J.; ANTONUCCI, J.M. and LIN-GIBSON, S. "*In situ* formation of silver nanoparticles in photocrosslinking polymers." **Journal of Biomedical Materials Research. Part B, Applied biomaterials**, v. 97, p. 1, p. 124-131, 2011.
5. DALLAS, P.; SHARMA, V.K. and ZBORIL, R. "Silver polymeric nanocomposites as advanced antimicrobial agents: classification, synthetic paths, applications, and perspectives." **Advances in Colloid and Interface Science**, 2011. 166(1-2): p. 119-135.
6. WILSON, A.D. "A hard decade's work: steps in the invention of the glass-ionomer cement." **Journal of Dental Research**, v. 75, n. 10, p. 1723-1727, 1996.
7. WILSON, A.D. and KENT, B.E. "A new translucent cement for dentistry. The glass ionomer cement." **British Dental Journal**, v. 132, n. 4, p. 133-135, 1972.
8. UPADHYA, N.P. and KISHORE, G. "Glass ionomer cement: The different generations." **Trends Biomater Artif Organs**, v. 18, n. 2, p. 158-165, 2005.
9. CRISP, S. and WILSON, A.D. "Reactions in glass ionomer cements: V. Effect of incorporating tartaric acid in the cement liquid." **Journal of Dental Research**, v. 55, n. 6, p. 1023-1031, 1976.
10. WILSON, A.D. and CRISP, S. "Ionomer cements." **British Polymer Journal**, v. 7, n. 5, p. 279-296, 1975.

11. CRISP, S.; LEWIS, B.G.; WILSON, A.D. "Characterization of glass-ionomer cements. 5. The effect of the tartaric acid concentration in the liquid component." **Journal of Dentistry**, v. 7, n. 4, p. 304-312, 1979.
12. SCED, I.R. and WILSON, A.D. **Poly(carboxylic acid) hardenable compositions**. B. Pat, Editor. 1980.
13. MCLEAN, J.W. and GASSER, O. "Glass-cermet cements." **Quintessence International**, v. 16, n. 5, p. 333-343, 1985.
14. PROSSER, H.J.; POWIS, D.R.; WILSON, A.D. "Glass-ionomer cements of improved flexural strength." **Journal of Dental Research**, v. 65, n. 2, p. 146-148, 1986.
15. NICHOLSON, J.W. "Chemistry of glass-ionomer cements: a review." **Biomaterials**, v. 19, n. 6, p. 485-494, 1998.
16. WOOD, D. and HILL, R. "Structure-property relationships in ionomer glasses." **Clinical Materials**, v. 7, p. 301-312, 1991.
17. STANTON, K. and HILL, R. "The role of fluorine in the devitrification of  $\text{SiO}_2 \cdot \text{Al}_2\text{O}_3 \cdot \text{P}_2\text{O}_5 \cdot \text{CaO} \cdot \text{CaF}_2$  glasses." **Journal of Materials Science**, v. 7, n. 4, p. 301-312, 2000.
18. WILSON, A.D. "The chemistry of dental cements." **Chemistry Society Review**, v. 7, n. 2, p. 265-296, 1978.
19. STAMBOULIS, A. and WANG, F. "Ionomer Glasses: design and characterization." **Advanced Biomaterials: Fundamentals**, 2010: 768 p.
20. WILSON, A.D. "Experimental luting agents based on the glass ionomer cements." **British Dental Journal**, v. 142, n. 4, p. 117-122, 1977.
21. CRISP, S.; LEWIS, B.G. and WILSON, A.D. "Gelation of polyacrylic acid aqueous solutions and the measurement of viscosity." **Journal of Dental Research**, v. 54, n. 6, p. 1173-1175, 1975.
22. MCLEAN, J.W.; WILSON, A.D. and PROSSER, H.J. "Development and use of water-hardening glass-ionomer luting cements." **Journal of Prosthetic Dentistry**, v. 52, n. 2, p. 175-181, 1984.
23. BARRY, T.I.; CLINTON, D.J. and WILSON, A.D. "The Structure of a Glass-Ionomer Cement and its Relationship to the Setting Process." **Journal of Dental Research**, v. 58, n. 3, p. 1072-1079, 1979.

24. CRISP, S. and WILSON, A.D. "Reactions in glass ionomer cements: III. The precipitation reaction." **Journal of dental research**, v. 53, n. 6, p. 1420-1424, 1973.
25. MITRA, S.B. "Adhesion to dentin and physical properties of a light-cured glass-ionomer liner/base." **Journal of dental research**, v. 70 , n. 1, p. 72-74, 1990.
26. ANUSAVICE, K.J. *et al.*, **Phillips' science of dental materials**. 5<sup>a</sup>. ed. Saunders, Elsevier Health Sciences, 2012, 764 p.
27. GRIFFIN, S.G. and HILL, R.G. "Influence of glass composition on the properties of glass polyalkenoate cements. Part I: influence of aluminium to silicon ratio." **Biomaterials**, v. 20, n. 17, p. 1579-86. 1999.
28. CRISP, S.; PRINGUER, M.A.; WARDLEWORTH, D. *et al.* "Reactions in Glass Ionomer Cements: II. An Infrared Spectroscopic Study." **Journal of Dental Research**, v. 53, n. 6, p. 1414-1419. 1974.
29. NICHOLSON, J.W.; BROOKMAN, P.J.; LACY, O.M. and WILSON A.D. "Fourier transform infrared spectroscopic study of the role of tartaric acid in glass-ionomer dental cements." **Journal of Dental Research**, v. 67, n. 12, p. 1451-1454, 1988.
30. PROSSER, H.J.; RICHARDS, C.P. and WILSON, A.D. "NMR spectroscopy of dental materials. II. The role of tartaric acid in glass-ionomer cements." **Journal of Biomedical Material Research**, v. 16, n. 4, p. 431-445, 1982.
31. HATTON, P.V. and BROOK, I.M. "Characterisation of the ultrastructure of glass-ionomer (poly-alkenoate) cement." **British Dental Journal**, v. 173, n. 8), p. 275-277, 1992.
32. WASSON, E.A. and NICHOLSON, J.W. "Change in pH during setting of polyelectrolyte dental cements." **Journal of Dentistry**, v. 21, n. 2, p. 122-126, 1993.
33. YOUNG, A.M.; RAFEEKA, S.A. and HOWLETT, J.A. "FTIR investigation of monomer polymerisation and polyacid neutralisation kinetics and mechanisms in various aesthetic dental restorative materials." **Biomaterials**, v. 25, n. 5, p. 823-833. 2004.
34. MUNHOZ, T., KARPUKHINA, N.; HILL, R.G. *et al.* "Setting of commercial glass ionomer cement Fuji IX by (27)Al and (19)F MAS-NMR." **Journal of Dentistry**, v. 38, n. 4, p. 325-330, 2010.
35. WILSON, A.D., PROSSER, H.J. and POWIS, D.M. "Mechanism of adhesion of polyelectrolyte cements to hydroxyapatite." **Journal of Dental Research**, v. 62, n. 5, p. 590-592, 1983.

36. YOSHIDA, Y.; VAN MEERBEEK, B.; NAKAYAMAET, Y. *et al.* "Evidence of chemical bonding at biomaterial-hard tissue interfaces." **Journal of Dental Research**, v. 79, n. 2, p. 709-714, 2000.
37. FRENCKEN, J.E.; PETERS, M.C.; MANTON, D.J. *et al.* "Minimal intervention dentistry for managing dental caries - a review: report of a FDI task group." **International Dental Journal**, v. 62, n. 5, p. 223-243, 2012.
38. FEJERSKOV, O.; KIDD, E.A.M. and NYVAD, B. "Defining the disease: an introduction", in **Dental Caries. The Disease and its Clinical Management**. Blackwell Publishing Ltd: Oxford. 2008, p. 3-6.
39. FERREIRA, S.H.; BERIA, J.U.; KRAMER, P.F. *et al.* "Dental caries in 0- to 5-year-old Brazilian children: prevalence, severity, and associated factors." **International Journal of Paediatric Dentistry**, v. 17, n. 4, p. 289-296, 2007.
40. FEATHERSTONE, J.D. "The science and practice of caries prevention." **Journal of American Dental Association**, v. 131, n. 7, p. 887-899, 2000.
41. FEJERSKOV, O. "Concepts of dental caries and their consequences for understanding the disease." **Community Dentistry and Oral Epidemiology**, v. 25, n. 1, p. 5-12. 1997.
42. KIDD, E.A.M. and FEJERSKOV, O. "What Constitutes Dental Caries? Histopathology of Carious Enamel and Dentin Related to the Action of Cariogenic Biofilms." **Journal of Dental Research**, v. 83, suppl 1, p. C35-C38, 2004.
43. SILLEN, A. and LEGEROS, R. "Solubility profiles of synthetic apatites and of modern and fossil bones." **Journal of Archaeological Science**, v. 18, n. 3, p. 385-397. 1991.
44. CCAHUANA-VASQUEZ, R.A. and CURY, J.A. "*S. mutans* biofilm model to evaluate antimicrobial substances and enamel demineralization." **Brazilian Oral Research**, v. 24, n. 2, p. 135-41, 2010.
45. CURY, J.A. and TENUTA, L.M. "Enamel remineralization: controlling the caries disease or treating early caries lesions?" **Brazilian Oral Researcj**, v. 23, suppl 1, p. 23-30. 2009.
46. AOBA, T. "Solubility properties of human tooth mineral and pathogenesis of dental caries." **Oral Disease**, v. 10, n. 5, p. 249-245, 2004.

47. TYAS, M.J.; ANUSAVICE, K.J.; FRENCKEN, J.E. *et al.* "Minimal intervention dentistry--a review. FDI Commission Project 1-97." **International Dental Journal**, v. 50, n. 1, p. 1-12, 2000.
48. FUSAYAMA, T. "Two layers of carious dentin; diagnosis and treatment." **Operative dentistry**, v. 4, n. 2, p. 63-70, 1979.
49. MASSARA, M.L.A.; ALVES, J.B. and BRANDÃO, P.R.G. "Atraumatic Restorative Treatment: Clinical, Ultrastructural and Chemical Analysis." **Caries Research**, v. 36, n. 6, p. 430-436, 2002.
50. YIP, H.K.; SMALES, R.J.; NGO, H.C. *et al.* "Selection of restorative materials for the atraumatic restorative treatment (ART) approach: a review." **Special Care Dentistry**, v. 21, n. 6, p. 216-221, 2001.
51. FRENCKEN, J.E. "The ART approach using glass-ionomers in relation to global oral health care." **Dental Materials**, v. 26, n. 1, p. 1-6, 2010.
52. SMALES, R.J.; NGO, H.C.; YIP, K.H.; YU, C. "Clinical effects of glass ionomer restorations on residual carious dentin in primary molars." **American Journal of Dentistry**, v. 18, n. 3, p. 188-193, 2005.
53. KARIN, L.W. and HENK, J.G. "The residual caries dilemma." **Community Dentistry and Oral Epidemiology**, v. 27, n. 6, p. 436-441, 1999.
54. OONG, E.M.; GRIFFIN, S.O.; KOHN, W.G.; GOOCH, B.F.; CAUFIELD, P.W. "The effect of dental sealants on bacteria levels in caries lesions: a review of the evidence." **Journal of the American Dental Association**, v. 139, n. 3, p. 271, 2008.
55. YIP, H.K.; TAY, F.R.; NGO, H.C.; SMALES, R.J.; PASHLEY, D.H. "Bonding of contemporary glass ionomer cements to dentin." **Dental Materials**, v. 17, n. 5, p. 456-70, 2001.
56. NGO, H., "Glass-ionomer cements as restorative and preventive materials." **Dental Clinics of North America**, v. 54, p. 551-563, 2010.
57. GANDOLFI, M.G.; CHERSONI, S.; ACQUAVIVA, G.L.; PIANA, G.; PRATI, C. Mongiorgi R. Fluoride release and absorption at different pH from glass-ionomer cements. **Dental Materials**, v. 22, n. 5, p. 441-449, 2006.

58. SMALES, R.J. and GAO, W. "In vitro caries inhibition at the enamel margins of glass ionomer restoratives developed for the ART approach." **Journal of Dentistry**, v. 28, n. 4, p. 249-256, 2000.
59. DONLAN, R.M. and COSTERTON, J.W. "Biofilms: survival mechanisms of clinically relevant microorganisms." **Clinical Microbiology Review**, v. 15, n. 2, p. 167-93, 2002.
60. DONLAN, R.M., "Biofilms: microbial life on surfaces." **Emerging Infectious Diseases**, v. 8, n.9, p. 881-90, 2002.
61. STEWART, P.S. and COSTERTON, J.W. "Antibiotic resistance of bacteria in biofilms." **Lancet**, v. 358, n. 9276, p. 135-8, 2001.
62. GU, H. and REN, D. "Materials and surface engineering to control bacterial adhesion and biofilm formation: A review of recent advances." **Frontiers of Chemical Science and Engineering**, v. 8, n. 1, p. 20-33, 2014.
63. SAUER, K.; CAMPER, A.K.; EHRLICH, G.D.; COSTERTON, J.W.; DAVIES, D.G. "Pseudomonas aeruginosa displays multiple phenotypes during development as a biofilm." **Journal of Bacteriology**, v. 184, n. 4, p. 1140-1154, 2002.
64. DUNNE, W.M., "Bacterial Adhesion: Seen Any Good Biofilms Lately?" **Clinical Microbiology Reviews**, v. 15, n. 2, p. 155-166, 2002.
65. STOODLEY, P.; SAUER, K.; DAVIES, D.G.; COSTERTON, J.W. "Biofilms as complex differentiated communities." **Annual Reviews in Microbiology**, v. 56, n. 1, p. 187-209, 2002.
66. HOUDT, R.V. and MICHIELS, C.W. "Role of bacterial cell surface structures in Escherichia coli biofilm formation." **Research in microbiology**, v. 156, p. 626-633, 2005.
67. PALMER, J.; FLINT, S. and BROOKS, J. "Bacterial cell attachment, the beginning of a biofilm." **J Ind Microbiol Biotechnol**, v. 34, n. 9, p. 577-88, 2007.
68. PLOUX, L.; PONCHE, A. and ANSELME, K. "Bacteria/material interfaces: role of the material and cell wall properties." **Journal of Adhesion Science and Technology**, v. 24, n. 13, p. 2165-2201, 2010.
69. RENNER, L.D. and WEIBEL, D.B. "Physicochemical regulation of biofilm formation." **MRS Bull**, v. 36, n. 5, p. 347-355, 2011.

70. SUNTHARALINGAM, P. and CVITKOVITCH, D.G. "Quorum sensing in streptococcal biofilm formation." **Trends Microbiol**, v. 13, n. 1, p. 3-6, 2005.
71. KOLENBRANDER, P.E.; PALMER, R.J.Jr.; PERIASAMY, S.; JAKUBOVICS, N.S. "Oral multispecies biofilm development and the key role of cell-cell distance." **Nat Rev Microbiol**, v. 8, n. 7, p. 471-80, 2010.
72. MARSH, P.D. "Are dental diseases examples of ecological catastrophes?" **Microbiology**, v. 149, n. 2, p. 279-94, 2003.
73. KOLENBRANDER, P.E. "Oral microbial communities: biofilms, interactions, and genetic systems." **Annual Review Microbiololy.**, v. 54, p. 413-37, 2000.
74. MARSH, P.D. "Microbiology of dental plaque biofilms and their role in oral health and caries." **Dental Clinics of North America**, v. 54, n. 3, p. 441-454, 2010.
75. KOLENBRANDER, P.E.; ANDERSEN, R.N.; BLEHERT, D.S.; EGLAND, P.G.; FOSTER, J.S.; PALMER, R.J.Jr. "Communication among oral bacteria." **Microbiology and Molecular Biology Reviews**, v. 66, n. 3, p. 486, 2002.
76. BURNE, R.A.; AHN, S.J.; WEN, Z.T.; ZENG, L.; LEMOS, J.A.; ABRANCHES, J.; NASCIMENTO, M. "Opportunities for disrupting cariogenic biofilms." **Advances in Dental Research**, v. 21, n. 1, p. 17-20, 2009.
77. FILOCHE, S.; WONG, L. and SISSONS, C.H. "Oral biofilms: emerging concepts in microbial ecology." **Journal of Dental Research**, v. 89, n. 1, p. 8-18, 2010.
78. LOESCHE, W.J. "Clinical and microbiological aspects of chemotherapeutic-agents used according to the specific plaque hypothesis." **Journal of Dental Research**, v. 58, n. 12, p. 2404-2412, 1979.
79. AAS, J.A.; GRIFFEN, A.L.; DARDIS, S.R.; LEE, A.M.; OLSEN, I.; DEWHIRST, F.E. *et al.* "Bacteria of dental caries in primary and permanent teeth in children and young adults." **Journal of clinical microbiology**, v. 46, n. 4, p. 1407-1417. 2008.
80. BEIGHTON, D. "The complex oral microflora of high-risk individuals and groups and its role in the caries process." **Community Dent Oral Epidemiol**, v. 33, n. 4, p. 248-55, 2005.
81. LEMOS, J.A.; QUIVEY, R.G.Jr.; KOO, H.; ABRANCHES, J. "*Streptococcus mutans*: a new Gram-positive paradigm?" **Microbiology**, v. 159, n. 3, p. 436-45, 2013.

82. BEYTH, N.; FARAH, S.; DOMB, A.J.; WEISS, E.I. "Antibacterial dental resin composites." **Reactive and Functional Polymers**, v. 75, p.81-88, 2013.
83. ØGAARD, B.; BRANTLEY, W.A. and ELIADES, T. "Oral microbiological changes, long-term enamel alterations due to decalcification, and caries prophylactic aspects." In: **Orthodontic materials. Scientific and clinical aspects**. Thieme Stuttgart, New York, 2001.
84. XU, X. and BURGESS, J.O. "Compressive strength, fluoride release and recharge of fluoride-releasing materials." **Biomaterials**, v. 24, n. 14, p. 2451-61, 2003.
85. YAP, A.U.; KHOR, E. and FOO, S.H. "Fluoride release and antibacterial properties of new-generation tooth-colored restoratives." **Operative dentistry**, v. 24, n. 5, p. 297-305, 1998.
86. YAMAMOTO, K.; OHASHI, S.; AONO, M.; KOKUBO, T.; YAMADA, I.; YAMAUCHI, J. "Antibacterial activity of silver ions implanted in SiO<sub>2</sub> filler on oral streptococci." **Dent Mater.**, v. 12, n. 4, p. 227-9, 1996.
87. KAWASHITA, M.; TSUNEYAMA, S.; MIYAJI, F.; KOKUBO, T.; KOZUKA, H.; YAMAMOTO, K. "Antibacterial silver-containing silica glass prepared by sol-gel method." **Biomaterials**, v. 21, p. 4; p. 393-8, 2000.
88. SPENCER, C.G.; CAMPBELL, P.M.; BUSCHANG, P.H.; CAI, J.; HONEYMAN, A.L. "Antimicrobial effects of zinc oxide in an orthodontic bonding agent." **Angle Orthod**, v. 79, n. 2, p. 317-22, 2009.
89. ALLAKER, R.P. and MEMARZADEH, K. "Nanoparticles and the control of oral infections." **International Journal of Antimicrobial Agents**, v. 43, n. 2, p. 95-104, 2014.
90. TÜZÜNER, T.; KUSGÖZ, A.; ER, K.; TASDEMİR, T.; BURUK, K.; KEMER, B. "Antibacterial activity and physical properties of conventional glass-ionomer cements containing chlorhexidine diacetate/cetrimide mixtures." **Journal of Esthetic Restoration Dentistry** v. 23, n. 1, p. 46-55, 2011.
91. TAKAHASHI, Y.; IMAZATO, S.; KANESHIRO, A.V.; EBISU, S.; FRENCKEN, J.E.; TAY, F.R. "Antibacterial effects and physical properties of glass-ionomer cements containing chlorhexidine for the ART approach." **Dental Materials**, v. 22, n. 7, p. 647-52, 2006.

92. YOSHIDA, K.; TANAGAWA, M. and ATSUTA, M. "Characterization and inhibitory effect of antibacterial dental resin composites incorporating silver-supported materials." **Journal of Biomedical Materials Research**, v. 47, n. 4, p. 516-22, 1999.
93. IMAZATO, S.; EBI, N.; TAKAHASHI, Y.; KANEKO, T.; EBISU, S.; RUSSELL, R.R. "Antibacterial activity of bactericide-immobilized filler for resin-based restoratives." **Biomaterials**, v. 24, n. 20, p. 3605-9, 2003.
94. ALLAKER, R.P. "The use of nanoparticles to control oral biofilm formation." **Journal of Dental Research**, v. 89, p. 11, p. 1175-86, 2010.
95. LIN, J.; QIU, S.; LEWIS, K.; KLIBANOV, A.M. "Bactericidal properties of flat surfaces and nanoparticles derivatized with alkylated polyethylenimines." **Biotechnololy Progress**, v. 18, n. 5, p. 1082-6, 2002.
96. MONTEIRO, D.R.; GORUP, L.F.; TAKAMIYA, A.S.; RUVOLLO-FILHO, A.C.; DE CAMARGO, E.R.; BARBOSA, D.B. "The growing importance of materials that prevent microbial adhesion: antimicrobial effect of medical devices containing silver." **International Journal of Antimicrobial Agents**, v. 34, n. 2, p. 103-110, 2009.
97. SEVINC, B.A. and HANLEY, L. "Antibacterial activity of dental composites containing zinc oxide nanoparticles." **Journal of Biomedical Materials Research B Applied Biomaterials**, v. 94, n. 1, p. 22-31, 2010.
98. DAMM, C.; MÜNSTEDT, H. and RÖSCH, A. "The antimicrobial efficacy of polyamide 6/silver-nano- and microcomposites." **Materials Chemistry and Physics**, v. 108, n. 1, p. 61-66, 2008.
99. KASSAEE, M.Z.; AKHAVAN, A.; SHEIKH, N. and SODAGA, A. "Antibacterial effects of a new dental acrylic resin containing silver nanoparticles." **Journal of Applied Polymer Science**, v. 110, n. 3, p. 1699-1703, 2008.
100. AHN, S.J.; LEE, A.-J.; KOOK, J.-K.; LIM, B.-S. "Experimental antimicrobial orthodontic adhesives using nanofillers and silver nanoparticles." **Dental Materials**, v. 25, n.2, p. 206-213, 2009.
101. CHENG, L.; ZHANG, K.; MELO, M.A.S.; WEIR, M.D.; ZHOU, X.; XU, H.H.K. "Anti-biofilm dentin primer with quaternary ammonium and silver nanoparticles." **Journal of dental research**, v. 91, n. 6, p. 598-604, 2012.

102. ZHANG, K.; MELO, M.A.; CHENG, L.; WEIR, M.D.; BAI, Y.; XU, H.H. "Effect of quaternary ammonium and silver nanoparticle-containing adhesives on dentin bond strength and dental plaque microcosm biofilms." **Dental Materials**, v. 28, n. 8, p. 842-52, 2012.
103. LI, F.; WEIR, M.D.; CHEN, J.; XU, H.H. "Comparison of quaternary ammonium-containing with nano-silver-containing adhesive in antibacterial properties and cytotoxicity." **Dental Materials : Official Publication of the Academy of Dental Materials**, v. 29, n. 4, p. 450-461, 2013.
104. XIE, D.; WENG, Y.; GUO, X.; ZHAO, J.; GREGORY, R.L.; ZHENG, C. "Preparation and evaluation of a novel glass-ionomer cement with antibacterial functions." **Dental Materials**, v. 27, n. 5, p. 487-496, 2011.
105. WENG, Y.; HOWARD, L.; CHONG, V.J.; SUN, J.; GREGORY, R.L. XIE, D. "A novel furanone-modified antibacterial dental glass ionomer cement." **Acta Biomaterialia**, v. 8, n. 8, p. 3153-3160, 2012.
106. ALEXANDER, J.W. "History of the medical use of silver." **Surgical infections**, v. 10, n. 3, p. 289-292, 2009.
107. RICHARD, D.G.; JOHN, M.M.; JAMES, E.H. "Generation of Metal Nanoparticles from Silver and Copper Objects: Nanoparticle Dynamics on Surfaces and Potential Sources of Nanoparticles in the Environment." **ACS Nano**, v. 5, n. 11, p. 8950-8957, 2011.
108. CHERNOUSOVA, S. and EPPLE, M. "Silver as antibacterial agent: ion, nanoparticle, and metal." **Angew Chem Int Ed Engl**, v. 52, n. 6, p. 1636-1653, 2013.
109. KIM, J.S.; KUK, E.; YU, K.N.; KIM, J.H.; PARK, S.J.; LEE, H.J. *et al.* "Antimicrobial effects of silver nanoparticles." **Nanomedicine**, v. 3, n. 1, p. 95-101. 2007.
110. MATSUMURA, Y.; YOSHIKATA, K.; KUNISAKI, S.; TSUCHIDO, T. "Mode of bactericidal action of silver zeolite and its comparison with that of silver nitrate." **Applied and Environmental Microbiology**, v. 69, n. 7, p. 4278-4281, 2003.
111. GUPTA, A.; MAYNES, M.; SILVER, S. "Effects of halides on plasmid-mediated silver resistance in *Escherichia coli*." **Appl Environ Microbiol**, v. 64, n. 12, p. 5042-5045, 1998.

112. YAMANAKA, M.; HARA, K.; KUDO, J. "Bactericidal actions of a silver ion solution on *Escherichia coli*, studied by energy-filtering transmission electron microscopy and proteomic analysis." **Appl Environ Microbiol**, v. 71, n. 11, p. 7589-7593, 2005.
113. FENG, Q.L.; WU, J.; CHEN, G.Q.; CUI, F.Z.; KIM, T.N.; KIM, J.O. "A mechanistic study of the antibacterial effect of silver ions on *Escherichia coli* and *Staphylococcus aureus*." **Journal of Biomedical Materials Research**, v. 52, n. 4, p. 662-668, 2000.
114. CHOI, O.; DENG, K.K.; KIM, N.J.; ROSS, L.Jr.; SURAMPALLI, R.Y.; HU, Z. "The inhibitory effects of silver nanoparticles, silver ions, and silver chloride colloids on microbial growth." **Water Res**, v. 42, n. 12, p. 3066-3074, 2008.
115. BRETT, D.W. "A discussion of silver as an antimicrobial agent: alleviating the confusion." **Ostomy/wound management**, v. 52, n. 1, p. 34-41, 2005.
116. TEEGUARDEN, J.G.; HINDERLITER, P.M.; ORR G.; THRALL, B.D.; POUNDS, J.G. "Particokinetics in vitro: dosimetry considerations for in vitro nanoparticle toxicity assessments." **Toxicological sciences : an official journal of the Society of Toxicology**, v. 95, n. 2, p. 300-312, 2007.
117. SILVER, S. "BioMetals: a historical and personal perspective." **Biometals**, v. 24, n. 3, p. 379-390. 2011.
118. SILVER, S. "Bacterial silver resistance: molecular biology and uses and misuses of silver compounds." **FEMS Microbiol Rev**, v. 27, n. 2-3, p. 341-53, 2003.
119. SILVER, S.; PHUNG, L.E.; SILVER, G. "Silver as biocides in burn and wound dressings and bacterial resistance to silver compounds." **Journal of Industrial Microbiology and Biotechnology**, v. 33, n. 7, p. 627-634, 2006.
120. PAL, S.; TAK, Y.K.; SONG, J.M. "Does the Antibacterial Activity of Silver Nanoparticles Depend on the Shape of the Nanoparticle? A Study of the Gram-Negative Bacterium *Escherichia coli*." **Applied and Environmental Microbiology**, v. 73, n. 6, p. 1712-1720, 2007.
121. NAIR, L.S. and LAURENCIN, C.T. "Silver Nanoparticles: Synthesis and Therapeutic Applications." **Journal of Biomedical Nanotechnology**, v. 3, n. 4, p. 301-316, 2007.

122. MORONES, J.R.; ELECHIGUERRA, J.L.; CAMACHO, A.; HOLT, K.; KOURI, J.B.; RAMÍREZ, J.T.; YACAMAN, M.J. “The bactericidal effect of silver nanoparticles.” **Nanotechnology**, v. 16, n. 10, p. 2346-2353, 2005.
123. MARTIN, M.N.; ALLEN, A.J.; MACCUSPIE, R.I.; HACKLEY, V.A. “Dissolution, agglomerate morphology, and stability limits of protein-coated silver nanoparticles.” **Langmuir**, v. 30, n. 38, p. 11442-11452, 2014.
124. LIU, J.; SONSHINE, D.A.; SHERVANI, S.; HURT, R.H. “Controlled release of biologically active silver from nanosilver surfaces.” **ACS Nano**, v. 4, n. 11, p. 6903-13, 2010.
125. SOTIRIOU, G.A. and PRATSINIS, S.E. “Antibacterial activity of nanosilver ions and particles.” **Environmental science & technology**, v. 44, n. 14, p. 5649-5654, 2010.
126. ESPINOSA-CRISTÓBAL, L.F.; MARTÍNEZ-CASTAÑÓN, G.A.; TÉLLEZ-DÉCTOR, E.J.; NIÑO-MARTÍNEZ, N.; ZAVALA-ALONSO, N.V.; LOYOLA-RODRÍGUEZ, J.P. “Adherence inhibition of *Streptococcus mutans* on dental enamel surface using silver nanoparticles.” **Material Science Engineering C Materi Biol Appl.**, v. 33, n. 4, p. 2197-202, 2013.
127. KIM, T.-H.H.; KIM, M.; PARK, H.S.; SHIN, U.S.; GONG, M.S.; KIM, H.W. “Size-dependent cellular toxicity of silver nanoparticles.” **Journal of Biomedical Materials Research. Part A**, v. 100, n. 4, p. 1033-1043, 2012.
128. GORTH, D.J.; RAND, D.M.; WEBSTER, T.J. “Silver nanoparticle toxicity in *Drosophila*: size does matter.” **International Journal of Nanomedicine**, v. 6, p. 343-350, 2011.
129. PARK, M.V.; NEIGH, A.M.; VERMEULEN, J.P.; DE LA FONTEYNE, L.J.; VERHAREN, H.W.; BRIEDÉ, J.J.; VAN LOVEREN, H. “The effect of particle size on the cytotoxicity, inflammation, developmental toxicity and genotoxicity of silver nanoparticles.” **Biomaterials**, v. 32, n. 36, p. 9810-9817, 2011.
130. LIU, W.; WU, Y.; WANG, C.; LI, H.C.; WANG, T.; LIAO, C.Y. *et al.* “Impact of silver nanoparticles on human cells: effect of particle size.” **Nanotoxicology**, 4(3): p. 319-30. 2010.

131. WILLETS, K.A. and V.R.P. DUYNE, "Localized surface plasmon resonance spectroscopy and sensing." **Annual Reviews of Physical Chemistry**, v. 58, p. 267–297, 2007.
132. GARCIA, M.A. "Surface plasmons in metallic nanoparticles: fundamentals and applications." **Journal of Physics D: Applied Physics**, v. 44, n. 28, 2011.
133. MULVANEY, P. "Surface plasmon spectroscopy of nanosized metal particles." **Langmuir**, v. 12, n. 3, p. 788-800, 1996.
134. LIZ-MARZAN, L.M. "Nanometals: Formation and color." **Materials Today**, v. 7, n. 2, p. 26-31, 2004.
135. TOMA, H.E.; ZAMARION, V.M.; TOMA; S.H.; ARAKI, K. "The coordination chemistry at gold nanoparticles." **Journal of the Brazilian Chemical Society**, v. 21, n. 7, p. 1158-1176, 2010.
136. SAU, T.K. and ROGACH, A.L. "Nonspherical noble metal nanoparticles: colloid-chemical synthesis and morphology control." **Advanced Materials**, v. 22, n. 16, p. 1781-804, 2010.
137. ABOU EL-NOUR, K.M.M.; EFTAIHA, A.; AL-WARTHANB, A.; AMMARB, R.A.A. "Synthesis and applications of silver nanoparticles." **Arabian Journal of Chemistry**, v. 3, n. 3, p. 135-140, 2010.
138. HEICKLEN, J. **Colloid formation and growth a chemical kinetics approach**. Academic Press Inc., London, Copyright © 1976, Elsevier Inc. 2015.
139. SAKAMOTO, M.; FUJISTUKA, M.; MAJIMA, T. "Light as a construction tool of metal nanoparticles: Synthesis and mechanism." **Journal of Photochemistry and Photobiology C-Photochemistry Reviews**, v. 10, n. 1, p. 33-56, 2009.
140. HOFFMANN, N. "Photochemical reactions as key steps in organic synthesis." **Chemical Reviews**, v. 108, n. 3, p. 1052-1103, 2008.
141. MUELLER, F. and MATTAY, J. "Photocycloadditions: control by energy and electron transfer." **Chemical Reviews**, v. 93, n. 1, p. 99-117, 1993.
142. WESSIG, P. "Organocatalytic enantioselective photoreactions." **Angewandte Chemie International Edition in English**, v. 45, n. 14, p. 2168-2171, 2006.
143. BALZANI, V.; CREDI, A.; VENTURI, M. "Light powered molecular machines." **Chemical Society Review**, v. 38, n. 6, p. 1542-50, 2009.

144. LI, L. and ZHU, Y.J. "High chemical reactivity of silver nanoparticles toward hydrochloric acid." **Journal of Colloid Interface Science**, v. 303, n. 2, p. 415-418, 2006.
145. MAYER, A.B.R.; JOHNSON, R.W.; HAUSNER, S.H.; MARK, J.E. "Colloidal silver nanoparticles protected by water-soluble nonionic polymers and "soft" polyacids." **Journal of Macromolecular Science: Part A**, v. 36, n. 10, p. 1427-1441, 1999.
146. TEMPLETON, A.C.; WUELFING, W.P. AND MURRAY, R.W. "Monolayer-protected cluster molecules." **Accounts of Chemical Research**, v. 33, n. 1, p. 27-36, 2000.
147. KÉKI, S.; TÖRÖK, J.; DEÁK, G.; DARÓCZI, L.; ZSUGA, M. "Silver Nanoparticles by PAMAM-Assisted Photochemical Reduction of Ag(+)." **Journal of Colloid and Interface Science**, v. 229, n. 2, p. 550-553, 2000.
148. LU, Y.; MEI, Y.; SCHRINNER, M.; BALLAUFF, M.; MÖLLER, M.W.; BREU, J. "In Situ Formation of Ag Nanoparticles in Spherical Polyacrylic Acid Brushes by UV Irradiation." **Journal of Physical Chemistry C**, v. 111, n. 21, p. 7676-7681, 2007.
149. LINNERT, T.; MULVANEY, P.; HENGLEIN, A.; WELLER, H. "Long-lived nonmetallic silver clusters in aqueous solution: preparation and photolysis." **Journal of the American Chemistry Society**, v. 112, n. 12, p. 4657-4664, 1990.
150. HENGLEIN, A.; LINNERT, T.; MULVANEY, P. "Reduction of Ag<sup>+</sup> in aqueous polyanion solution: some properties and reactions of long-lived oligomeric silver clusters and metallic silver particles." **Berichte der Bunsengesellschaft für physikalische Chemie**, v. 94, n. 12, p. 1449-1457, 1990.
151. ZHANG, Z.; PATEL, R.C.; KOTHARI, R.; JOHNSON, C.P.; FRIBERG, S.E. "Stable silver clusters and nanoparticles prepared in polyacrylate and inverse micellar solutions." **The Journal of Physical Chemistry B**, v. 104, n. 6, p. 1176-1182, 2000.
152. MALLICK, K.; WITCOMB, M.J.; SCURRELL, M.S. "Polymer stabilized silver nanoparticles: a photochemical synthesis route." **Journal of Materials Science**, v. 39, n. 14, p. 4459-4463, 2004.
153. HU, Y.X.; GE, J.; LIM, D.; ZHANG, T.; YI, Y. "Size-controlled synthesis of highly water-soluble silver nanocrystals." **Journal of Solid State Chemistry**, v. 181, n. 7, p. 1524-1529, 2008.
154. ZHANG, T.; GE, J.; HU, Y.; YIN, Y. "A general approach for transferring hydrophobic nanocrystals into water." **Nano letters**, v. 7, n. 10, p. 3203-3207, 2007.

155. HUANG, H. and Y. YANG, "Preparation of silver nanoparticles in inorganic clay suspensions." **Composites Science and Technology**, v. 68, n. 14, p. 2948-2953, 2008.
156. LAVINIA, B.; SCHNEIDER, R.; LOUGNOT, D.J. "A new and convenient route to polyacrylate/silver nanocomposites by light-induced cross-linking polymerization." **Progress in Organic Coatings**, v. 62, n. 3, p. 351–357, 2008.
157. WILSON, A.D.; HILL, R.G.; WARRENS, C.P.; LEWIS, B.G. "The influence of polyacid molecular weight on some properties of glass-ionomer cements." **Journal of Dental Research**, v. 68, n. 2, p. 89-94, 1989.
158. DOWLING, A.H.; FLEMING, G.J. "The influence of poly(acrylic) acid number average molecular weight and concentration in solution on the compressive fracture strength and modulus of a glass-ionomer restorative." **Dental Materials**, v. 27, n. 6, p. 535-43, 2011.
159. SCHNEIDER, C.A.; RASBAND, W.S.; ELICEIRI, K.W. "671 nih image to imageJ: 25 years of image analysis." **Nature Methods**, v. 9, n. 7, p. 671-5, 2012.
160. PAIVA, L., FIDALGO, T.K.S.; MAIA, L.C. "Mineral content of ionomer cements and preventive effect of these cements against white spot lesions around restorations." **Brazilian Oral Research**, v. 28, n. 1, p. 1-9, 2014.
161. INTERNATIONAL ORGANIZATION FOR STANDARDIZATION. "9917 Dentistry—Water based cements." in Part 1: Powder/Liquid acid-base cements. 2007: Switzerland. p. 22.
162. MIAO, H.; RATNASINGAM, S.; PU, C.S.; DESAI, M.M.; SZE, C.C. "Dual fluorescence system for flow cytometric analysis of *Escherichia coli* transcriptional response in multi-species context." **Journal of Microbiological Methods**, v. 76, n. 2, p.109-19, 2009.
163. WONG, L. and SISSONS, C. "A comparison of human dental plaque microcosm biofilms grown in an undefined medium and a chemically defined artificial saliva." **Archives of Oral Biology**, v. 46, n. 6, p. 477-486, 2001.
164. HEYDORN A.; NIELSEN, A.T.; HENTZER, M.; STERNBERG, C.; GIVSKOV, M., ERSBØLL, B.K. MOLIN, S. "Quantification of biofilm structures by the novel computer program COMSTAT." **Microbiology**, v. 146, n. 10, p. 2395-407, 2000.

165. KRAIGSLY, A.M.; TANG, K.; LIPPA, K.A. "Effect of polymer degree of conversion on *Streptococcus mutans* biofilms." **Macromolecular Bioscience**, v. 12, n. 12, p. 1706-13, 2012.
166. KUPTSOV, A.H. and ZHIZHIN, G. **Handbook of Fourier transform Raman and infrared spectra of polymers**. v. 45. 1998: Elsevier.
167. LIN-VIEN, D. *et al.* **The handbook of infrared and Raman characteristic frequencies of organic molecules**. Elsevier. 1991: Elsevier.
168. KACZMAREK, H.; KAMIŃSKA, A.; ŚWIATEK, M.; RABEK, J.F. "Photo-oxidative degradation of some water-soluble polymers in the presence of accelerating agents." **Die Angewandte Makromolekulare Chemie**, v. 261-262, n. 1, p. 109-121, 1998.
169. SHUKLA, N.B.; DARABOINA, N. and MADRAS, G. "Oxidative and photooxidative degradation of poly(acrylic acid)." **Polymer Degradation and Stability**, v. 94, n. 8, p. 1238-1244, 2009.
170. MARQUSEE, J.A. and ROSS, J. "Theory of Ostwald Ripening - Competitive Growth and Its Dependence on Volume Fraction." **Journal of Chemical Physics**, v. 80, n. 1, p. 536-543, 1984.
171. TONTI, D.; MOHAMMED, M.B.; AL-SALMAN, A.; PATTISON, P. "Multimodal distribution of quantum confinement in ripened CdSe nanocrystals." **Chemistry of Materials**, v. 20, n. 4, p. 1331-1339, 2008.
172. DAGTEPE, P. and CHIKAN, V. "Quantized Ostwald Ripening of Colloidal Nanoparticles." **Journal of Physical Chemistry C**, v. 114, n. 39, p. 16263-16269, 2010.
173. PODGORNIK, R. and LICER, M. "Polyelectrolyte bridging interactions between charged macromolecules." **Current Opinion in Colloid & Interface Science**, v. 11, n. 5, p. 273-279, 2006.
174. FARROKHPAY, S.; MORRIS, G.E.; FORNASIERO, D. *et al.* "Effects of chemical functional groups on the polymer adsorption behavior onto titania pigment particles." **Journal of Colloid Interface Science**, v. 274, n. 1, p. 33-40, 2004.
175. BANASH, M.A. and CROLL, S.G. "A Quantitative study of polymeric dispersant adsorption onto oxide-coated titania pigments." **Progress in Organic Coatings**, v. 35, n. 1-4, p. 37-44, 1999.

176. RIVERO, P.J.; GOICOECHEA, J.; URRUTIA, A.; ARREGUI, F.J. "Effect of both protective and reducing agents in the synthesis of multicolor silver nanoparticles." **Nanoscale Research Letters**, v. 8, n. 1, p. 101, 2013.
177. POKHREL, L.R.; DUBEY, B.; SCHEUERMAN, P.R. "Impacts of select organic ligands on the colloidal stability, dissolution dynamics, and toxicity of silver nanoparticles." **Environmental Science & Technology**, v. 47, n. 22, p. 12877-12885, 2013.
178. HUBER, K.; WITTE, T.; HOLLMANN, J.; KEUKER-BAUMANN, S. "Controlled formation of ag nanoparticles by means of long-chain sodium polyacrylates in dilute solution." **Journal of American Chemistry Society**, v. 129, n. 5, p. 1089-1094, 2007.
179. GREGOR, H.P.; LUTTINGER, L.B.; LOEBL, E.M. "Metal-Polyelectrolyte Complexes. I. The Polyacrylic Acid-Copper Complex." **The Journal of Physical Chemistry**, v. 59, n. 1, p. 34-39, 1955.
180. FLEMING, G.J.; FAROOQ, A.A.; BARRALET, J.E. "Influence of powder/liquid mixing ratio on the performance of a restorative glass-ionomer dental cement." **Biomaterials**, v. 24, n. 23, p. 4173-4179, 2003.
181. KILPATRICK, N.M.; MURRAY, J.J.; MCCABE, J.F. "The use of a reinforced glass-ionomer cermet for the restoration of primary molars - a clinical-trial." **British Dental Journal**, v. 179, n. 5, p. 175-179, 1995.
182. DAMM, C.; MUNSTEDT, H.; ROSCH, A. "The antimicrobial efficacy of polyamide 6/silver-nano- and microcomposites." **Materials Chemistry and Physics**, v. 108, n. 1, p. 61-66, 2008.
183. EL BADAWY, A.M.; LUXTON, T.P.; SILVA, R.G.; SCHECKEL, K.G.; SUIDAN, M.T.; TOLAYMAT, T.M. "Impact of environmental conditions (pH, ionic strength, and electrolyte type) on the surface charge and aggregation of silver nanoparticles suspensions." **Environment Science and Technology**, v. 44, n. 4., p. 1260-1266, 2010.
184. DAMM, C. and MUNSTEDT, H. "Kinetic aspects of the silver ion release from antimicrobial polyamide/silver nanocomposites." **Applied Physics A:Materials Science & Processing**, v. 91, n. 3, p. 479-486, 2008.

185. EBI, N.; IMAZATO, S.; NOIRI, Y.; EBISU, S. "Inhibitory effects of resin composite containing bactericide-immobilized filler on plaque accumulation." **Dental Materials**, v. 17, n. 6, p. 485-491, 2001.
186. MULLER, R.; EIDT, A.; HILLER, K.A.; KATZUR, V.; SUBAT, M.; SCHWEIKL, H.; IMAZATO, S.; RUHL, S.; SCHMALZ, G. "Influences of protein films on antibacterial or bacteria-repellent surface coatings in a model system using silicon wafers." **Biomaterials**, v. 30, n. 28, p. 4921-4929, 2009.
187. CRISP, S.; KENT, B.E.; LEWIS, B.G.; FERNER, A.J.; WILSON, A.D. "Glass-ionomer cement formulations. II. The synthesis of novel polycarboxylic acids." **Journal of dental research**, v. 59, n. 6, p. 1055-1063, 1980.
188. YAMAZAKI, T.; BRANTLEY, W.; CULBERTSON, B.; SEGHI, R.; SCHRICKER, S. "The measure of wear in N-vinyl pyrrolidinone (NVP) modified glass-ionomer cements." **Polymers for Advanced Technologies**, v. 16, n. 2-3, p. 113-116, 2005.
189. MOSHAVERINIA, A.; ANSARI, S.; MOSHAVERINIA, M.; ROOHPUR, N.; DARR, J.A.; REHMAN, I. "Effects of incorporation of hydroxyapatite and fluoroapatite nanobioceramics into conventional glass ionomer cements (GIC)." **Acta Biomaterialia**, v. 4, n. 2, p. 432-440, 2008.
190. XIE, D.; ZHAO, J.; YANG, Y.; PARK, J.; CHU, T.M.; ZHANG, J.T. "Preparation and evaluation of a high-strength biocompatible glass-ionomer cement for improved dental restoratives." **Biomedical Materials**, v. 3, n. 2, p. 025-012, 2008.
191. FAN, C.; CHU, L.; RAWLS, H.R.; NORLING, B.K.; CARDENAS, H.L.; WHANG, K. "Development of an antimicrobial resin--a pilot study." **Dental Materials**, v. 27, n. 4, p. 322-328, 2011.
192. EICK, S.; GLOCKMANN, E.; BRANDL, B.; PFISTER, W. "Adherence of *Streptococcus mutans* to various restorative materials in a continuous flow system." **Journal of oral rehabilitation**, v. 31, n. 3, p. 278-285, 2004.
193. CHENG, L.; EXTERKATE, R.A.; ZHOU, X.; LI, J.; TEN CATE, J.M. "Effect of *Galla chinensis* on growth and metabolism of microcosm biofilms." **Caries Research**, v. 45, n. 2, p. 87-92, 2010.
194. MARSH, P.D.; MOTER, A.; DEVINE, D.A. "Dental plaque biofilms: communities, conflict and control." **Periodontology**, v. 55, n. 1, p. 16-35, 2011.

195. LI, Y.H.; HANNA, M.N.; SVENSÄTER, G.; ELLEN, RP; CVITKOVITCH, D.G. "Cell density modulates acid adaptation in *Streptococcus mutans*: implications for survival in biofilms." **Journal of Bacteriology**, v. 183, n. 23, p. 6875-84, 2001.
196. LI, Y.H.; TANG, N.; ASPIRAS, M.B.; LAU, P.C.; LEE, J.H.; ELLEN, R.P.; CVITKOVITCH, D.G. "A quorum-sensing signaling system essential for genetic competence in *Streptococcus mutans* is involved in biofilm formation." **Journal of Bacteriology**, v. 184, n. 10, p. 2699-2708, 2002.
197. OPPERMANN, R.V.; RØLLA, G.; JOHANSEN, J.R.; ASSEV, S. "Thiol groups and reduced acidogenicity of dental plaque in the presence of metal ions *in vivo*." **Scandinavian Journal of Dental Research**, v. 88, n. 5, p. 389-396, 1980.
198. LI, Y.H.; LAU, P.C.; LEE, J.H.; ELLEN, R.P.; CVITKOVITCH, D.G. "Natural genetic transformation of *Streptococcus mutans* growing in biofilms." **Journal of bacteriology**, v. 183, n. 3, p. 897-908, 2001.
199. MEI, M.L.; CHU, C.H.; LO, E.C.; SAMARANAYAKE, L.P. "Fluoride and silver concentrations of silver diammine fluoride solutions for dental use." **International Journal of Paediatric Dentistry**, v. 23, n. 4, p. 279-85, 2013.
200. CHU, C.H.; LO, E.C.M.; LIN, H.C. "Effectiveness of silver diamine fluoride and sodium fluoride varnish in arresting dentin caries in Chinese pre-school children." **Journal of Dental Research**, v. 81, n. 11, p. 767-770, 2002.
201. LLODRA, J.C.; RODRIGUEZ, A.; FERRER, B.; MENARDIA, V.; RAMOS, T.; MORATO, M. "Efficacy of silver diamine fluoride for caries reduction in primary teeth and first permanent molars of schoolchildren: 36-month clinical trial." **Journal of Dental Research**, v. 84, n. 8, p. 721-724, 2005.
202. FUNG, M.; WONG, M.; LO, E.; CHU, C. "Arresting Early Childhood Caries with Silver Diamine Fluoride-A Literature Review." **Journal of Oral Hygiene & Health**, v. 1, n. 3, p. 1000117, 2013.
203. GOTJAMANOS, T. "Pulp response in primary teeth with deep residual caries treated with silver fluoride and glass ionomer cement ('atraumatic' technique)." **Australian Dental Journal**, v. 41, n. 5, p. 328-334, 1996.
204. MCCABE, J.F.; YAN, Z.; AL NAIMI, O.T.; MAHMOUD, G.; ROLLAND, S.L. "Smart materials in dentistry." **Australian Dental Journal**, v. 56, n. 1, p. 3-10, 2011.

205. KNIGHT, G.M.; MCINTYRE, J.M.; CRAIG, G.G.; MULYANI; ZILM, P.S.; GULLY, N.J. "Inability to form a biofilm of *Streptococcus mutans* on silver fluoride- and potassium iodide-treated demineralized dentin." **Quintessence International**, v. 40, n. 2, p. 155-161, 2009.
206. CHU, C.; LEE, A.H.; ZHENG, L.; MEI, M.L.; CHAN, G.C. "Arresting rampant dental caries with silver diamine fluoride in a young teenager suffering from chronic oral graft versus host disease post-bone marrow." **BMC Research Notes**, v. 7, n. 3, 2014. doi:10.1186/1756-0500-7-3

## ***ANNEX (Cotutelle UFRJ-UHA)***

---

### ***Introduction***

---

La carie dentaire est encore un problème de santé bucco-dentaire grave dans les pays développés économiquement, puisqu'elle affecte 60 à 90% des enfants d'âge scolaire et la grande majorité des adultes. Elle est également la maladie bucco-dentaire la plus répandue dans de nombreux pays en Asie et en Amérique Latine, mais semble être moins fréquente et moins sévère dans la plupart des pays africains. [1]

Le traitement préféré des caries avec cavitation est l'ablation du tissu dentaire déminéralisé et contaminé par préparation de la cavité, suivie par le remplacement des tissus perdus par des matériaux dentaires tels que des alliages métalliques, des résines composites, des ciments verres ionomères ou de la céramique.

De par la nécessité de remplacer les amalgames à base de mercure en dentisterie, les ciments verres ionomères (CVI), une catégorie particulière de matériaux dentaires bioactifs, ont été introduits par Wilson et Kent [2]. Ces ciments de polyalkenoate, formés de verres de fluoro-alumino-silicate et d'une solution aqueuse de poly(acide acrylique), sont toujours l'un des matériaux les plus prometteurs parmi les matériaux dentaires actuels et ont été appliqués avec succès en dentisterie depuis plus de 30 ans. Une réaction acide-base conduit

à la formation d'une phase de gel composite (sels carboxylates) incrusté de particules de verre qui n'ont pas réagi.

Les CVI sont souvent utilisés dans la pratique clinique à cause de leurs caractéristiques singulières. L'importance de ces ciments est attribuée à leur rôle dans la gestion clinique des caries, en Intervention Restauratrice Minimale (IRM), et en gestion des caries par l'évaluation des risques (CAMBRA). Leurs propriétés anti-cariogéniques comme la libération de fluorure, l'échange d'ions à l'interface interne entre le CVI et la dent, l'adhésion directe à la structure dentaire et aux bases métalliques, la réduction des microfuites à l'interface dent-émail, un coefficient linéaire de dilatation thermique similaire à celui de la dentine et une faible cytotoxicité sont des propriétés uniques qui permettent des applications spécifiques de ces ciments. Cependant leurs inconvénients tels que leur sensibilité précoce à l'eau, leur faible résistance à la compression et leur résistance à l'usure réduite ont limité l'utilisation des CVI classiques dans certaines applications cliniques. Malgré ces problèmes, les CVI ont un champ d'applications spécifiques en pédodontie, dans lesquels la carie dentaire présente une morbidité élevée. Compte tenu du temps de chaise réduit et d'autres difficultés de traitement inhérentes au comportement des enfants, les CVI sont indiqués en raison de la simplicité de la technique et des effets préventifs observés seulement pour cette classe de matériaux. Ainsi, contrairement aux résines composites dentaires utilisées pour la restauration définitive de la carie dentaire, ils restent comme le matériau approprié pour des restaurations de court et moyen terme dans de nombreuses situations dans la pratique dentaire.

L'utilisation du fluorure dans la prévention de la carie est déjà établie en médecine dentaire, mais actuellement il apparaît nécessaire d'élargir l'arsenal des produits de

prévention par des thérapies antibactériennes efficaces, afin de permettre à la prévention de devenir moins dépendante des produits fluorés [3]. Dans ce contexte, les nanoparticules d'argent (AgNP) se sont montrées particulièrement efficaces quand elles sont associées à des matériaux, car elles peuvent changer leur charge de surface, leur hydrophobie, et d'autres caractéristiques physico-chimiques importantes pour le processus d'adhésion et de maturation du biofilm bactérien à l'origine des caries [4]. En outre, l'immobilisation des AgNP dans la matrice polymérique qui fonctionne comme réservoir d'ions argent, permet de réduire leur toxicité car cela empêche l'absorption directe des particules par les cellules de mammifère [5].

Récemment, les nanocomposites à base de résine remplis d'AgNP ont été largement étudiés comme matériaux antibactériens pour les applications dentaires. Ces matériaux sont appliqués aux restaurations permanentes, qui exigent une stabilité des couleurs et des propriétés mécaniques durables. Toutefois, les matériaux à base de résine ne sont pas aussi bioactifs que le CVI conventionnel à cause du flux d'eau non liée à travers le matériau que ce dernier présente. La bioactivité des matériaux à base aqueuse est une exigence majeure pour la lutte contre les caries actives, et aussi la principale raison de l'applicabilité des CVI dans les approches cliniques modernes, comme l'IRM. Ainsi, la présence des AgNP dans les CVI à base aqueuse peut donner des propriétés antibactériennes à ce matériau grâce à la libération d'ions d'argent. Cette activité alliée à la libération connue de fluorure pourrait aussi donner une fonction cariostatique aux CVI.

Poussés par la motivation d'attribuer des propriétés antibactériennes aux CVI, nous souhaitons analyser si la présence des AgNP pouvait modifier les propriétés du CVI conventionnel. Le but de cette étude était de synthétiser et de caractériser de nouveaux

poly(acide acrylique) (AgNP-PAA) associés avec des nanoparticules d'argent via la technique de photoréduction, d'évaluer les propriétés *in vitro* du CVI ainsi formé et valider également ses propriétés antibactériennes, en étudiant la formation de biofilms à la surface des ciments.

## *Revue de Littérature*

---

En 1972, Wilson et Kent ont mis au point un matériau palliant aux inconvénients des silicates utilisés depuis le début du siècle pour les restaurations dentaires. Ils ont inventé une nouvelle classe de biomatériaux: les ciments verres ionomères (notés dans la littérature française CVI et en anglais GIC: Glass Ionomer Cements) qui sont principalement utilisés en pédodontie.

Les premiers ciments présentaient des inconvénients tels qu'une prise lente et une manipulation délicate. Au fil des années, ces matériaux se sont améliorés. Mac Lean et Gasser (1984), ont incorporé lors du frittage, des particules de métal (Ag) à des poudres de verre afin d'obtenir une liaison charge-matrice. Une nouvelle catégorie de ciment a ainsi été obtenue: les CVI composites verre-métal appelés CERMETS. Depuis 1986 nous assistons au développement de CVI modifiés par addition de résine (les CVIMAR).

Les CVI traditionnels sont classiquement composés d'une poudre et d'un liquide à mélanger. Ils sont le résultat d'une réaction acide-base où l'acide est le liquide et la base est

la poudre. Le matériau possède donc une structure qu'on pourrait presque qualifier de "composite" avec une matrice renforcée par des charges. Trois phases peuvent être décrites dans la réaction de prise: la phase de relargage ionique; la phase de formation de la matrice hydrogel (prise initiale) qui commence de 2 à 3 minutes après le début du mélange et dure à peu près 5 minutes; et la phase de formation d'un hydrogel matriciel gélifié (prise finale) qui démarre après la prise initiale et peut continuer pendant 24h ou plusieurs jours. Une bonne connaissance de la réaction de prise permet au praticien d'optimiser la manipulation et l'efficacité clinique de ces matériaux. Au sein du CVI pris, il y a 20 à 25 % d'eau. L'hydrophilie de ce matériau est donc une propriété directement issue de sa composition.

La carie est une pathologie du tissu dentaire due à la production locale d'acides organiques par les bactéries cariogènes de la plaque (Streptococcus, Lactobacillus, Actinomyces) lorsque ces dernières sont en contact avec des sucres fermentescibles. Ces bactéries produisent de l'acide quand elles sont disposées sous la forme d'un biofilm à la surface des dents. Cette acidité est responsable d'une déminéralisation de l'émail quand le pH passe en dessous de 5,5 puis de la dentine, plus fragile, en dessous de 6,5.

Les CVI libèrent des ions fluorures dans la salive et vers la dent ce qui engendre une augmentation de la résistance à la solubilité des tissus dentaires en milieu acide. Pour cette raison le ciment verre ionomère est un outil important dans la lutte contre les caries. Il peut être considéré comme un réservoir de fluorure et d'autres ions dans la cavité buccale, et comme une barrière mécanique qui protège la surface de la dent contre les bactéries.

Lorsque la carie se trouve à un stade où l'émail est complètement détruit, la cavité qui se forme dans la dentine est irréversible et nécessite donc des soins de restauration

(soins conservateurs). En l'absence de traitement, l'évolution peut se faire vers des complications aboutissant à la perte de la dent, avec des conséquences fonctionnelles et esthétiques et des problèmes infectieux.

Une variété de modifications des matériaux dentaires a été développée dans les dernières années pour leur attribuer des propriétés antibactériennes dans le but de réduire l'adhérence bactérienne et la formation de biofilm à leur surface, et donc la production d'acides qui provoquent la carie. Parmi ces stratégies, des nanoparticules d'argent ont été utilisées avec succès dans la matrice de matériaux polymères à base de résine, d'où elles sont relarguées lentement et agissent comme des réservoirs d'ions d'argent qui sont connus pour leur effet biocide à large spectre.

L'utilisation de méthodes photochimiques pour la synthèse de nanoparticules d'argent présente certains avantages comme la réaction sans solvant, la haute résolution spatiale, la production contrôlée d'agents réducteurs, et le fait de pouvoir se faire sur différents substrats. Ces agents de réduction activés par une lumière ionisante (telle que la lumière ultraviolette) en présence d'une matrice polymérique (jouant le rôle d'agent de stabilisation) induit la réduction des ions d'argent en AgNP.

En raison de leurs propriétés optiques de résonance plasmonique de surface, les nanoparticules d'argent ont des bandes d'absorption dont la longueur d'onde et la largeur à mi-hauteur varient en fonction de leur taille moyenne et de la distribution en taille de la population de particules.

## *Objectifs*

---

### **GÉNÉRAL**

L'évaluation d'un nouveau ciment verre ionomère experimental contenant nanoparticules d'argent (AgNP-CVI) avec diverses teneurs d'argent était le but principal de ce travail.

### **OBJETIFS SPÉCIFIQUES**

- La synthèse *in situ* des nanoparticules d'argent dans la solution de poly(acide acrylique) de CVI;
- Les propriétés mécaniques, physico-chimiques, toxicologiques et antibactériennes *in vitro* AgNP-CVI ont été analysés pour valider leur applicabilité comme ciments à base d'eau dans la pratique clinique.

## *Matériaux et Méthodes*

---

Le CVI développé ici a été constitué par l'association d'une solution de poly(acide acrylique) (PAA) fournie par Sigma-Aldrich et une poudre de verre ionomère de fluoro-alumino-silicate produite par le Laboratoire de Physique Dentaire de la Queen Mary University de Londres (Angleterre).

La solution de polyélectrolyte (liquide ionomère) utilisée dans toutes les expériences était composée d'un poly(acide acrylique) (PAA) ( $M_w \sim 100\,000\text{ g mol}^{-1}$ , 35% en poids dans  $\text{H}_2\text{O}$ ) et d'acide L-(+)-tartrique (TA) (99,5%). Une méthode photochimique par transfert direct d'électrons a été utilisée afin d'induire la formation de nanoparticules d'argent stables dans une solution de matrice de polyélectrolyte de PAA et TA. Le nitrate d'argent ( $\text{AgNO}_3$ ) (99%) (Sigma-Aldrich) a été ajouté à la formulation liquide ionomère décrite ci-dessus pour préparer des solutions de polyacrylate d'argent ( $[-\text{CH}_2-\text{CH}(\text{COOAg})-]_n$  ou Ag-PA) contenant une quantité croissante de sels d'argent (0, 0,05, 0,10 ou 0,50 en % en poids) et d'acide tartrique (5 ou 10 en % en poids). Ces solutions de polyacrylate d'argent contenant de l'acide tartrique (Ag-PA-TA) sont la base de la réduction en AgNP.

Les solutions d'Ag-PA-TA ont été progressivement irradiées par une lumière UV directe et suivie par spectroscopie UV-Vis afin de sélectionner la meilleure configuration en fonction des bandes de spectres UV-Vis autour de 430 nm. Après différents temps d'irradiation (0, 10, 30, 60 et 90 min) les formulations ont été séchées sur une plaque de verre, et analysées par FTIR-ATR.

La stabilité colloïdale a été évaluée en fonction de leur aspect visuel et suivie par spectroscopie UV-Vis. L'analyse morphologique des AgNP a été réalisée par microscopie électronique en transmission. Des solutions contenant des AgNP étaient directement déposées sur des grilles 400 mesh pour l'analyse.

Sur la base de la quantité de sel d'argent ajoutée dans les formulations de polyélectrolytes, les échantillons d'AgNP-CVI ont été classés en quatre groupes: Without Ag (contrôle négatif); Low Ag (0,05%); Medium Ag (0,10%) et High Ag (0,50%).

Les échantillons d'AgNP-CVI ont été caractérisés par les techniques suivantes:

- ✓ Temps de prise (ISO 9917-1:2007);
- ✓ Résistance à la compression (ISO 9917-1:2007);
- ✓ Plasma à couplage inductif - spectrométrie d'émission optique (ICP-EOS);
- ✓ Spectroscopie photoélectronique de Rayons X (XPS);
- ✓ Test de cytotoxicité indirect (essai MTT);
- ✓ Test de diffusion en gélose (test antibactérien général avec *E. coli* SCC1);
- ✓ Essais d'activités antibactériennes spécifiques (avec *Streptococcus mutans* CIP 103220):
- ✓ Etude de l'adhérence bactérienne au bout de 3 heures d'incubation dans la salive artificielle avec observation *in situ* grâce à un microscope confocal à balayage laser (MCBL);
- ✓ Etude de la structure du biofilm bactérien au bout de 24 heures d'incubation dans la salive artificielle avec observation *in situ* grâce à un microscope confocal à balayage laser (MCBL);

- ✓ Test de viabilité du biofilm bactérien au bout de 24 heures d'incubation dans la salive artificielle par essai MTT .
- ✓ Le test  $t$  de Student a été appliqué pour l'analyse statistique et un intervalle de confiance supérieur à 95% ( $p$ -value  $< 0,05$ ) a été considéré comme significatif.

## *Résultats et Discussion*

---

Les structures moléculaires des polyélectrolytes (solutions aqueuses de PAA et PAA-TA) ont été analysées après irradiation UV par spectroscopie FTIR en présence ou en absence de sel d'argent. Les spectres d'absorption FTIR ont montré que les groupes carboxyliques de PAA ne sont pas significativement affectés par la lumière UV, avec ou sans argent ajouté à la solution. D'autre part, les spectres d'absorption des solutions Ag-PAA-TA suggèrent que la synthèse de nanoparticules d'argent se passe entre 10 et 30 minutes d'irradiation UV, alors qu'après 60 minutes les chaînes de PAA se dégradent.

Les groupes carboxyliques des molécules de TA sont plus susceptibles d'interagir avec les ions d'argent que ceux des PAA. Ceci peut s'expliquer par le fait que les molécules plus petites sont censées avoir une réactivité fonctionnelle plus élevée que les molécules polymères à longue chaîne.

La cinétique de photoréduction dans les formulations de PAA contenant les rapports  $\text{AgNO}_3$  / TA: (A) 0,05 / 5 pour Low Ag; (B) 0,10 / 10 pour Medium Ag et (C) 0,50 / 10

pour High Ag montrent une évolution de la bande d'absorption plasmon dans la région de 410 à 470 nm. Ce phénomène reflète le caractère de taille nanométrique de la dispersion colloïdale de particules d'argent sphéroïdales produites par cette méthode. Une augmentation de la conversion induite par la lumière UV est accompagnée d'une croissance du cluster et de la formation de nanoparticules. La surveillance des nanoparticules à long terme (180 jours) a montré qu'elles étaient stables en milieu aqueux en raison de la présence des chaînes polymères de PAA, qui agissent comme stabilisants. La taille moyenne des nanoparticules en solution étaient de 7, 8 et 10 nm, respectivement, pour Low Ag, Medium Ag et High Ag.

Lors de la caractérisation des AgNP-CVI, les temps de prise ont été jugés acceptables selon les valeurs prévues par la norme, et les valeurs de résistance à la compression ont été augmentées pour High Ag. Les sels d'argent en excès agissent comme agents d'ancrage des chaînes de polymère, ce qui augmente la résistance interne du ciment. En revanche, une diminution de la résistance à la compression du PAA irradié en absence de sel d'argent est une indication supplémentaire de la possible photo-dégradation subie par le PAA lorsque les radicaux libres générés par la lumière UV ne peuvent pas agir directement sur le transfert d'électrons aux ions d'argent.

La caractérisation biologique du ciment a montré que la quantité d'argent libérée par High Ag est toxique pour les cellules HGF-1. De plus, l'inhibition de la croissance bactérienne observée autour des AgNP-CVI suggère que les nanoparticules agissent comme un réservoir d'argent, provoquant la libération d'ions argent de la matrice du ciment à l'environnement par diffusion. En parallèle, il a été observé que les valeurs de la biomasse au bout de 3h d'incubation sont inversement proportionnelles à la quantité d'ions argent

libérés dans l'eau mesurée par analyse ICP, à partir respectivement de High Ag, Low Ag et Medium Ag. Il est cohérent de mettre en évidence que la formation de biofilm (après 24h) est principalement liée à une quantité croissante d'AgNP qui seraient exposées à la surface du CVI, et seraient ensuite oxydées pour libérer des ions d'argent. Par contre, les bactéries adhérentes (après 3h) souffrent également de l'influence de la diffusion des ions à partir des AgNP-CVI dans les premiers stades de la réaction de prise lorsque la plus grande quantité d'eau non liée et le flux de l'eau à travers les ciments sont censés attribuer une bioactivité supérieure.

La comparaison des valeurs obtenues à partir de la littérature montrent que les AgNP-CVI ont plus d'argent libéré de leur matrice et donc une plus grande bioactivité que les matériaux à base de résine pour la même quantité de sel d'argent ajoutée.

La quantité d'ions argent libérés par diffusion à partir de High Ag ( $\sim 1 \times 10^{-3}$  M), ainsi que l'oxydation des AgNP exposées à la surface des ciments ont inactivé la croissance de la population de bactéries sessiles et affecté la structure du biofilm. Par conséquent, la quantité totale d'ions d'argent a probablement atteint la concentration minimale inhibitrice (CMI) dans ces conditions, et a réduit la viabilité des bactéries à la surface du High Ag. Par contre, des concentrations plus faibles d'argent qui n'étaient pas en mesure de réduire la viabilité des bactéries, tel que Medium Ag, peuvent aussi affecter des paramètres de structure importants du biofilm. En faisant l'analogie avec les résultats d'action de biocides pour un taux sous-critique sur des biofilms oraux, on peut suggérer que les ions argent pourraient interférer avec le système de détection du quorum du biofilm et donc modifier sa structure, même si les bactéries sont encore viables.

Une des raisons pour laquelle les ions argent pourraient être un agent antibactérien stratégique dans l'environnement buccal est due au fait qu'ils ne devraient pas avoir une interaction à longue distance avec la microflore buccale en raison de leur grande affinité pour les ions chlorure abondants dans la salive (tendant à former des sels d'argent peu solubles). Ainsi, l'homéostasie microbienne des biofilms formés loin de surfaces contenant de l'Ag n'est pas susceptible d'être perturbée, alors que les biofilms formés sur ces surfaces pourraient être plus facilement enlevés.

Enfin, la libération d'ions fluorure connue pour les CVI combinée à la présence d'ions argent également libérés par les ciments pourrait attribuer à ces matériaux une activité cariostatique qui leur donne un grand potentiel d'application pour le traitement de la carie.

## ***Conclusions***

---

➤ Des nanoparticules d'argent ont été synthétisées *in situ* dans la solution de poly(acide acrylique) contenant de l'acide tartrique par irradiation UV induisant un transfert d'électrons à partir des groupes carboxylates non liés du polyélectrolyte vers l'espèce Ag<sup>+</sup>.

➤ Les nanoparticules d'argent sphéroïdales dont la distribution en taille est centrée de 7 à 10 nm en fonction de la formulation initiale, sont restées stables dans la matrice de polyélectrolytes jusqu'à 180 jours.

➤ Le système colloïdal a été maintenu par une stabilisation électrostatique en contrôlant la concentration initiale de l'acide tartrique (rapport molaire  $\text{Ag}^+/\text{COO}^-$ ) et le temps d'exposition à la lumière UV de chaque formulation.

➤ Malgré le temps de prise augmenté par l'addition des AgNP, la réaction de prise reste acceptable selon les exigences de la norme ISO9917:1.

➤ La résistance à la compression n'a pas été modifiée par la synthèse *in situ* des AgNP dans les CVI, et la résistance à la compression de High Ag a même augmenté par rapport au contrôle. Medium Ag et Low Ag ont des valeurs similaires à celles du matériau de référence (Vitro Molar™), indiquant une utilisation potentielle des AgNP-CVI pour l'application dentaire.

➤ High Ag a libéré une quantité plus grande d'argent lors d'une incubation dans de l'eau déminéralisée pendant 24h par rapport à Medium Ag et Low Ag.

➤ Après adsorption de protéines salivaires à la surface des ciments, la quantité d'argent exposée directement aux bactéries est diminuée.

➤ La viabilité des HGF-1 diminue significativement dans le groupe High Ag à cause de la grande quantité d'ions d'argent libérés à partir de ces ciments.

➤ Tous les groupes contenant de l'argent montrent des différences significatives d'inhibition de croissance de *E. coli* par diffusion sur gélose, suggérant une bioactivité des AgNP-CVI.

➤ Les bactéries adhérees sur les matériaux (3h) ont montré une tendance à former des microcolonies de bactéries agglomérées sur les surfaces d'AgNP-CVI par rapport au témoin (FB) ( $p$ -value < 0,05), et les valeurs de la biomasse étaient significativement différentes du Without Ag ( $p$ -value < 0,05).

➤ Les valeurs de biomasse du biofilm (24h) sur les groupes Medium Ag et High Ag ont montré des différences statistiquement significatives par rapport au contrôle (FB) ( $p$ -value < 0,05), ainsi que par rapport à Without Ag ( $p$ -value < 0,05).

➤ Medium Ag affecte des paramètres importants de la structure du biofilm, comme la biomasse, l'épaisseur moyenne et le rapport surface sur volume par rapport à Without Ag, mais la viabilité mesurée par l'activité MTT n'est pas modifiée de manière significative ni pour les bactéries formant les biofilms, ni pour les cellules HGF-1.

➤ La quantité d'ions argent relarguée à partir de High Ag est efficace pour inactiver la croissance de la population de bactéries sessiles et affecte la structure du biofilm, réduisant la viabilité des bactéries, mais aussi celle des cellules HGF-1.

➤ On peut affirmer que le nouveau AgNP-CVI développé dans ce travail s'est avéré avoir un effet biocide contre les biofilms de *S. mutans*, suggérant la dissolution oxydative des ions d'argent à partir de la matrice du ciment, sans causer d'effet cytotoxique sur les cellules HGF-1 ni réduire la résistance à la compression du ciment final.

## *Proposition d'Études Futures*

---

- La synthèse d'AgNP par photoréduction *in situ* dans la solution de PAA d'un CVI disponible dans le commerce;
- La synthèse d'AgNP par photoréduction *in situ* dans différentes solutions d'homopolymères et de copolymères de PAA;
- L'étude de l'influence des différentes compositions de verres ionomères sur la bioactivité et les activités biocides d'AgNP-CVI;
- L'exploration du mécanisme de purification du PAA par le processus de synthèse photochimique *in situ* des AgNP en solution;
- L'étude du mécanisme par lequel un niveau sous-critique d'ions d'argent peut perturber la formation du biofilm, soit parce qu'il peut être lié à une interférence avec le système de détection du quorum des bactéries cariogéniques, soit à leur production d'acide, leur tolérance à l'acide et / ou leur résistance;
- L'évaluation *ex vivo* de l'échange d'ions du AgNP-CVI avec les tissus dentaires et l'inhibition *in vitro* des caries;
- L'évaluation de l'effet cytotoxique des AgNP-CVI sur les odontoblastes et la réponse histologique des tissus pulpaire à travers la barrière de la dentine.